Synthesis and electrochemical modulation of the actuator properties of poly(phenazine-2,3-diimino (pyrrol-2-yl))

UNIVERSITY *of the*
WESTERN CAPE

Shanielle Veronique Botha

A full thesis submitted in partial fulfillment of the requirements for the degree of

Magister Scientiae in the Department of Chemistry,

University of the Western Cape

Supervisor: Prof. Emmanuel I. Iwuoha

Co- supervisor: Prof. Priscilla GL Baker

November 2008

Synthesis and electrochemical modulation of the actuator properties of poly(phenazine-2,3-diimino (pyrrol-2-yl))

Shanielle V. Botha

KEYWORDS

Conducting polymer

Polypyrrole

Phenazine

Poly (phenazine-2, 3-diimino (pyrrol-2-yl))

Actuator

Electrochemical Impedance Spectroscopy

Film thickness

Controlled drug release

Synthesis and electrochemical modulation of the actuator properties of poly(phenazine-2,3-diimino (pyrrol-2-yl))

ABSTRACT

A novel Schiff- base compound, phenazine-2,3-diimino(pyrrol-2-yl), was chemically synthesized by the condensation reaction of 2,3-diaminophenazine and pyrrole-2-carboxaldehyde and its structure confirmed by FTIR, NMR and SEM. Poly(phenazine-2,3-diimino(pyrrol-2-yl)) (PPDP) doped with 1,2-naphthaquinone-4-sulfonic acid (NQSA) was then electrochemically synthesized on a glassy carbon electrode in 0.1M HCl. Electrochemical impedance spectroscopy (EIS) was used to assess the actuating mechanism of PDPP by investigating the change in film thickness in various aqueous media, i.e. 0.1M NaCl, HCl, KCl and $CaCl_3$, at the reduction potential. Surface analysis of the synthesized polymer, were also done on screen printed carbon electrodes to investigate its morphology. Cyclic Voltammetry showed two redox couples, i.e. a quasi- reversible couple due to the pyrrole moiety and an irreversible couple due to phenazine's electrochemistry, with a surface concentration of $1.89x10^{-9}mol.cm^{-2}$, a diffusion coefficient of $4.61x10^{-7}cm^2.s^{-1}$ and a rate constant of $1.48x10^{-3}cm.s^{-1}$. Osteryoung Square Wave Voltammetry gave a formal potential of +320 mV vs Ag/AgCl. The trend in film thickness (as determined from EIS) for the different solvents were KCl>$CaCl_2$>NaCl>HCl, which is attributed to the increase in the cationic radius of the charged species. The film thickness of PPDP/NQSA at +320mV in 0.1M HCl was found to be 1.007μm, which increased by 0.023μm at the reduction potential in the same solvent. Polypyrrole doped with NQSA showed a change of 0.012 μm under the same conditions. PPDP was found to

undergo a greater change in film thickness, compared to PPy, making it a better actuator material as it can accommodate more ions in its structure. This actuator material can find possible application in controlled-release studies where they can act as hydrogels, swelling upon changes in the properties of the medium and leading to regulated release of ions into its environment.

DECLARATION

I declare that ***Synthesis and Electrochemical modulation of the actuator properties of poly(phenazine-2,3-diimino (pyrrol-2-yl)***) is my own work, that it has not been submitted before for any degree or examination in any other university, and that all the sources I have used or quoted have been indicated and acknowledged as complete references.

Shanielle Veronique Botha November 2008

……..

ACKNOWLEDGEMENTS

I would like to give thanks to God the Almighty for seeing me through this journey.

To my supervisor, Prof. Emmanuel Iwuoha, my sincere thanks for giving me the opportunity to be your student, for your guidance, support and direction throughout my studies.

Thank you to the Department of Chemistry for all your help and my sponsor, NRF, for the funding of my studies.

To my family, thank you for the motivation and the support throughout my studies.

To all my friends who helped me make this a success, through your understanding, encouragement and support, thank you.

LIST OF ABBREVIATIONS

A = surface area of electrode

C = capacitance

CP = conducting polymers

CPE = constant phase element

CV = Cyclic Voltammetry

DAP = 2, 3-diaminophenazine

DBS= dodecylbenzenesulfonate

D_e = diffusion coefficient

DMF = Dimethyl formamide

EIS = Electrochemical Impedance Spectroscopy

E^o = formal potential

FTIR = Fourier Transform Infrared Spectroscopy

GC = glassy carbon

IPMC = ionic polymer metal composites

k_0 = rate constant

L = film thickness

NMR = Nuclear Magnetic Resonance

NQSA = 1,2- naphthaquinone- 4- sulfonic acid

OSWV = Osteryoung Square Wave Voltammetry

PANI = Polyaniline

PDAP= Poly (2,3- diaminophenazine)

PDP = Phenazine -2,3- diimino (pyrrol-2-yl))

PPDP = Poly (phenazine -2,3- diimino (pyrrol-2-yl))

PPy = Polypyrrole

Pt = Platinum

R_{ct} = charge transfer resistance

SEM = Scanning Electron Microscopy

SPCE = screen printed carbon electrode

Γ^* = surface concentration of electroactive species

ε_o = vacuum permittivity

ε_r = dielectric constant

LIST OF FIGURES

LIST OF TABLES

Table of Contents

Page number

INTRODUCTION

1.1 Introduction

An actuator is a device which promotes mechanical work under the application of an external stimulus (Vidal F et al., 2006). Conventional actuators, i.e. piezoelectric polymers, ceramics, shape memory alloys, and acrylics have limited use, mostly due to the high driving voltages required to produce small strains and their lack of steady state responses (Baughmann RH, 1996). Conjugated conducting polymers (CP) are a viable and interesting alternative as actuators, since they work with low potentials and they experience volume changes that are associated with conformational changes in their structure (Hara S et al., 2004; Otero TF, 1997). CP actuators offer several advantages, such as large dimensional changes, high stress generation and high work per cycle (Baughmann RH, 1996). Electronically conducting polymers have many interesting and unique physical, chemical and optical properties (MacDiarmid AG, 2001). Most of these polymers are insulators in their neutral state and become conducting only when doped with counter- ions. These CP actuators are referred to as electrochemomechanical devices, in which an electric signal causes a chemical reaction, resulting in mechanical motion (Vidanapathirana KP, 2002). The mechanical motion results from a movement of solvated counter-ions into and out of the polymer chain, causing expansion and contraction respectively, upon either oxidation or reduction of the electroactive polymer (Otero TF et al., 1997).

In the last few decades, conducting polymer actuators undergoing volume change during redox processes have been intensively studied (Smela E, 2003; Baughmann RH, 1996). Among the conducting polymers, polypyrrole and its derivatives have attracted considerable attention due to their stability and electroactivity. During oxidation or reduction, the polymer chain has a net positive or negative charge due to the movement of electrons into or out of the polymer backbone respectively. These charged chains repulse each other, resulting in the generation of free space, which is subsequently occupied by counter-ions from the solution, accompanied by solvent molecules to neutralize the charge, resulting in an increase in the volume of the film (Otero TF et al., 1997). Upon reversal of the redox state of the polymer, the generated free space is diminished, causing the counter-ions and solvent molecules to migrate out of the polymer, resulting in the polymer film returning to its original volume. It is this mechanism that makes polymer actuator materials promising for microscopic valves and pumps, microflaps for aircraft wings, actuators for adaptive optics and steerable catheters, drug delivery systems and artificial muscle for robotic and prosthetic devices (Careem MA et al., 2006; Han G and Shi G, 2006).

Actuators mimic the movement of natural (skeletal) muscle, by the mechanism of expansion and contraction that a muscle undergoes upon application of a stimulus, which is comparable to the expansion and contraction mechanism of conducting polymers upon application of the appropriate potential. Many polypyrrole materials have been developed as possible artificial muscle for prosthesis or robotics. These

include PPy/ClO_4^- (Otero TF et al., 1997), PPy/BF_4^- (Skaarup S et al., 2007) and a microrobot based on polypyrrole doped with dodecylbenzenesulfonate, PPy/DBS (Pei and Inganas, 1993), that could grab and lift a 100µm glass bead. Controlled drug release systems, which uses the principle of conducting polymer actuators, is a viable and interesting alternative to conventional polymers used in controlled drug delivery. Such systems works on the same principle of expansion and contraction and are based on bilayer, trilayer or hydrogel composites of conducting polymers. Polypyrrole actuators that have been developed as possible controlled drug release systems include a bilayer of PPy (electropolymerized on a gold electrode) and polydimethylsiloxane (Tsai HA and Madou M, 2007). Another bilayer, which was developed by Xu et al, was made in the shape of flaps hinged on one side to a valve consisting of evaporated gold and electrochemically deposited PPy (Xu H et al., 2006).

1.2 Rationale and motivation

The main purpose of controlled drug delivery is the elimination of potential under- and overdosing, while achieving more effective therapeutic methods. Polymer controlled drug release systems are reproducible, but they are unable to respond to varying therapeutic needs of a patients since the drugs are released at a pre-determined rate. Drug delivery technology can be substantially improved by designing 'smart' polymers or devices that fulfills the patient's therapeutic requirements by delivering a certain amount of drug in response to a biological stimulus (Low LM et al., 2000). Controlled release systems, which uses the principle of conducting polymer actuators is a viable and interesting alternative.

Although tremendous technological progress has been made since the days of the wooden leg, contemporary prosthetic limbs cannot perform as well as their biological counterparts (Herr H et al., 2003). People suffering from leg disabilities still experience balance difficulties and thus the need to develop muscle- like materials is of critical importance. Conjugated conducting polymers are feasible as actuators; since they possess the characteristics named above and they are capable to imitate the operation of natural muscles.

The actuating mechanism of conducting polymers is governed by the movement of counterions into and out of the polymer backbone. Accommodation of these counterions and their associated solvated species is favoured by weak polymer interchain intercalations (Baughmann RH, 1996). 'Classical' conducting polymer

actuators, such as polypyrrole and polyaniline, has limited maximum strain by the inability of the polymer backbone to significantly change length to accommodate further ions. Thus, conducting polymer backbones with larger changes in their length, in response to electrically induced changes in oxidation state should be designed. These include molecules that can undergo volume changes due to the stacking of redox units and “accordion- like” structures that have a molecular structure that can be extended and tightly folded (Anquetil PA et al., 2002). Such “accordion- like” structures have been prepared vis. a calix-4-arene hinged quaterthiopene polymer (Anquetil PA et al., 2002) and a poly calix-4-arene with terminal N-substituted pyrrole units (Chen Z et al., 1995).

1.3 Objectives

The focus of this study is to synthesize a novel hinged polymer actuator. The linking molecule (hinge) is phenazine with interconnected dipyrrole units. To achieve this, the following must be met:

- Synthesis of phenazine-2, 3- diimino (pyrrol-2-yl) by the condensation reaction of 2,3-diaminophenazine and pyrrole-2- carboxaldehyde and substantiating the formation of the product by FTIR, NMR and SEM.
- Electrochemically polymerize the phenazine-2, 3- diimino (pyrrol-2-yl) monomer in the presence of 1,2- naphthaquinone 4- sulfonic acid dopant (NQSA).
- Investigate the electrochemical parameters by Cyclic Voltammetry and Osteryoung Square Wave Voltammetry.
- Assess the change in film thickness of poly (phenazine -2,3- diimino (pyrrol-2-yl)) in different solvents at the reduction potential using Electrochemical Impedance Spectroscopy and comparing it to Polypyrrole doped NQSA.

1.4 Layout of thesis

This thesis consists of 5 chapters, which is layout as follows:

Chapter 1 *Introduction*

Chapter 1 gives an introduction to actuators and conducting polymers as actuating materials. The rationale and motivations of this project are also given, as well as the objectives that must be met.

Chapter 2 *Literature Review and Background*

Chapter 2 introduces the history, electrochemistry and actuating mechanism of conducting polymers. This is followed by an in depth description of the electrochemical and actuating properties of polypyrrole. Other polymer actuators are also discussed and applications, i.e. artificial muscle and controlled drug release systems, of conducting polymers are given. The chapter is concluded by literature work on electrochemical impedance spectroscopy, and its utilization for measuring film thickness.

Chapter 3 *Materials and Methods*

In Chapter 3 the materials used and methods implemented are discussed. This includes the synthesis of phenazine-2,3-diimino(pyrrol-2-yl), its electropolymerization, characterization by Cyclic Voltammetry, Osteryoung Square Wave Voltammetry, Scanning Electron Microscopy and Electrochemical Impedance Spectroscopy.

Chapter 4 *Results and Discussion*

In Chapter 4 all the results obtained are given and discussed in detail. FTIR, NMR and SEM characterize the formation of the desired Schiff base product PDP. CV gives information about the redox activity of the polymer, i.e. reversibility, rate constant, diffusion coefficient and the number of electrons involved in the redox processes. OSWV provides the formal potential, which was used in EIS to assess the film thickness of PPDP in the different solvents.

Chapter 5 *Conclusion and Future Work*

The study is concluded with a concise discussion of the most significant points relevant to the applicability of the synthesized polymer as an actuator material. Recommendations made, the relevance, implications and future work are discussed.

1.5 References

Anquetil, Patrick A.; Yu, Hsiao-hua; Madden, John David; Madden, Peter Geoffrey; Swager, Timothy M.; Hunter, Ian Warwick. **Thiophene -based conducting polymer molecular actuators.** Proceedings of SPIE-The International Society for Optical Engineering (2002), 4695(Electroactive Polymer Actuators and Devices (EAPAD)), 424-434.

Ballardini, Roberto; Balzani, Vincenzo; Credi, Alberto; Gandolfi, Maria Teresa; Venturi, Margherita. **Molecular-level artificial machines based on photoinduced electron-transfer processes.** Structure and Bonding (Berlin, Germany) (2001), 99 163-188.

Careem, M. A.; Velmurugu, Y.; Skaarup, S.; West, K. **A voltammetry study on the diffusion of counter ions in polypyrrole films.** Journal of Power Sources (2006), 159(1), 210-214.

Chen, Zheng; Gale, Philip A.; Beer, Paul D. **Synthesis and electrochemical polymerization of calix[4]arenes containing N-substituted pyrrole moieties.** Journal of Electroanalytical Chemistry (1995), 393(1-2), 113-17.

Han, Gaoyi; Shi, Gaoquan. **Electrochemical actuator based on single-layer polypyrrole film.** Sensors and Actuators, B: Chemical (2006), B113(1), 259-264.

Madden, John D. **Actuator selection for variable camber foils.** Proceedings of SPIE-The International Society for Optical Engineering (2004), 5385(Electroactive Polymer Actuators and Devices (EAPAD)), 442-448.

Otero, T. F.. **Conducting polymers as biomimetic materials.** Boletin de la Sociedad Espanola de Ceramica y Vidrio (1997), 36(2-3), 230-237.

Hara, Susumu; Zama, Tetsuji; Takashima, Wataru; Kaneto, Keiichi. **Artificial muscles based on polypyrrole actuators with large strain and stress induced electrically.** Polymer Journal (Tokyo, Japan) (2004), 36(2), 151-161.

Pei, Qibing; Inganaes, Olle. **Conjugated polymers as smart materials, gas sensors and actuators using bending beams.** Synthetic Metals (1993), 57(1), 3730-5.

Skaarup, Steen; Bay, Lasse; West, Keld. **Polypyrrole actuators working at 2-30Hz.** Synthetic Metals (2007), 157(6-7), 323-326.

Tsai, Han-Kuan A.; Madou, Marc. **Microfabrication of bilayer polymer actuator valves for controlled drug delivery.** JALA (2007), 12(5), 291-295.

Vidal, Frederic; Plesse, Cedric; Palaprat, Guillaume; Kheddar, Abderrahmane; Citerin, Johan; Teyssie, Dominique; Chevrot, Claude. **Conducting IPN actuators: From polymer chemistry to actuator with linear actuation.** Synthetic Metals (2006), 156(21-24), 1299-1304.

Smela, Elisabeth; Inganaes, Olle; Pei, Qibing; Lundstroem, Ingemar. **Electrochemical muscles: micromachining fingers and corkscrews.** Advanced Materials (Weinheim, Germany) (1993), 5(9), 630-2.

Vidanapathirana, K. P.; Careem, M. A.; Skaarup, S.; West, K. **Force exerted by polypyrrole/dodecylbenzenesulphonate artificial muscles.** Solid State Ionics: Trends in the New Millennium, Proceedings of the Asian Conference, 8th, Langkawi, Malaysia, Dec. 15-19, 2002 (2002), 831-838.

Xu, Han; Wang, Chong; Wang, Chunlei; Zoval, Jim; Madou, Marc. **Polymer actuator valves toward controlled drug delivery application.** Biosensors & Bioelectronics (2006), 21(11), 2094-2099.

LITERATURE REVIEW AND BACKGROUND

2.1 Conducting polymers

In 1977 Shirakawa, MacDiarmid and Heeger discovered the electrical conductivity of certain doped polymers, for which they were awarded the Nobel Prize in Chemistry in 2000. Prior to their discovery, polymers were considered to be insulators, but they showed that the electrical conductivity of polyacetylenes on exposure to halogen vapours increased significantly (Shirakawa H et al., 1977). From this discovery the synthesis of conducting polypyrrole (Kanazawa KK et al., 1979), polyaniline and polythiophene (Diaz AF et al., 1980), via the then new method of electrochemical polymerization, followed.

Conducting polymers are compounds whose chemical structure enables them to conduct electrons without possessing free electrons. They are conducting due to the overlap of π- molecular orbitals via a high degree of π- bond conjugation (Audebert P and Miomandre F, 2007).

Polymers are insulating materials in their neutral state. When a π- electron is removed from the polymer backbone, it becomes a radical cation (polaron) that is delocalized over 3-4 monomer units. On removal of a second electron, a dication (bipolaron) is formed. The formation of these bipolarons is energetically more favorable and they are spread over the polymer (Brocks G, 2001; Audebert P and Miomandre F, 2007). Polarons and bipolarons are mobile in an electric field and they are the charge carriers responsible for the electrical conductivity of conjugated polymer chains.

2.1.1 Electrochemistry of conducting polymers

Conjugated conducting polymers consist of a variety of macromolecules, i.e. polyacetylenes, polypyrroles, polythiophenes, polyanilines, etc (Figure 1). These polymers are intrinsically insulating with conductivities ranging between 10^{-10} - 10^{-5} S/cm (in their neutral states) but which can be improved to 10^{2} – 10^{3} S/cm in their conductive states (Otero TF et al., 2001, Inzelt G et al., 2000).

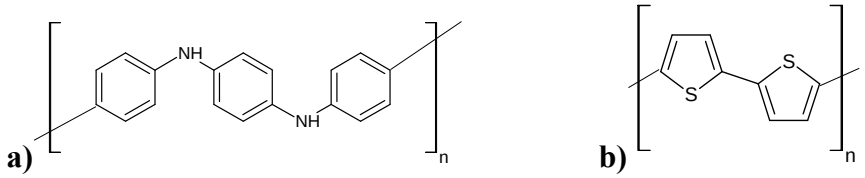

Fig 1: Repeating units of some conductive polymers i.e.,a) polyaniline and b)polythiophene.

Conducting polymers can be synthesized both chemically and electrochemically, the latter being more favorable due to control of film thickness (by controlling the applied potential), its environmentally friendliness (no by-products formed), and it is a one step reaction.

Different electrochemical techniques can be used including potentiostatic (constant-potential), galvanostatic (constant current) and potentiodynamic (potential scanning *i.e.* cyclic voltammetry) methods. Electrochemical polymerization occurs in a three electrode cell, consisting of a working electrode, reference electrode and counter (auxiliary) electrode with the monomer dissolved in appropriate solvent containing the desired doping salt. A potential is applied to the working electrode which initiates

the formation of oligomers and finally polymers at the working electrode surface (Heinze J, 2001; Otero TF et al., 2001).

Conductivity is brought about by a process referred to as doping, i.e. addition of electrons or removal of electrons from the π-conjugated system, forming a charged species called a bipolaron. This results in an improvement of ion movement along the polymer backbone and/or movement of solvent into or out of the modified polymer. Doping can be achieved electrochemically or via photodoping (Audebert P and Miomandre F, 2007; Zotti G, 1995). P-doping refers to the loss of electrons from the valence band resulting in a positively charged molecule. This occurs upon oxidation and results in a flux of anions, into the polymer backbone to neutralize the charge. N-doping occurs during reduction when electrons are added to the valence band, forming a negatively charged moiety, which is neutralized by the flux of cations into the polymer backbone. In addition to changes in conductivity, doping can produce several effects, i.e. changes in colour, volume and porosity (Madden et al., 1999; Brocks G, 2001, Inzelt G et al., 2000). These changes are related to the oxidation state of the polymer and can be controlled electrochemically, i.e. the neutral, reduced and oxidized polymer as well as any intermediary state can be reached by applying the appropriate potential (Heinze J, 1991). Due to the alternating double bond in the conjugated polymer backbone, the charged species formed upon doping are able to move along the carbon chain (delocalization) allowing electron transport giving an electronically conductive material.

In recent years conducting polymers have drawn considerable attention. Among the wide range of conducting organic polymers; polypyrrole, polyaniline and polythiophene are all relatively stable in air and moisture. This makes them the most attractive and they have been extensively studied the past two decades. Many applications have been developed based on their unique properties, i.e. electroactivity, electrical conductivity, environmental stability, physical and chemical properties. Potential applications include polymeric batteries, photovoltaics, electrochromic devices, ion selective membranes, electrical wires, corrosion inhibitors, sensors and electrochemomechanical actuators (Cosnier S et al., 2004).

2.2 Actuation properties of conducting polymers

Conducting polymers are suitable for the production of actuator systems because of their low operation voltages (~ 1V), large stress (higher than that of natural muscles), large strain, the possibility to fabricate actuators in different shapes (fibres, yarns, films, tubes, multilayers), good work density per cycle, high degree of compliance, electrochemopositioning and good lifetime (Lee DY et al., 2008; Otero TF et al., 1998; Baughmann RH, 1996).

Strains are typically 2-10% (Kaneto et al. recently showed that actuator strokes can reach 40%) and rates of actuation tend to be low (<<1%/s), due to the relative slow transport of ions within the polymer and the large degree of doping sometimes used (Kaneto K et al.,2007, Hara S et al., 2005). The rates of actuation can exceed 10%/s by using metal contacts, porous polymers, fast changing methods or thin films and fibres. High quality electrochemically grown films and solution-spun fibres have tensile strengths of 100MPa or higher. Small strains (<0.2%) are achieved at loads of 100 MPa with typical operating stresses ≈1-34 MPa. Work densities approach 100MJ/m^3 and operating voltages are ≈2V, though higher voltages of up to 10V are sometimes used to increase the actuation rate (Madden et al., 2007).

2.3 Polypyrrole (PPy)

Polypyrrole (Fig 2) and its derivatives are the most extensively studied conducting polymers due to the easily oxidizable monomer that is soluble in water and commercially available, the high electrical conductivity, good electrochemical properties, thermal and environmental stability and the high mechanical strength of polypyrrole which is easily generated both chemically and electrochemically (Wang L et al., 2001). Hence, polypyrrole has several advantages, including environmental stability, good redox properties and the ability to give high electrical conductivities (Mabrouk PA, 2005; Truba M et al., 2005). As a result of these intrinsic properties, polypyrrole has been utilized in many applications, including batteries, supercapacitors, electrochemical (bio) sensors, conductive textiles and fabrics, drug delivery systems and mechanical actuators (Sayyah SM et al., 2005; Baba A et al., 2002; Li G et al., 2007). However, its poor mechanical properties (e.g. brittleness) and low processibility minimizes their practical utilization (Migahed MD et al., 2004).

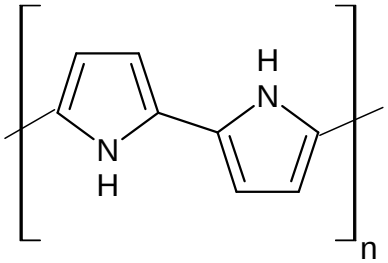

Fig 2: Repeating unit of polypyrrole

2.3.1 Electropolymerization of PPy

Chemical polymerization occurs by the chemical oxidation of pyrrole monomers in a solvent by a suitable catalyst, e.g. $FeCl_3$, other salts of iron (III) and copper (II), and Lewis acids and halogens have been used (Vernitskaya TV and Efimov ON, 1997).

Electrochemical polymerization is achieved by applying a potential to a solution containing monomer, solvent and supporting electrolyte in a three electrode cell. The choice of solvent is of particular importance in electrochemistry since both the solvent and electrolyte should be stable at the oxidation potential of the monomer and it should also provide an ionically conductive medium (Lee CW et al., 2002). Organic solvents like acetonitrile and propylene carbonate have very large potential windows and high relative permittivities, which allows good dissociation of the electrolyte and thus good conductivity. Since pyrrole has a relatively low oxidation potential, electropolymerization can be carried out in aqueous solvents, which is not possible for thiophene and benzene. As a result of the initial oxidation, the radical cation of the monomer is formed and reacts with other monomers present in solution to form oligomeric products and then the polymer (Zhou M et al., 2002; Warren MR and Madden JD, 2006). The extended conjugation in the polymer results in a lowering of the oxidation potential compared to the monomer. Therefore, the synthesis and doping of the polymer are generally done simultaneously. The anion is incorporated into the polymer to ensure the electrical neutrality of the film and, at the end of the reaction, a polymeric film of controllable thickness is formed at the working

electrode. The working electrode can be made of a variety of materials including platinum, gold, glassy carbon, and tin or indium–tin oxide (ITO) coated glass. The properties of polypyrrole are highly dependent on electropolymerization conditions, i.e. solvent type, pH, dopant, temperature, etc (Mabrouk PA et al., 2005; Li G et al., 2007; Truba M et al., 2005). An understanding of the mechanism of electropolymerization is thus of great importance, which will ultimately lead to improved chemical and electrochemical properties.

2.3.2 Mechanism of electropolymerization

The mechanism most widely used to describe pyrrole polymerization is that of Diaz et al. (Figure 3) (Genies, Bidan and Diaz, 1983; Funt and Diaz, 1991), which was confirmed by theoretical studies based on the correlation between the reactivity and the unpaired electron density of the radical cations by Waltman and Bargon (Waltman and Bargon, 1984; Waltman and Bargon, 1985).

Both chemical and electrochemical polymerization involves the generation of radical cations by the oxidation of the monomer. According to Diaz et al two radical cations couple and results in the formation of a bond between their α-positions and the formation of the dication, which is neutralised to the dimmer form by the loss of two protons. The dimmer is then oxidised to the radical cation dimmer, which reacts with a monomer radical cation to form the trimer cation, which deprotonates to the neutral trimmer. Propogation continues via the sequence of steps: oxidation, coupling and

deprotonation until the insoluble polymer film is produced (Sabouraud G et al., 2000; Genies GM et al, 1983; Funt and Diaz, 1991).

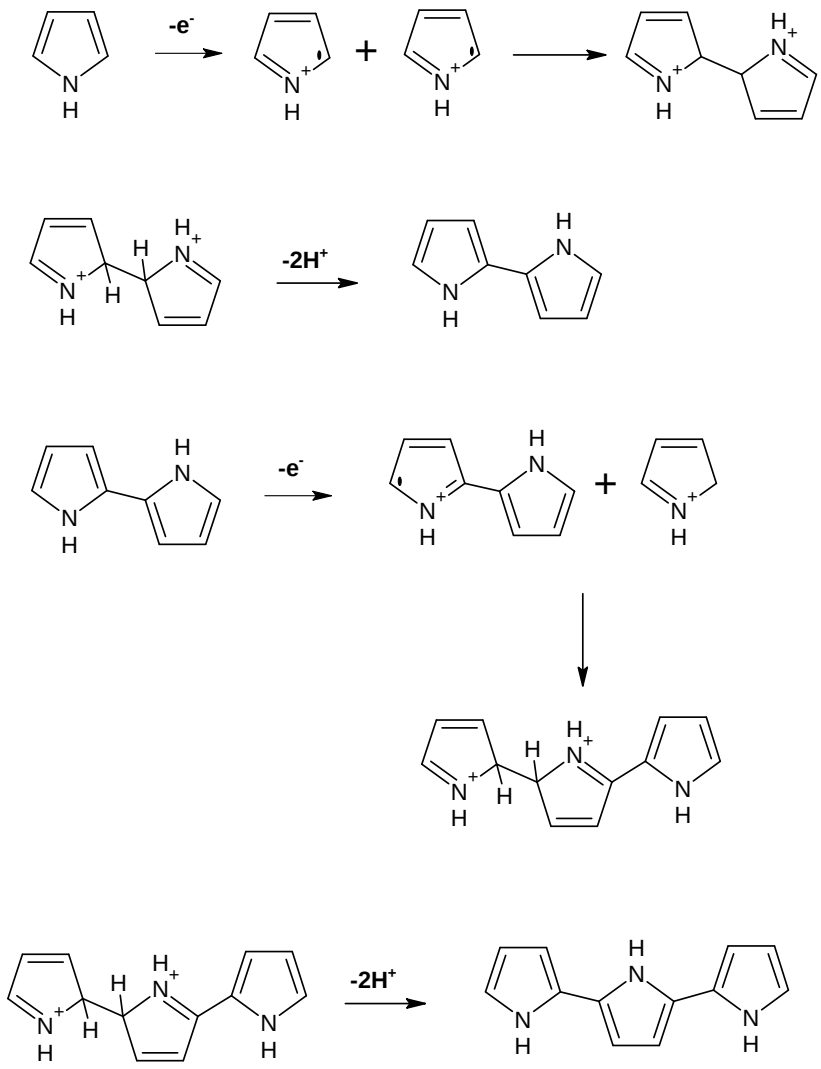

Fig 3: Mechanism of Pyrrole polymerization according to the Diaz mechanism.

2.3.3 Actuation mechanism of Polypyrrole

Oxidation of a p-doped polymer can maintain electroneutrality via two methods. The polymer can be doped with a mobile small anion in an electrolyte solution with mobile cations and anions. The insertion and removal of anions during the redox reaction will maintain the neutrality along the polymer backbone (Burgmayer P and Murray RW, 1982). Eq. (1) shows the insertion of ClO_4^- anions upon oxidation (Otero TF, 1997).

$$PPy^+ (ClO_4^-) + e^- \underset{\text{Oxidation}}{\overset{\text{Reduction}}{\rightleftharpoons}} PPy^0 + ClO_{4\,aq}^- \quad \ldots\ldots\ldots (1)$$

If the polymer is doped with a non-mobile and big anion such as dodecylbenzenesulfonate (DBS^-) in an electrolyte containing mobile and small cations (X^+), the latter will be inserted and removed during the redox reaction to maintain electroneutrality. In eq. (2) X^+ cations are inserted in a DBS^- doped polypyrrole (Pei Q and Inganaes O, 1993).

$$PPy^+ (DBS^-) + X^+aq \underset{\text{Oxidation}}{\overset{\text{Reduction}}{\rightleftharpoons}} PPy^0 (DBS^-X^+) \quad \ldots\ldots\ldots (2)$$

Otero et al. developed a model that explains the volume changes in conducting polymers taking into account the electrostatic repulsion between charged polymeric chains (Otero TF et al., 1997). According to this model, when a conducting polymer (PPy) is oxidized, positive charges are generated along the polymeric chains. These positive charges produce electrostatic repulsions between the chains, resulting in conformational changes in the polymeric structure and generation of free space. These free spaces facilitate the insertion of solvated counter-anions, maintaining the electroneutrality of the polymer resulting in an increase in its volume. Thus upon oxidation of a conducting polymer doped with a small mobile anion, its volume increases proportionally to the formed positive charges (expansion). When the conducting polymer is reduced the positive charges are neutralized by the addition of electrons from the potentiostat. The electrostatic repulsions are eliminated, diminishing the free space and counter ions move out of the chain to maintain the electroneutrality in the polymer. Thus, upon reduction, its volume decreases (contraction) due to the de-insertion of the counter ions from its structure into the electrolyte (refer to Figure 4 and 5). Otero et al. supported their model with density measurements in polypyrrole films. In the oxidized state the film mass is 50% higher than in the reduced state due to the incorporation of counter ions (Otero TF et al., 1997).

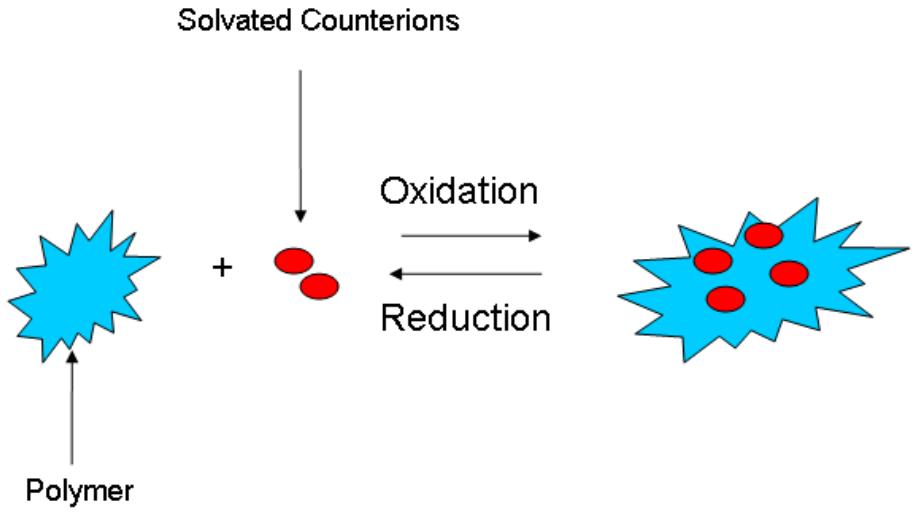

Fig 4: Illustration showing the volume changes that occur in a conducting polymer during a redox reaction. In this example, during oxidation the polymer undergoes expansion due to the insertion of solvated counterions to neutralize the positive charges formed. During reduction the positive charges are neutralized by the addition of electrons from the potentiostat. The counterions migrate out of the polymer to maintain electroneutrality.

Otero et al., was the first to design an actuator of this type, i.e. a bilayer of PPy(ClO_4^-) with an adherent inactive and flexible polymer, named an electro-chemo-mechanical device or artificial muscle (Otero TF, 1997). Its denomination arises from the fact that an electrochemical reaction on the polymer produces conformational changes on its structure, which is finally transformed into motion. This bilayer showed motions up to 180^o in aqueous solution of $LiClO_4$. The behavior of the bilayer was studied in solutions of acetonitrile/ $LiClO_4$, propylene carbonate/ $LiClO_4$ and water/ $LiClO_4$. It was observed that water as solvent gave the greatest molecular interaction between the solvent and the polymer (Otero TF, 1997). This can be rationalized by the penetration of counterions accompanied by water during the oxidation process, causing greater swelling of the PPy in aqueous media (Madden et al., 2006). Thus the

polymeric swelling occurred easier and in greater extent when aqueous solutions were used.

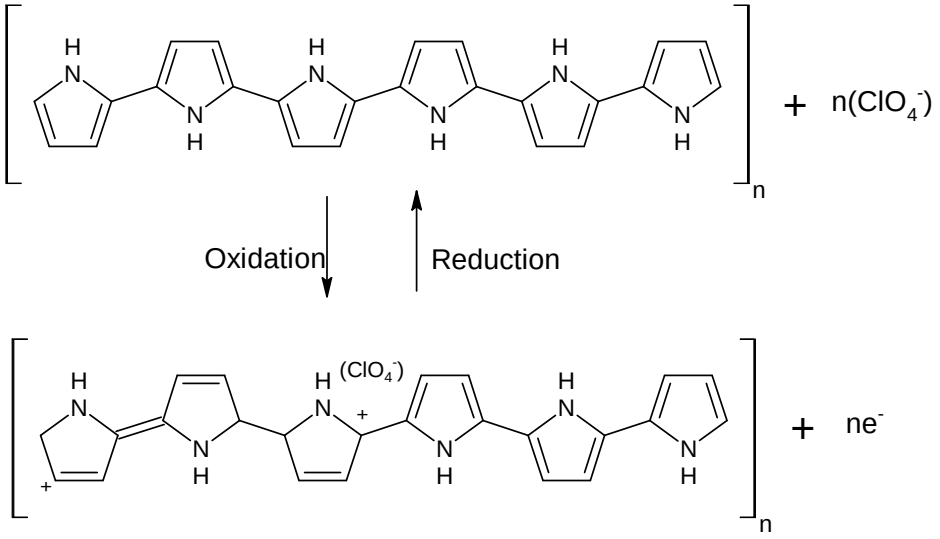

Fig 5: Schematic representation of the redox reaction of PPy in the presence of ClO_4^- anions. The electroneutrality during oxidation is maintained by the incorporation of the ClO_4^- anions inside the polymer chain. During reduction the positive charges are neutralized and the anions move outside the polymer to maintain neutrality.

When the conductive polymer is doped with a large, immobile anion (like DBS^-), the mechanism of actuation differs from that described by Otero et al. Figure 6 gives a schematic representation of PPy doped with DBS^- (as demonstrated in eq 2).

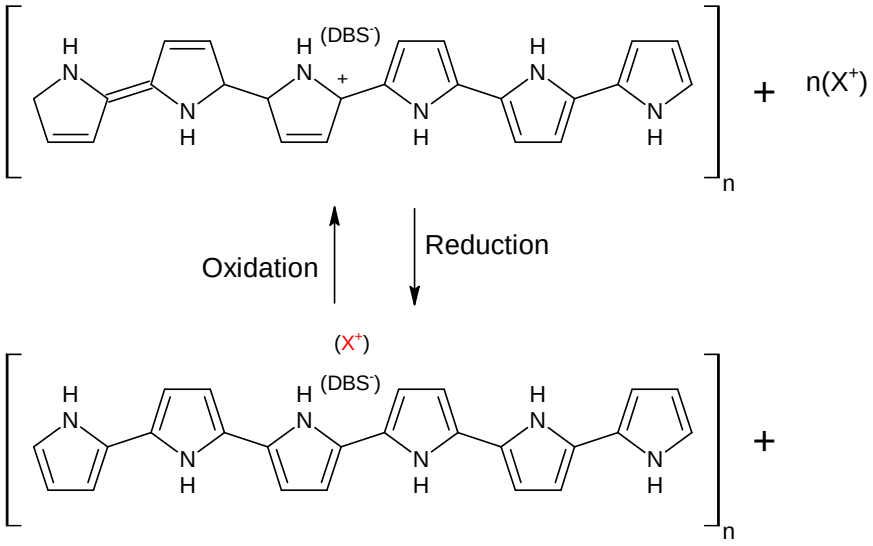

Fig 6: Schematic representation of the redox reaction of PPy in the presence of DBS^- anions. The electroneutrality during reduction is maintained by the incorporation of the X^+ cations inside the polymer chain. During oxidation the negative charges are neutralized and the cations move outside the polymer to maintain neutrality.

Upon reduction of the PPy/DBS^- the overall negative charge that is generated across the polymer chain causes repulsion between these chains, leading to the generation of free spaces. The polymer is neutralized by the movement of small mobile cations, accompanied by solvent molecules into the chain, resulting in an increase in its volume. Thus expansion occurs upon reduction. When electrons are removed, as occurs during oxidation, the electrostatic repulsions are neutralized and the cations move out of the chain to maintain electroneutrality. This results in a decrease in the volume or contraction.

Research has shown that the ionic flux in conducting polymers depends on the size of the cations and anions, thickness of the polymer film, applied voltage and the time

scale. Applying a potential causes a change in the oxidation state of the polymer and the inserted ions and solvent occupy the free space generated. When these are inserted, the polymer expands and vice versa upon removal of the ions. Thus, the volume change is dependent on the applied voltage, the electrolyte and the dopant. Volume changes in conducting polymers are thus due to the movements of ions in and out of the polymer backbone during an electrochemical reaction (Madden JD et al., 2001).

2.3.4 Electrochemical actuators based on Polypyrrole (PPy)

Due to the different inherent properties of polypyrrole, it is favorable as an actuator device. Polypyrrole actuator materials possess the properties listed below (K J. Kim and S Tadokoro, 2007).

- low-voltage (1–3 V),
- moderate to large strain (2–35%),
- relatively high stress (up to 34 MPa),
- Moderate to low strain rates (11%/s),
- and frequency response of several hertz.

A polypyrrole film synthesized electrochemically from a methyl benzoate solution of tetra-n- butylammonium tetrafluoroborate ($TBABF_4$) exhibited 12.4% strain and 22 MPa stress (Hara S et al., 2004). Faster responses (>1 kHz) are predicted in nanostructured materials (K J. Kim and S Tadokoro, 2007). Skaarup et al.

synthesized a PPy/BF_4 film with frequencies of 2-30Hz by utilizing the change in stiffness compared to the change of length as the polymer is redox cycled (Skaarup et al., 2007).

Different polypyrrole actuator devices have been electrochemically synthesized the past two decades and can be constructed in linear or bending (bilayer) formations.

2.3.4.1 Linear PPy actuators

The simplest actuators are linear actuators. These materials are formed by a doped or undoped electrochemically synthesized conducting polymer film. The actuation mechanism is based on the longitudinal expansion and contraction of the polymer due to the insertion and de- insertion of ions. A PPy film doped with benzenesulfonate anions (BS^-) was characterized electrochemically by Della Santa (Della Santa A et al., 1997). This polymer film was obtained under the trade name Lutamer and underwent swelling that produced a linear dimension change by 2%. The lifetime of the actuator also decreased significantly at charges higher than 0.3C. Other linear polypyrrole actuators include PPy/DBS (Careem et al., 2006), PPy/ tetrafluoroborate (Hara et al., 2004) and PPy/hexafluorophosphate (Madden JD et al., 2002), all obeying the mechanism as shown in eq. 2. Hutchison et al. developed a linear PPy/ toluenesulfonic acid, which was tested directly or sputter coated with platinum before mechanical analysis (Hutchison et al., 2000). PPy/PF_6 tubes were also grown on top

of a helical Pt wire and successfully evaluated as actuator materials by Lu et al. (Lu et al., 2002).

2.3.4.2 PPy bilayer actuators

A bilayer is formed by an electrochemically synthesized conducting polymer layer and a flexible, insulating layer, which bends under electric power. As mentioned previously, the first conductive polymer actuator was made combining a PPy film with a non- volume changing layer into a bilayer structure, i.e. PPy doped with ClO_4^-/ adherent tape (Otero et al., 1997) (Figure 7). Upon oxidation, the PPy film undergoes an increase in its volume as described earlier for a film that has a mobile small dopant anion. This results in the adherent tape shrinking, causing the polymer to bend into the adherent tape. Upon reduction the opposite is noted due to a decrease in the volume of the polymer film.

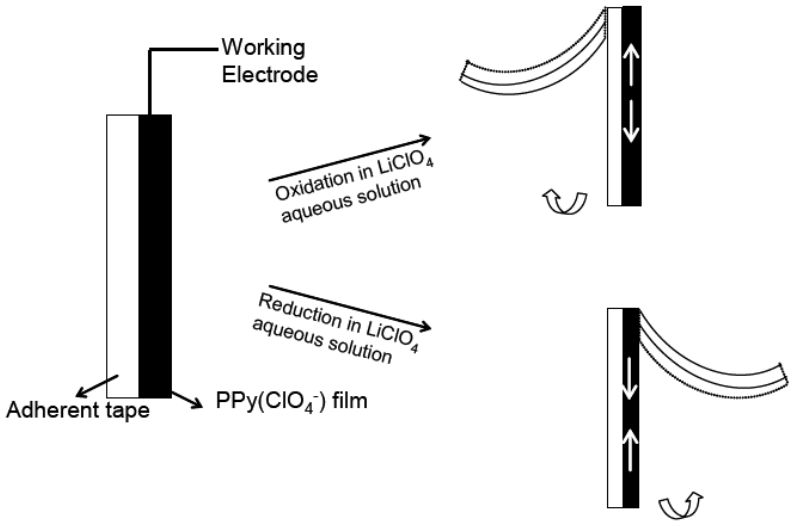

Fig 7: Schematic representation of a bilayer device formed by PPy (ClO_4^-) film and adherent tape (Adapted from Cortes MT and Moreno JC, 2003).

2.3.4.3 PPy triple layer actuators

The bilayer was improved by a triple layer design, i.e. conducting polymer/ intermediate layer/ conducting polymer. It is formed by electrochemically depositing a polymer film, followed by drop coating or electrochemical deposition of an intermediate layer and finally electrochemically depositing another layer of polymer over the two layers. To work in air, this triple layer should have an intermediate layer that allows ion motion without electric contact.

Figure 8 illustrates the actuation mechanism of a triple layer PPy actuator. In the middle is an amorphous, porous polyvinylidene fluoride (PVDF) layer that serves as a backing material and storage tank for the electrolyte. On both sides of the PVDF is PPy layers. On application of a voltage, the anions will be driven into and oxidize the PPy layer and cause it to expand, while the other PPy layer on the cathode side will be reduced and contract. The simultaneous contraction and expansion leads to bending of the actuator (Fang et al., 2008).

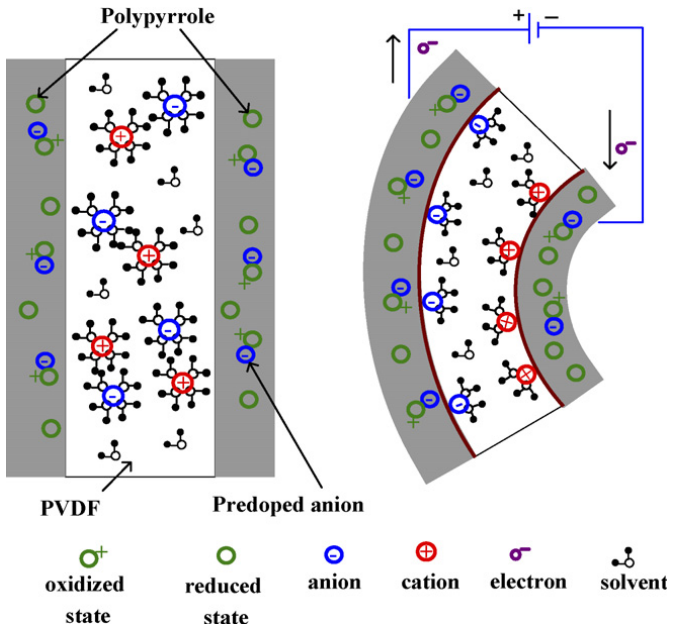

Fig 8: Illustration of the actuation mechanism of trilayer polypyrrole actuator (Adapted from Fang et al., 2008)

Another tri-layer conducting polymer composite film consisting of polypyrrole/polythiophene/polypyrrole was electrochemically synthesized by the successive oxidation of polypyrrole in aqueous solutions and thiophene in boron trifluoride diethyl ether (BFEE) solution, respectively (Han G and Shi G, 2004). One of the polypyrrole layers was doped with a small perchlorate anion, while the other was doped with a large anion, dodecylbenzenesulfonate. The tri-layer film underwent conformational changes during redox reactions of the polypyrrole (refer to eq.1 and 2), while the polythiophene layer provided a high strength polymeric support and acted as current collector for the actuator. The loading capacity of the tri-layer film was much higher than that of the bi-ionic film, mainly due to the polythiophene layer providing a strong mechanical support for the actuator and also enhanced its

loading capacity. Furthermore, at a given driving condition, the movement rate of the tri-layer composite film was faster than that of the bi-ionic polypyrrole film. The simple structure and easy electrosynthesis process of the tri-layer composite conducting polymer film may be very promising for fabrication of the actuator with excellent high strength and loading capacity.

Another design built to obtain actuators that work in air is the encapsulated device. This system uses a triple layer that is covered by a jacket containing the electrolyte. It is generally limited by an increase of stiffness that decreases the performance capacity.

The promising properties of polypyrrole actuators has led to a number of applications being developed and prototypes being built including a variable camber foil, shape changing stents and an active Braille screen (Spinks GM et al., 2003; Madden JD et al., 2004; K J. Kim and S Tadokoro,2007).

2.4 Other polymer- actuators

2.4.1 Polyaniline (PANI)

Polyaniline has many similarities to polypyrrole. However it has other attributes that differ significantly from that of the other conducting polymers. It is one of the most studied conducting polymers due to its high processability, environmental stability, electroactivity and pH switching properties and this has made it one of the most promising organic conducting polymers for commercialization (Han MG et al., 2002; Zhang Z et al., 2005). The main drawback of this polymer is its poor processibility in melt and solution forms due to its stiff backbone and it insolubility in most organic and inorganic solvents (undoped PANI is soluble only in strong acids and in N-methylpyrollidone) (Michira I et al., 2007). PANI follows the same actuating mechanism as PPy (Okabayashi K et al., 1987; Smela E et al., 2005; Smela E and Mattes BR, 2005).

Smela and Mattes synthesized PANI doped with 2-acrylamido-2-methyl-propane-1-sulfonic acid (AMPS) and studied its actuation properties in aqueous methanesulfonic acid as well as a polyaniline (PANI)/Au bending bilayer. In the same year Smela et al prepared a PANI- AMPS and investigated its properties in HCl (Smela E et al., 2005).

Layered composites of polyaniline (PANI), single-walled carbon nanotubes (CNTs) and polypyrrole (PPy) were produced by coating PANI or PANI/CNT on a PPy hollow fibre containing a platinum (Pt) helix. The actuation behaviour of PANI/PPy and PANI/CNT/PPy composites was compared with that of neat PPy (Spinks GM et

al., 2006). The carbon- nanotubes reinforced polyaniline fibers possess improved breaking strength and higher operating stress levels than neat polyaniline (Spinks GM et al., 2006). These fibers have tensile strengths of 255 MPa and operate I stress levels in excess of 100MPa, which is 3 times higher than previously reported for conducting polymer actuators.

2.4.2 Polythiophene (PT)

Polythiophene is another conjugated conducting polymer. Polythiophene (PT) and its derivatives are not as well studied as the above polymers as actuator devices. The main advantages of PT include high conductivity (10^2 S/cm), stability in air and moisture, structural versatility and a wide electrochemical potential window. PT follows the same actuating mechanism as PPy and PANI.

Different actuators based on PT have been synthesized from monomers for particular actuation purposes (Fuchiwaki M et al., 2002; Tourillon G and Garnier F, 1984; Wu Y et al., 2007). One polythiophene derivative that has been developed recently is Poly (calix [4]arene bis-bithiophene). This molecule uses a deformable hinge molecule, calix[4]arene, that interconnects rigid rods of redox active quaterthiophene units (Anquetil PA et al., 2002, Zanuy D et al., 2006). Due to the redox active sites that are closer in proximity, there is an overlap of π-orbitals. Expansion occurs upon oxidation of the material, due to the electrostatical repulsion of positive charges formed along the quaterthiophene blocks. This is followed by the deprotonation of the oxygens of the calixarene forming the quinoid form. Electrostatic repulsion of

these deprotonated oxygens causes the material to contract into a folded molecular structure (Figure 9) (Zanuy D et al., 2006).

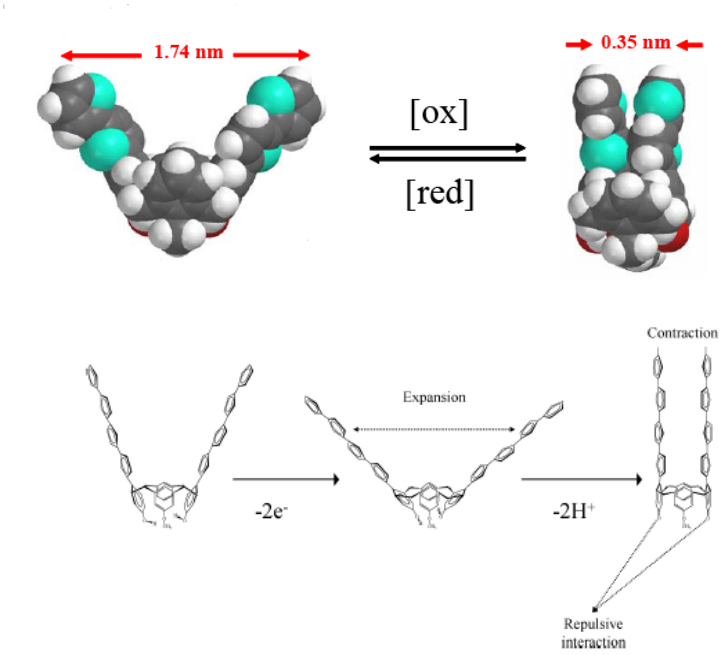

Fig 9: Space fill model and schematic representation of the actuation mechanism of a molecular actuator based on PT chains interconnected with a highly versatile calixarene molecule (Adapted from Anquetil PA et al., 2002; Zanuy D et al., 2006).

A similar hinged polymer was prepared by Chen et al. They prepared a calix-4-arene with terminal N- substituted pyrrole moieties (Chen Z et al., 1995). The polymer was formed by polymerization of the pyrrole units, resulting in a block polymer. This phenomenon of π-π stacking results in the generation of a larger free space compared to that of classic linear polymers. This greater free space can thus accommodate more ions and cause a greater degree of volume change.

2.4.3 Ionic polymer metal composites (IPMC's)

IPMC's are electroactive polymers that are obtained from an ionic polymer, capable of ion exchange, which is then chemically treated with an ionic salt solution of a metal, followed by chemically reduction to yield the IPMC (Sun L and Zhao Y, 2008). They have been extensively studied in the application of smart structures, bio-medical devices and biomimetic robots (Oh IK at al, 2006) due to their high reliability and flexibility. Typical ion exchange polymers employed include perfluorinated alkenes (with terminal ionic groups) and styrene/ divinylbenzene based polymers (substitution on the phenyl rings with ionic groups) where the nitrogen atom is fixed to the ionic group (Shahinpoor M and Kim KL, 2001). As an electrical current is applied to the electrode surfaces, the metallic cations and water molecules move to the anode. Therefore, one side will swell and the other side will shrink, resulting in the mechanical bending of the cantilevered actuators as shown in Figure 10 (Jeon JH et al., 2007).

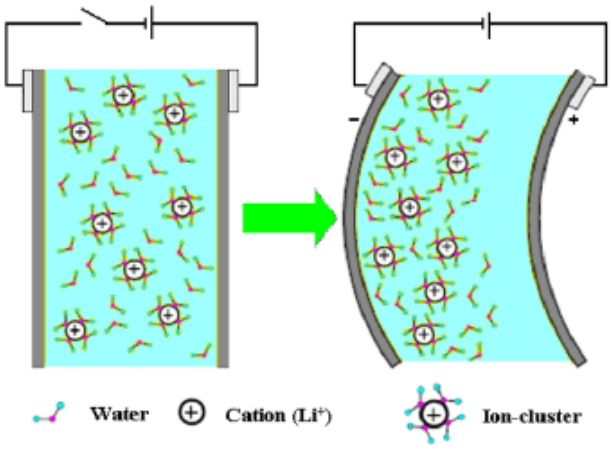

Fig 10: Schematic representation of the actuation principle in IPMC's (Adapted from Jeon JH et al., 2007).

Recently an introduction of perfluorocarboxylate gold composite with two types of cations, tetra-n-butylammonium and lithium, instead of sodium, made the most significant improvement of the material's electroactivity. Under less than 3 volts, such IPMC materials were shown to induce bending beyond a complete loop. The bending characteristic of IPMC offered an attractive actuation capability for a dust wiper in planetary applications (Bar- Cohen Y et al., 2002).

2.4.4 Electroactive polymer gels

An electroactive polymer gel can be described as an intermediate between a liquid and a solid, consisting of a polymer network and interstitial fluid (Figure 11) (Popovic S, 2001).

The properties of the gel are due to the interaction between the polymer and the liquid. These polymer gels can swell, shrink, bend, and curl upon application of a stimulus. These stimuli include changes in pH, solvent, temperature and electric stimulation (Yao L and Krause S, 2002; Yoshioko Y and Calvert P, 2002, Yamauchi T et al., 2005). The key feature of the gels as actuators is their ability to drastically change volume. This expansion and contraction mechanism is due to the diffusion of water or solvent in and out of the matrix. Factors that influence the rate and quantity of volume change include: the gels' rubber elasticity, polymer- polymer affinity and the hydrogen ion pressure (Yao L and Krause S, 2002; Yoshioko Y and Calvert P, 2002). The most studied electroactive polymer gels are based on polyacrylic acid and this work has been reviewed recently. The gel swells strongly by taking up water in

response to a change from pH 3 to pH 5, which ionizes the polymer. In its ionized form, the polymer shrinks as the solvent is changed from water to acetone or another water-miscible solvent (Yoshioko Y and Calvert P. 2001).

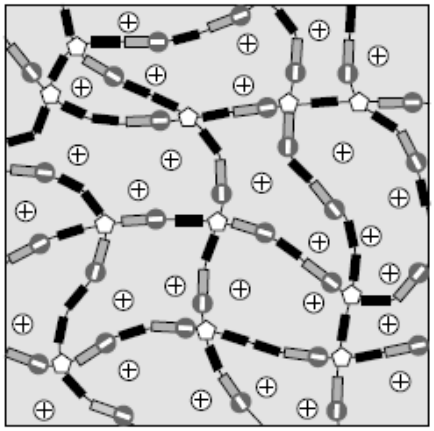

	Chemical Composition	*Example*
▬	backbone monomer	acrylamide
▬⊖	electrolyte comonomer	$acrylate^-$
⊕	mobile counterion	Na^+
⬠	crosslinking comonomer	bisacrylamide
□	solvent	H_2O

Fig 11: Schematic representation of a polymer network with fixed anionic groups and mobile cations (Adapted from Wallmersperger T et al., 2002).

2.5 Artificial muscle

Skeletal muscles are devices that convert chemical energy into mechanical energy and heat at a constant temperature. The muscular motion is initiated with an electric pulse that is generated in the brain and transported into the nervous system, resulting in an increase in the concentration of Ca^{2+} ions around the muscular fibres, which causes conformational changes in the troponin-tropomyosin complex and consequently results in muscular contraction (Figure 2). Thus a natural muscle is an electro-chemo-mechanical device, in which an electric signal initiates a chemical reaction that leads to the production of mechanical energy (Figure 12) (Cortes MT and Moreno JC, 2003).

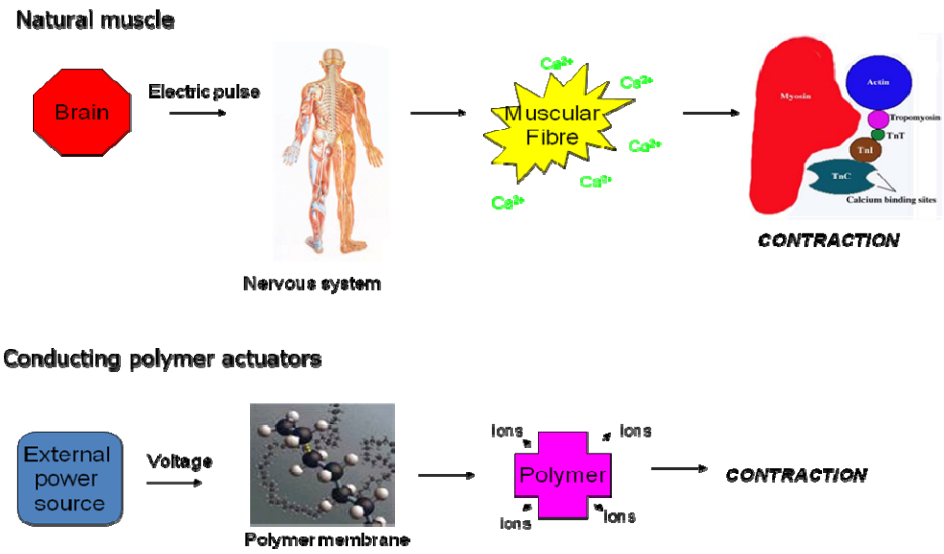

Fig 12: Schematic representation of the action of natural muscle compared to conductive polymer actuators

Conducting polymer actuators exhibit similarities in operation and structure to natural muscles (Figure 12). These polymers possess reversibility in their reduction and oxidation processes (Meijer K et al., 2001). This allows the insertion and de-insertion of ions into their backbone, causing conformational changes that leads to volume changes and ultimately results in the generation of motion, i.e. contraction and expansion (Mirfakhrai Y et al., 2007) that is similar to that of natural muscle. Both systems are initiated by an electric pulse which causes chemical reactions and lead to the generation of movement. In both systems there is a direct conversion of chemical energy to mechanical energy and conducting polymers, like natural muscles, exhibit a controlled mechanical motion (He X, 1994). The polymers work in an aqueous media of ionized salts at a constant temperature and these conducting polymers have a macromolecular structure that is similar to the protein structure of natural muscles.

There are differences between these two systems (Otero TF, 1997).

Natural muscles are driven by chemical energy which is produced by the combustion of glucose at a constant temperature. In conducting polymers the driving power is the electric charge which is consumed during the redox reaction. The reversibility of muscular motion is achieved by the operation of a second muscle (Cortes MT and Moreno JC, 2003), while both contraction and expansion in conducting polymers are due to the insertion and removal of ions to and from its structure.

2.6 Controlled drug delivery

Controlled drug delivery is the process of releasing a drug or active ingredient from a material in a pre-designed manner, which may be constant over a time period. Release may be cyclic over a time period, or may be triggered by the environment or other external events (Robinson JR and Rubenstein A, 1987).

Traditional tablets or injections, follows a drug profile in which the level in the blood rises after each administration of the drug, and then decreases until the next administration. In controlled- drug delivery, the drug level in the blood remains constant, ranging from a day to several years. Thus the main purpose of drug delivery is the elimination of potential under- and overdosing by maintaining the concentration of active ingredient constant in the blood stream over a period of time. Other advantages of using controlled drug delivery systems includes the maintaining drug levels within the desired range, fewer administrations, optimal use of the drug of interest and increased patient compliance(Mikos AG, 1994). Controlled drug delivery is crucial in situations requiring slow release of water- soluble drugs, fast release of low- solubility drugs, drug delivery using nanoparticulate systems, delivery of two or more agents with the same formulation, and systems whose carriers can dissolve or degrade and easily be eliminated (Cleary GW, 1993).

Polymers that have been used in these systems include polyurethanes, polysiloxanes, polyethylene, PVC, PMMA, polylactides, polyglycolides and polyanhydrides. These polymers use diffusion, degradation or swelling followed by diffusion as mechanisms

for drug release. The stimulus responsible for the release can be pH, ionic strength, chemical, magnetic or thermal (Heller J, 1985; Kim SW, 1996).

2.6.1 Actuators as controlled drug release materials

Polymer controlled release systems are reproducible, but they are unable to respond to varying therapeutic needs of a patients since the drugs are released at a pre-determined rate. Drug delivery technology can be substantially improved by designing 'smart' polymers or devices that fulfills the patient's therapeutic requirements by delivering a certain amount of drug in response to a biological stimulus (Low LM et al., 2000). Controlled release systems, which uses the principle of conducting polymer actuators is a viable and interesting alternative. Such systems would work on the principle of polymer expansion and contraction on oxidation or reduction. Hydrogels are water swollen three- dimensional networks of hydrophilic homopolymers or co-polymers with cross links formed by covalent or ionic bonds (Peppas NA and Mikos AG, 1986). They are considered to be the most efficient polymers in transforming molecular energy into mechanical energy. Hydrogel- based actuator systems has potential applications in the development of robots with noiseless and life- like movements. Temperature, pH, radiation and electrical field (Lee YM et al., 1996) control the actuating mechanism. Madou and co- workers have recently demonstrated that polymeric actuator systems can act as valves that will electrochemically control the opening of microsized channels (Low LM et al., 2000), and reservoirs (Xu H et al., 2006). Lou et al used a blend of polyaniline and poly (2-hydroxy-ethylmethacrylate)- poly (N- vinylpyrrolidinone) deposited on a gold

electrode (Loe M et al., 2000). At the reduction potential of -0.2V, the polymer blend was in its shrunken state and the grid's holes were open, while at the oxidation potential (+0.3V) the swollen state had the holes almost closed. Lira and Cordoba de Torresi electropolymerized aniline inside the porous structure of polyacrylamide (Lira LM and Cordoba de Torresi SI, 2005). The electroactive network of polyaniline and polyacrylamide retains the swelling capabilities of hydrogels, which allows the use of this material for the electrochemically controlled release of large molecules, such as safranin and pyrocathecol violet (Lira LM et al., 2007), due to the free space inside the blend that allows storing of the molecules. Polypyrrole microvalve actuators that have been developed as possible drug delivery systems include a bilayer of Ppy (electropolymerized on a gold electrode) and polydimethylsiloxane (Tsai HA and Madou M, 2007). Another bilayer was developed by Xu et al, where the bilayer structure was made in the shape of flaps hinged on one side to a valve consisting of evaporated gold and electrochemically deposited PPy (Xu H et al., 2006). The pre- stored drugs are released on bending of the bilayer flaps away from the substrate upon application of potential.

Thus hydrogels, comprising of conducting polymers in their network, shows promise as controlled drug release materials.

2.7 Electrochemical Impedance Spectroscopy

Electrical resistance is defined by Ohm's law as the ability of a circuit to resist the flow of current. However, the real world contains circuit elements that exhibit more complex behavior and thus the concept of resistance is replaced by impedance, Z, which is a measure of a circuit's tendency to resist (or impede) the flow of an alternating electrical current (Barcia OE et al.,2002). The impedance of a system can be calculated using Ohm's law as:

$$Z_{(w)} = \Delta E_{(w)} / \Delta I_{(w)} \quad \text{..... (3)}$$

Electrochemical Impedance Spectroscopy (EIS) is a powerful technique for the characterization of electrochemical systems. EIS has found widespread applications in the field of characterization of materials, i.e. coatings, batteries and fuel cells. It has also been extensively used to investigate mechanisms of electrodeposition, electrodissolution, passivity and corrosion studies. Recently it has gained popularity in the investigation of the diffusion of ions across membranes and in the study of semiconductor interfaces.

The fundamental approach of EIS is the application of a small amplitude sinusoidal excitation signal, i.e. current or voltage, to the system under investigation. The response that is measured is either current, voltage or another signal of interest. Thus by applying an AC potential to an electrochemical cell the current through the cell is measured.

The impedance of a system is a complex quantity with a magnitude and a phase shift which depends on the frequency of the applied signal (Barcia et al., 2002). Therefore by varying the frequency of the applied signal one can get the impedance of the system as a function of frequency. Typically in electrochemistry, a frequency range of 100 kHz – 0.1 Hz is used. To characterize impedance, Z, you must specify its magnitude, |Z|, phase angle, Θ, and the frequency, f (in cycles per second, or Hertz), at which it was measured. These three parameters are often plotted on what is known as a Bode plot (Figure 13). The plot of the real part of impedance against the imaginary part gives a Nyquist Plot (Figure 13). The shape of the resulting curve (or semicircle) is important in making qualitative interpretations of the data. Electrochemical Impedance plots sometime contain several semicircles and often only a portion of the semicircle is seen. Both plotting formats are used because each has its strengths. The advantage of Nyquist representation is that it gives a quick overview of the data and one can make some qualitative interpretations (Penner and Martin, 1989). The disadvantage of the Nyquist representation is that one loses the frequency dimension of the data. One way of overcoming this problem is by labeling the frequencies on the curve.

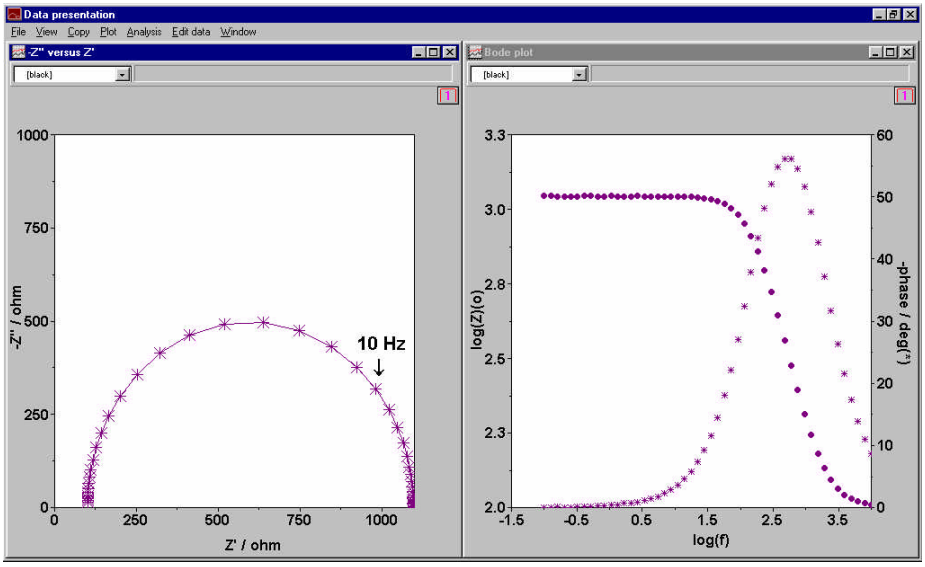

Fig 13: Representation of Nyquist and Bode plots

Electrochemical systems such as coated surfaces or corroding metals often behave like simple electronic circuits. Thus to quantitatively analyze the data from the Nyquist or Bode plot, it has to be fitted to an equivalent circuit where the values of the electrical components are associated with the physical/ chemical properties of the electrochemical system under investigation (Barcia OE et al., 2002). The equivalent circuit model provides a simple way of understanding what may be a complicated electrochemical system. The equivalent circuit is a combination of capacitor(s) and resistor(s).

One commonly used equivalent circuit is the Randles circuit (Figure 14). When this model is applied to a coated electrode surface immersed in an electrolyte, R_s represents the resistance of the electrolyte solution between the reference electrode tip and the surface of the coating. It is also called the uncompensated resistance and is

generally a few ohms if the electrolyte's salt has a low concentration. The capacitor, C_{dl}, represents the coating and can be characterized by the thickness and dielectric constant of the coating material. The resistor R_{ct}/R_p is associated with the resistance of the coating and varies with the thickness and composition of the coating. Coating resistances can be quite high for a good epoxy coating.

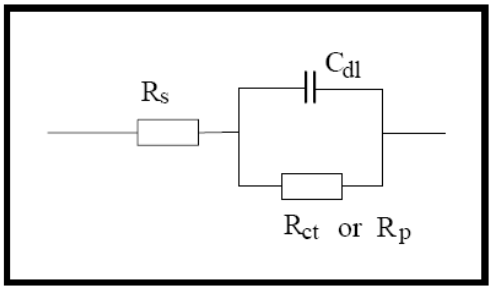

Fig 14: Schematic diagram of the Randle Cell

As mentioned, the capacitance can give quantitative information about the dielectric constant and film thickness of a coated electrode surface. This capacitance from the impedance data can be obtained from:

$$C = (1/ Z_{CPE}\, j\omega)^{-\alpha} \quad \ldots\ldots\ldots\ldots (4)$$

where α is a fractional exponent, having values between 0 and 1, $j = \sqrt{1}$, $\omega = 2\Pi f$ is the angular frequency and Z_{CPE} is the real impedance. When α=0, C describes an ideal resistor, for α=1 it describes an ideal capacitor and for α=0.5 it represents homogenous semi- infinite diffusion (Lasia A. et al., 1999; MacDonald JR and

Johnson WB., 1987). When an inhomogenous film is characterized C is replaced by a CPE (constant phase element). The CPE describes the distribution of relaxation times of the process occurring in the inhomogeneous polymer film (Martini M. et al., 2000; Bisquert J et al., 2000; Krause S, 2003). When a CPE or C is parallel to a resistor, a depressed semi- circle (Cole- element) is produced (Hallik A et al., 2006).

2.7.1 EIS as a tool to measure film thickness

The electrochemical behaviour of conducting polymers has been extensively studied with the aim of elucidating the nature of ionic doping, conduction and charge accumulation in these materials. Diverse electrochemical and non-electrochemical techniques have been used for this purpose, among them electrochemical impedance spectroscopy (EIS). This technique has several advantages including i) coverage of a wide range of frequencies, which allows the determination of both kinetic and mass transport parameters, and ii) small perturbation of the system from its steady state. As mentioned, impedance results are analyzed by means of equivalent circuits (Drexler and Steinem, 2003), where the values of the electrical components are associated with the physical/ chemical properties of the electrochemical systems (Barcia et al., 2002). In particular, the value of the thickness of an electroactive film can be estimated from the values of the equivalent circuit elements, which are obtained through complex methods of fitting of the experimental data to their respective circuits (Macdonald, 1992; Penner and Martin, 1989). Measuring the thickness of a polymer actuator film

in its neutral and expanded state allows the determination of the degree of volume change that occurs as counterions move into the polymer network upon expansion by the application of the potential at which expansion occurs.

Verge et al. showed that the film thickness can be estimated from equation 5,

$$L = \varepsilon_r \varepsilon_o A/C \ldots\ldots. (5)$$

L is the film thickness, ε_r is the dielectric constant, ε_o is the vacuum permittivity, A is the geometrical electrode surface area and C is the capacitance determined from curve fitting (Verge et al., 2004). Leinad Gnana Lissy et al. used EIS to assess the effect of counter ion on the film thickness of PANI. They found that an increase in the film thickness is associated with an increase in the size of counter-ion and higher C_{dl} (double layer capacitance) values (Leinad Gnana Lissy et al., 2002). The impedance response of electrochemically synthesized poly- (o-toluidine) was also investigated in $HClO_4$ solutions as a function of film thickness and electrolyte concentration (Presa et al., 1998). They found that an increase in film thickness results in a decrease in the capacitance, substantiating equation 4. Various PPy composites have been developed and characterized via EIS including a dodecylsulfate doped PPy (Martini et al., 2000; Lee et al., 2002; Hallik et al., 2006).

2.8 REFERENCES

Anquetil, Patrick A.; Yu, Hsiao-hua; Madden, John David; Madden, Peter Geoffrey; Swager, Timothy M.; Hunter, Ian Warwick. **Thiophene -based conducting polymer molecular actuators.** Proceedings of SPIE-The International Society for Optical Engineering (2002), 4695(Electroactive Polymer Actuators and Devices (EAPAD)), 424-434.

Audebert, P.; Miomandre, Fabien. Electrochemistry of conducting polymers. Handbook of Conducting Polymers (3rd Edition) (2007).

Baba, Akira; Advincula, Rigoberto C.; Knoll, Wolfgang. **Evaluation of the electropolymerization process of pyrrole on micropatterned self-assembled monolayers.** PMSE Preprints (2002), 86, 48-49.

Barcia, O. E.; D'Elia, E.; Frateur, I.; Mattos, O. R.; Pebere, N.; Tribollet, B. **Application of the impedance model of de Levie for the characterization of porous electrodes.** Electrochimica Acta (2002), 47(13-14), 2109-2116.

Bar-Cohen, Yoseph. **Electroactive polymers as artificial muscles: a review.** Journal of Spacecraft and Rockets (2002), 39(6), 822-827.

Barthus, Rosangela C.; Lira, Luiz M.; Cordoba de Torresi, Susana I. **Conducting polymer- hydrogel blends for electrochemically controlled drug release devices.** Journal of the Brazilian Chemical Society (2008), 19(4), 630-636.

Baughman, R. H. **Conducting polymer artificial muscles.** Synthetic Metals (1996), 78(3), 339-353.

Brocks, Geert. **Charged oligothiophene dimers and π -stacks: the bipolaron revisited.** Synthetic Metals (2001), 119(1-3), 253-254.

Burgmayer, Paul; Murray, Royce W. **Increasing the rate of charging of redox polymer films with extended surface electrodes.** Journal of Electroanalytical Chemistry and Interfacial Electrochemistry (1982), 135(2), 335-42.

Careem, M. A.; Velmurugu, Y.; Skaarup, S.; West, K. **A voltammetry study on the diffusion of counter ions in polypyrrole films.** Journal of Power Sources (2006), 159(1), 210-214.

Chen, Zheng; Gale, Philip A.; Beer, Paul D. **Synthesis and electrochemical polymerization of calix[4]arenes containing N-substituted pyrrole moieties.** Journal of Electroanalytical Chemistry (1995), 393(1-2), 113-17.

Cleary, Gary W.. **Transdermal delivery systems: a medical rationale.** Top. Drug Bioavailability, Bioequivalence, Penetration (1993), 17-68.

Cortes, Maria Teresa; Moreno, Juan Carlos. **Artificial muscles based on conducting polymers.** e-Polymers (2003).

Della Santa, A.; De Rossi, D.; Mazzoldi, A. **Performance and work capacity of a polypyrrole conducting polymer linear actuator.** Synthetic Metals (1997), 90(2), 93-100.

Diaz, A. F.; Logan, J. A. **Electroactive polyaniline films.** Journal of Electroanalytical Chemistry and Interfacial Electrochemistry (1980), 111(1), 111-14.

Drexler, Janine; Steinem, Claudia. **Pore-Suspending Lipid Bilayers on Porous Alumina Investigated by Electrical Impedance Spectroscopy.** Journal of Physical Chemistry B (2003), 107(40), 11245-11254.

Fang, Fei Fei; Cho, Min Seong; Choi, Hyoung Jin; Yoon, Sang Soon; Ahn, Wha-Seung. **Electrorheological characteristics of conducting polypyrrole /swollen MCM-41 nanocomposite.** Journal of Industrial and Engineering Chemistry (Seoul, Republic of Korea) (2008), 14(1), 18-21.

Fuchiwaki, Masaki; Takashima, Wataru; Kaneto, Keiichi. **Soft actuators based on poly(3-alkyl thiophene) films upon electrochemical oxidation and reduction.** Molecular Crystals and Liquid Crystals Science and Technology, Section A: Molecular Crystals and Liquid Crystals (2002), 374 513-520.

Gelling, Victoria Johnston; Vetter, Christopher; Somayajula, Subramanyam V. Kasi; Qi, Xiaoning. **Polypyrrole as a corrosion inhibitor.** Polymer Preprints (American Chemical Society, Division of Polymer Chemistry) (2008), 49(2), 642-643.

Genies, E. M.; Bidan, G.; Diaz, A. F. **Spectroelectrochemical study of polypyrrole films.** Journal of Electroanalytical Chemistry and Interfacial Electrochemistry (1983), 149(1-2), 101-13.

Genies, E. M.; Bidan, G.; Diaz, A. F. **Spectroelectrochemical study of polypyrrole films.** Journal of Electroanalytical Chemistry and Interfacial Electrochemistry (1983), 149(1-2), 101-13.

Hallik, Allan; Alumaa, Ants; Tamm, Jueri; Sammelselg, Vaeino; Vaeaertnou, Mart; Jaenes, Alar; Lust, Enn. **Analysis of electrochemical impedance of polypyrrole**

|sulfate and polypyrrole |perchlorate films. Synthetic Metals (2006), 156(5-6), 488-494.

Han, Moon Gyu; Cho, Seok Ki; Oh, Seong Geun; Im, Seung Soon. **Preparation and characterization of polyaniline nanoparticles synthesized from DBSA micellar solution.** Synthetic Metals (2002), 126(1), 53-60.

Hara, Susumu; Zama, Tetsuji; Tanaka, Noboru; Takashima, Wataru; Kaneto, Keiichi. **Artificial fibular muscles with 20% strain based on polypyrrole-metal coil composites.** Chemistry Letters (2005), 34(6), 784-785.

Hara, Susumu; Zama, Tetsuji; Takashima, Wataru; Kaneto, Keiichi. **Gel-like polypyrrole based artificial muscles with extremely large strain.** Polymer Journal (Tokyo, Japan) (2004), 36(11), 933-936.

He, Xiaoquan. **Artificial muscle polymers.** Gaofenzi Tongbao (1994), (4), 215-23.

Heinze, J. **Electrochemistry of conducting polymers.** Synthetic Metals (1991), 43(1-2), 2805-23.

Heinze, Jurgen. **Electrochemistry of conducting polymers.** Organic Electrochemistry (4th Edition) (2001), 1309-1339.

Heller, J.. **Controlled drug release from poly(ortho esters)-a surface eroding polymer.** Journal of Controlled Release (1985), 2 167-77.

Hutchison, A. S.; Lewis, T. W.; Moulton, S. E.; Spinks, G. M.; Wallace, G. G. **Development of polypyrrole -based electromechanical actuators.** Synthetic Metals (2000), 113(1-2), 121-127.

Inzelt, G.; Pineri, M.; Schultze, J. W.; Vorotyntsev, M. A. **Electron and proton conducting polymers: recent developments and prospects.** Electrochimica Acta (2000), 45(15-16), 2403-2421.

Jeon, Jin-Han; Oh, Il-Kwon; Han, Jae-Hung; Lee, Sun-woo. **Development of bio-mimetic patterned IPMC actuators with multiple electrodes.** Key Engineering Materials (2007), 334-335(Pt. 2, Advances in Composite Materials and Structures), 1005-1008.

Kanazawa, K. Keiji; Diaz, A. F.; Geiss, Roy H.; Gill, William D.; Kwak, James F.; Logan, J. Anthony; Rabolt, John F.; Street, G. Bryan. **'Organic metals': polypyrrole , a stable synthetic 'metallic' polymer.** Journal of the Chemical Society, Chemical Communications (1979), (19), 854-5.

Kaneto, Keiichi; Fujisue, Hisashi; Kunifusa, Masakatsu; Takashima, Wataru. **Conducting polymer soft actuators based on polypyrrole films-energy conversion efficiency.** Smart Materials and Structures (2007), 16(2), S250-S255.

Kim, Kwang J.; Shahinpoor, Mohsen. **A novel method of manufacturing three-dimensional ionic polymer-metal composites (IPMCs) biomimetic sensors, actuators and artificial muscles.** Polymer (2001), Volume Date 2002, 43(3), 797-802.

Kim, Sung Wan. **Temperature sensitive polymers for delivery of macromolecular drugs.** Advanced Biomaterials in Biomedical Engineering and

Drug Delivery Systems, [Iketani Conference on Biomedical Polymers], 5th, Kagoshima, Japan, Apr. 18-22, 1995 (1996), Meeting Date 1995, 126-133.

Lee, Chi-Woo; Yoon, Jung-Hyun; Cho, Hyun-Woo; Bae, Sang-Eun; Lee, Kang-Bong. **Electropolymerization of pyrrole applied to biosystem.** Journal of the Korean Electrochemical Society (2002), 5(4), 202-208.

Lee, Deuk Yong; Kim, Yena; Lee, Se-Jong; Lee, Myung-Hyun; Lee, Jai-Yeoul; Kim, Bae-Yeon; Cho, Nam-Ihn. **Characteristics of chemo-mechanically driven polyacrylonitrile fiber gel actuators.** Materials Science & Engineering, C: Biomimetic and Supramolecular Systems (2008), 28(2), 294-298.

Lee, Hochun; Yang, Haesik; Kwak, Juhyoun. **Effects of dopant anions and N-substituents on the electrochemical behavior of polypyrrole films in propylene carbonate solution.** Electrochemistry Communications (2002), 4(2), 128-133.

Leinad Gnana Lissy, S.; Pitchumani, S.; Jayakumar, K. **The effect of film thickness and counter ions on the double layer and redox capacitance of polyaniline thin film electrode.** Materials Chemistry and Physics (2002), 76(2), 143-150.

Li, Guang; Wang, You; Xu, Hui. **A hydrogen peroxide sensor prepared by electropolymerization of pyrrole based on screen-printed carbon paste electrodes.** Sensors (2007), 7(3), 239-250.

Lira, L. M.; Barthus, R. C.; Cordoba de Torresi, S. I. **Conducting polymers and hydrogels for electrochemically controlled drug release devices.** ECS Transactions (2007), 3(29), 105-114.

Lira, Luiz M.; Cordoba de Torresi, Susana I. **Conducting polymer-hydrogel composites for electrochemical release devices: Synthesis and characterization of**

semi-interpenetrating polyaniline-polyacrylamide networks. Electrochemistry Communications (2005), 7(7), 717-723.

Low, L.-M.; Seetharaman, S.; He, K.-Q.; Madou, M. J. **Microactuators toward microvalves for responsive controlled drug delivery.** Sensors and Actuators, B: Chemical (2000), B67(1-2), 149-160.

Mabrouk, Patricia Ann. **Oxidative electropolymerization of pyrrole from neat monomer solution.** Synthetic Metals (2005), 150(1), 101-105.
Macdonald J R **Impedance spectroscopy**. Annals of biomedical engineering (1992), 20(3), 289-305.

Madden, J. D.; Genereux, N.; Shkuratoff, K. A.; van der Star, A.; Poon, D.; Irwin, D.; Cheng, P.; Hsu, G.; Filipozzi, L. **Electroactive polymer actuator online database.** Proceedings of SPIE-The International Society for Optical Engineering (2007), 6524(Electroactive Polymer Actuators and Devices (EAPAD) 2007)

Madden, John D. **Actuator selection for variable camber foils.** Proceedings of SPIE-The International Society for Optical Engineering (2004), 5385 (Electroactive Polymer Actuators and Devices (EAPAD)), 442-448.

Madden, John D.; Madden, Peter G.; Anquetil, Patrick A.; Hunter, Ian W. **Load and time dependence of displacement in a conducting polymer actuator.** Materials Research Society Symposium Proceedings (2002), 698(Electroactive Polymers and Rapid Prototyping), 137-144.

Martinez, G.; Gomez, M. A. **Nanocomposite materials formed by carbon nanotubes and conducting polymers.** Revista de Plasticos Modernos (2008), 95(624), 500-508.

Martini, Milena; De Paoli, Marco-A. **Effect of the electrolyte cations and anions on the photocurrent of dodecyl sulphate doped polypyrrole films.** Solar Energy Materials and Solar Cells (2002), 73(3), 235-247.

McGovern, S. T.; Spinks, G. M.; Xi, B.; Alici, G.; Truong, V.; Wallace, G. G. **Fast bender actuators for fish-like aquatic robots.** Proceedings of SPIE (2008), 6927(Electroactive Polymer Actuators and Devices (EAPAD) 2008), 69271L/1-69271L/12.

Meijer, Kenneth; Rosenthal, Marc S.; Full, Robert J. **Muscle -like actuators? A comparison between three electroactive polymers.** Proceedings of SPIE-The International Society for Optical Engineering (2001), 4329(Electroactive Polymer Actuators and Devices), 7-15.

Michira, I.; Akinyeye, R.; Somerset, V.; Klink, M. J.; Sekota, M.; Al-Ahmed, A.; Baker, P. G. L.; Iwuoha, E. **Synthesis, characterisation of novel polyaniline nanomaterials and application in amperometric biosensors.** Macromolecular Symposia (2007), 255(Polymers for Advanced Applications), 57-69.

Mikos, Antonios G.; Murphy, Regina M.; Bernstein, Howard; Peppas, Nicholas A.; Editors. **Biomaterials for Drug and Cell Delivery. (Symposium held November 29 - December 1, 1993, Boston, Massachusetts.) [In: Mater. Res. Soc. Symp. Proc., 1994; 331].** (1994), 290 pp.

Mirfakhrai, Tissaphern; Madden, John D. W.; Baughman, Ray H. **Polymer artificial muscles.** Materials Today (Oxford, United Kingdom) (2007), 10(4), 30-38.

Oh, Il-Kwon; Jeon, Jin-Han; Lee, Yeon-Gwan. **Multiple electrode patterning of ionic polymer metal composite actuators.** Proceedings of SPIE-The International Society for Optical Engineering (2006), 6168(Electroactive Polymer Actuators and Devices (EAPAD)), 616828/1-616828/8.

Okabayashi, Katsuaki; Goto, Fumio; Abe, Katsushi; Yoshida, Takashi. **Electrochemical studies of polyaniline and its application.** Synthetic Metals (1987), 18(1-3), 365-70.

Otake, Mihoko; Kagami, Yoshiharu; Ishikawa, Kohei; Inaba, Masayuki; Inoue, Hirochika. **Shape design of gel robots made of electroactive polymer gel.** Proceedings of SPIE-The International Society for Optical Engineering (2001), 4234(Smart Materials), 194-202.

Otero, T. F.; Cortes, M. Teresa; Boyano, I. **Molar enthalpy of the polypyrrole electrochemistry.** Journal of Electroanalytical Chemistry (2004), 562(2), 161-165.

Otero, T. F.; Huerta, P. **Electrochemistry and conducting polymers : Soft, wet, multifunctional, and biomimetic materials.** Book of Abstracts, 219th ACS National Meeting, San Francisco, CA, March 26-30, 2000 (2000).

Otero, T. F.; Sansinena, J. M. **Bilayer dimensions and movement in artificial muscles.** Bioelectrochemistry and Bioenergetics (1997), 42(2), 117-122.

Otero, T. F.; Villanueva, S.; Cortes, M. T.; Cheng, S. A.; Vazquez, A.; Boyano, I.; Alonso, D.; Camargo, R. **Electrochemistry and conducting polymers : soft, wet, multifunctional and biomimetic materials.** Synthetic Metals (2001), 119(1-3), 419-420.

Otero, Toribio F.; Grande, Hans-Juergen; Rodriguez, Javier. **Reinterpretation of polypyrrole electrochemistry after consideration of conformational relaxation processes.** Journal of Physical Chemistry B (1997), 101(19), 3688-3697.

Otero, Toribio F.; Sansinena, Jose M. **Soft and wet conducting polymers for artificial muscles.** Advanced Materials (Weinheim, Germany) (1998), 10(6), 491-494.

Otero, Toribio Fernandez. **Conducting polymers , electrochemistry , and biomimicking processes.** Modern Aspects of Electrochemistry (1999), 33 307-434.

Pei, Qibing; Inganaes, Olle. **Conjugated polymers as smart materials, gas sensors and actuators using bending beams.** Synthetic Metals (1993), 57(1), 3730-5.

Penner, Reginald M.; Martin, Charles R. **Electrochemical investigations of electronically conductive polymers. 2. Evaluation of charge-transport rates in polypyrrole using an alternating current impedance method.** Journal of Physical Chemistry (1989), 93(2), 984-9.

Peppas, Nikolaos A.; Mikos, Antonios G. **Preparation methods and structure of hydrogels.** Hydrogels Med. Pharm. (1986), 1 1-25

Popovic, Suzana. **Design of electro-active polymer gels as actuator materials.** (2001), 162 pp.

Rubinstein, Abraham; Robinson, Joseph R.. **Controlled drug delivery.** Progress in Clinical Biochemistry and Medicine (1987), 4 71-107.

Sabouraud, Guillaume; Sadki, Said; Brodie, Nancy. **The mechanisms of pyrrole electropolymerization.** Chemical Society Reviews (2000), 29(5), 283-293.

Sayyah, S. M.; Abd El-Rehim, S. S.; El-Deeb, M. M. **Electropolymerization of pyrrole and characterization of the obtained polymer films.** Journal of Applied Polymer Science (2003), 90(7), 1783-1792.

Shirakawa, Hideki; Louis, Edwin J.; MacDiarmid, Alan G.; Chiang, Chwan K.; Heeger, Alan J. **Synthesis of electrically conducting organic polymers: halogen derivatives of polyacetylene, (CH)x.** Journal of the Chemical Society, Chemical Communications (1977), (16), 578-80.

Skaarup, Steen; Bay, Lasse; West, Keld. **Polypyrrole actuators working at 2-30Hz.** Synthetic Metals (2007), 157(6-7), 323-326.

Smela, Elisabeth; Lu, Wen; Mattes, Benjamin R. **Polyaniline actuators.** Synthetic Metals (2005), 151(1), 25-42.

Smela, Elisabeth; Mattes, Benjamin R. **Polyaniline actuators - Part 2. PANI(AMPS) in methanesulfonic acid.** Synthetic Metals (2005), 151(1), 43-48.

Somerset, V.; Klink, M.; Akinyeye, R.; Michira, I.; Sekota, M.; Al-Ahmed, A.; Baker, P.; Iwuoha, E. **Spectroelectrochemical reactivities of novel polyaniline nanotube pesticide biosensors.** Macromolecular Symposia (2007), 255(Polymers for Advanced Applications), 36-49

Spinks, Geoffrey M.; Mottaghitalab, Vahid; Bahrami-Samani, Mehrdad; Whitten, Philip G.; Wallace, Gordon G. **Carbon-nanotube-reinforced polyaniline fibers for high-strength artificial muscles.** Advanced Materials (Weinheim, Germany) (2006), 18(5), 637-640.

Spinks, Geoffrey M.; Wallace, Gordon G.; Ding, Jie; Zhou, Dezhi; Xi, Binbin; Scott, Timothy R.; Truong, Van-Tan. **Electroactive polymer actuator devices (EAPAD).** Proceedings of SPIE-The International Society for Optical Engineering (2003), 5051(Electroactive Polymer Actuators and Devices (EAPAD)), 21-28.

Sun, Li-qun; Zhao, Yao. **Progress in fabrication and modeling of IPMC.** Cailiao Kexue Yu Gongcheng Xuebao (2008), 26(3), 473-478.

Tourillon, G.; Garnier, F. **Electrochemical doping of polythiophene in aqueous medium. Electrical properties and stability.** Journal of Electroanalytical Chemistry and Interfacial Electrochemistry (1984), 161(2), 407-14.

Trueba, M.; Montero, A. L.; Rieumont, J. **Pyrrole nanoscaled electropolymerization. Effect of the proton.** Electrochimica Acta (2004), 49(25), 4341-4349.

Tsai, Han-Kuan A.; Madou, Marc. **Microfabrication of bilayer polymer actuator valves for controlled drug delivery.** JALA (2007), 12(5), 291-295.

Verge, M.-G.; Olsson, C.-O. A.; Landolt, D. **Anodic oxide growth on tungsten studied by EQCM, EIS and AES.** Corrosion Science (2004), 46(10), 2583-2600.

Vernitskaya, T. V.; Efimov, O. N. **Polypyrrole: a conducting polymer (synthesis, properties and applications).** Uspekhi Khimii (1997), 66(5), 489-505.

Wallmersperger, Thomas; Kroeplin, Bernd; Guelch, Rainer W. **Numerical simulation of a coupled chemo-electric-formulation for ionic polymer gels in electric fields.** Proceedings of SPIE-The International Society for Optical

Engineering (2002), 4695(Electroactive Polymer Actuators and Devices (EAPAD)), 303-314.

Waltman, Robert J.; Bargon, Joachim. **Reactivity/structure correlations for the electropolymerization of pyrrole: an INDO/CNDO study of the reactive sites of oligomeric radical cations.** Tetrahedron (1984), 40(20), 3963-70.

Waltman, Robert J.; Bargon, Joachim. **The electropolymerization of polycyclic hydrocarbons: substituent effects and reactivity/structure correlations.** Journal of Electroanalytical Chemistry and Interfacial Electrochemistry (1985), 194(1), 49-62.

Warren, M. R.; Madden, J. D.. **A structural, electronic and electrochemical study of polypyrrole as a function of oxidation state.** Synthetic Metals (2006), 156(9-10), 724-730.

Wu, Yanzhe; Ballantyne, Amy M.; Wagner, Pawel; Zhou, Dezhi; Spinks, Geoffrey M.; Officer, David; Wallace, Gordon G. **Electrochemical actuation properties of a novel solution-processable polythiophene.** Electrochimica Acta (2007), 53(4), 1830-1836.

Xu, Han; Wang, Chong; Wang, Chunlei; Zoval, Jim; Madou, Marc. **Polymer actuator valves toward controlled drug delivery application.** Biosensors & Bioelectronics (2006), 21(11), 2094-2099.

Yamauchi, T.; Tansuriyavong, S.; Doi, K.; Oshima, K.; Shimomura, M.; Tsubokawa, N.; Miyauchi, S.; Vincent, J. F. V. **Preparation of composite materials of polypyrrole and electroactive polymer gel using for actuating system.** Synthetic Metals (2005), 152(1-3), 45-48.

Yao, Li; Krause, Sonja. **Mechanism study of electromechanical deformation of ionic electroactive polymer gels in electric fields.** PMSE Preprints (2002), 86 28-29.

Yoshioka, Yuka; Calvert, Paul. **Electrically stimulated hydrogel as microactuators.** Polymeric Materials Science and Engineering (2001), 84 335-336.

Yoshioka, Yuka; Calvert, Paul. **Epoxy-based electroactive polymer gels.** Experimental Mechanics (2002), 42(4), 404-408.

Zanuy David; Casanovas Jordi; Aleman Carlos **Conformational features of an actuator containing calix[4]arene and thiophene : a molecular dynamics study**. The journal of physical chemistry. B (2006), 110(20), 9876-81.

Zhang, Zhiming; Wan, Meixiang; Wei, Yen. **Electromagnetic functionalized polyaniline nanostructures.** Nanotechnology (2005), 16(12), 2827-2832.

Zhou, Ming; Pagels, Markus; Geschke, Beate; Heinze, Juergen. **Electropolymerization of pyrrole and electrochemical study of polypyrrole. 5. Controlled electrochemical synthesis and solid-state transition of well-defined polypyrrole variants.** Journal of Physical Chemistry B (2002), 106(39), 10065-10073.

Zhou, Yuanyuan; Yu, Min; Li, Song; Li, Lei. **Electropolymerization of polypyrrole films doped with sulfonated polyaniline.** European Physical Journal: Applied Physics (2008), 42(2), 141-144.

Zotti, Gianni. **Electrochemistry of conducting polymers.** Chimica e l'Industria (Milan) (1995), 77(3), 156-62.

MATERIALS AND METHODS

3.1 Materials

Pyrrole-2-carboxaldehyde
2,3-diaminophenazine (DAP)
Acetic
Methanol
Pyrrole
1,2 –napthaquinone-4-sulfonic acid (NQSA)
Deionised water
Hydrochloric acid
Dimethyl formamide (DMF)

The pyrrole (98%), pyrrole-2-carboxaldehyde (95%), 2,3- diaminophenazine (90%), DMF, methanol, and acetic acid used was supplied by Sigma- Aldrich (Pty) Ltd., South Africa. The pyrrole was distilled at reduced pressure, kept in 1ml ampoules, saturated with argon gas and kept in the dark at 4^{o}C. The sodium salt of 1,2- napthaquinone- 4- sulfonic acid (BDH laboratory reagent) was used as dopant. Acetic acid (99.8%) and methanol (99.8%) was dried with molecular sieves before experiments. The electrolyte used for polymerization was prepared from hydrochloric acid (32%) (Fluka) and DMF in a 1:1 ratio, and that for electrochemical characterization experiments HCl only; both using distilled water (specific resistance 18MW MilliQ, Millipore).

3.2 Synthesis of phenazine-2, 3- diimino (pyrrol-2-yl)

All solvents were dried with molecular sieves to remove any trace of water. Phenazine-2, 3- diiimino (pyrrol-2-yl) (PDP) was synthesized by the condensation reaction between 1mmol (0.0951g) pyrrole-2-carboxaldehyde and 0.5mmol (0.1051g) 2, 3-diaminophenazine in 20ml acetic acid, under reflux for 48 hrs. The resulting black precipitate was then filtered, washed several times with methanol and dried under vacuum. The dried product was then subjected to NMR using a Varian Gemini 2000, FTIR (Perkin Elmer Spectrum-1) and SEM analysis (Hitachi X-650 SEMicroanalyzer) at 1100x magnification.

3.3 Voltammetric measurements

Cyclic voltammetry (CV) and Osteryoung square wave voltammetry (OSWV) measurements were made using a BAS 100W integrated automated electrochemical workstation (Bioanalytical Systems, Lafayette, IN, USA).

The three electrode cell configuration consisted of a glassy carbon electrode (GC) with a surface area of 0.071 cm^2 as working electrode which was polished to a shiny finish using slurries of 1µm, 0.3µm and 0.05µm fine alumina powder (Bueller, IL, USA), and rinsed with copious quantities of deionized water after each polishing step. The working electrode was then subjected to repeated potential scanning in 0.1M H_2SO_4 in the potential range between -1.2V and +1.5V, until a reproducible voltammogram was obtained. The reference electrode used was a Ag/AgCl electrode (3M NaCl type) (BAS MF-2052) and the counter electrode was a flame cleaned platinum wire, which involves flame cleaning the wire until white hot, followed by rinsing with deionised water. The cleaned electrodes were then used directly for polymer deposition.

The electrolyte used in all the electrochemical experiments, was 0.1M HCl. All solutions were degassed with Argon for 15 minutes prior to all experiments.

3.3.1 Electrochemical synthesis and characterization of doped and undoped poly(phenazine-2,3- diamino (pyrrol-2-yl)) on a glassy carbon electrode

The three electrode configuration was setup in a sealed 20ml electrochemical cell. The molar ratio of dopant to monomer is critical to produce a conductive polymer, and a ratio of 1: 10 (dopant: monomer) was used. The monomer/HCl solution was first degassed by passing argon through the solution for 15 minutes and an argon

blanket was then kept over the solution during electrosynthesis. A thin film of conducting poly (phenazine- 2,3- diimino (pyrrol-2-yl)) (PPDP) was grown potentiodynamically from a solution containing 0.5 mmol (0.182 g) (of phenazine -2,3- diimino (pyrrol-2-yl) and 0.05 mmol (0.013g) of the sodium salt of 1,2-naphthaquinone-4 –sulfonic acid dopant respectively in 20 ml of 0.1M HCl/DMF (1:1) at 50mV/s for 25 cycles using a potential window of 600mV to +700mV vs. Ag/AgCl. Undoped PPDP was also synthesized as above in the absence of NQSA. The PPDP-modified electrodes was rinsed with deionised water, and used as working electrode in subsequent studies.

3.3.2 Characterization of doped PPDP-modified glassy carbon electrode using cyclic voltammetry and OSWV

The solution from which the film was generated was replaced with a fresh electrolyte solution of 0.1M HCl only, in which all cyclic voltammetry experiments were then performed using the same three electrode cell configuration. The doped PPDP- modified electrode was then anodically scanned from -600mV to +700mV vs. Ag/AgCl at different scan rates i.e. 5, 10, 15, 25 and 50mV/s for one cycle only.

OSWV were performed at 5Hz at 15mV square wave amplitude using a potential step of 4mV in an oxidative direction (anodically) from initial potential , E_i of -600mV to a final potential, E_f of +700mV; and reductive direction (cathodically) from E_i of +700mV to a final potential, E_f of -600mV.

3.3.3 Polymerization and characterization of PPy/NQSA and PPy

Thin films of polypyrrole-doped NQSA and undoped polypyrrole were also prepared as done by Akinyeye et al., 2007.

Polypyrrole doped NQSA was grown under potentiodynamic conditions, from a solution containing 350 µl pyrrole monomer (0.0050 moles) and 0.130g (0.0005 moles) of 1,2- napthaquinone-4sulfonic acid dopant in 50ml of 0.1M HCl. The potential window used for polymerization and characterization studies was

-100mV to +700mV vs Ag/AgCl.

Undoped polypyrrole was grown using the same parameters above, but with no NQSA in the solvent during polymerization. The same parameters as 3.3.2 were then used for both polymers.

3.3.4 Polymerization and characterization of undoped DAP

Thin films of undoped 2,3-diaminophenazine-(DAP). PolyDAP was grown under potentiodynamic conditions, from a solution containing 0.1051g DAP monomer (0.50 mmoles) in 50ml of 0.1M HCl. The potential window used for polymerization studies was -200mV to +1500mV vs Ag/AgCl.

Undoped DAP was grown using the same parameters above, but with no NQSA in the solvent during polymerization. The same parameters as 3.3.2 were then used for both polymers.

3.4 Electrochemical Impedance Spectroscopy (EIS) measurements

EIS measurements were performed on the thin film of GC/PPDP-NQSA as well as the GC/PPy-NQSA using an IM6ex Zahner. The same three-electrode cell arrangement and electrolyte for cyclic voltammetry was used. An AC amplitude of 10mV at different applied potentials, over a frequency range from 10^5 to 10^{-2} Hz in 20 steps per frequency decade. Measurements were also taken at the reduction potential of the PPDP, as determined from CV in different solvents, i.e. 0.1M HCl, NaCl, KCl and $CaCl_2$. Data analysis was done by modeling with equivalent circuits using Zahner Thales- SIM software.

3.5 Scanning Electron Microscopy (SEM) analysis of PPDP/NQSA and PPy/NQSA

Scanning Electron Microscopy (SEM) was done to assess the morphology of the electrochemically prepared polymer films. A three electrode arrangement was setup in which the working electrode used was a screen- printed carbon electrode, with a Pt wire and Ag/AgCl as the counter and reference electrodes respectively. The same procedure as stated in Section 3.3.1 and 3.3.4 was followed for electropolymerization of PPDP/NQSA and PPy/NQSA respectively.

RESULTS AND DISCUSSION

4.1 Synthesis of phenazine -2, 3- diimino (pyrrol-2-yl) (PDP)

The novel Schiff- base compound, PDP, was synthesized according to scheme 1.

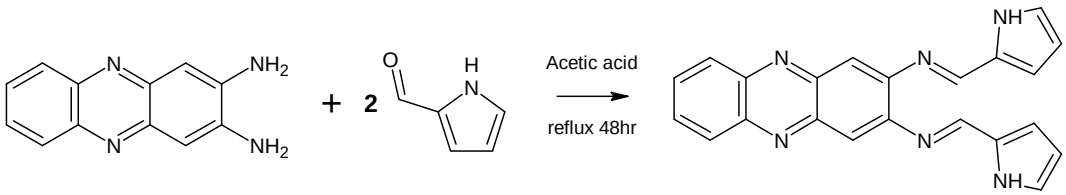

Scheme 1: Condensation reaction between pyrrole-2-carboxaldehyde and DAP resulting in the formation of the Schiff-base product (phenazine -2, 3- diimino (pyrrol-2-yl).

The resulting product showed a 61% yield. The phenazine-2, 3- diimino (pyrrol-2-yl) was then characterized by FTIR, NMR and SEM to confirm the synthesis of the desired product, after drying.

4.1.1 FTIR analysis

FTIR analysis was done to confirm the structure of the synthesized PDP by assessing the bonds that are present in this molecule compared to DAP and pyrrole-2-aldehyde at a frequency range of 400cm^{-1} to 4000 cm^{-1}.

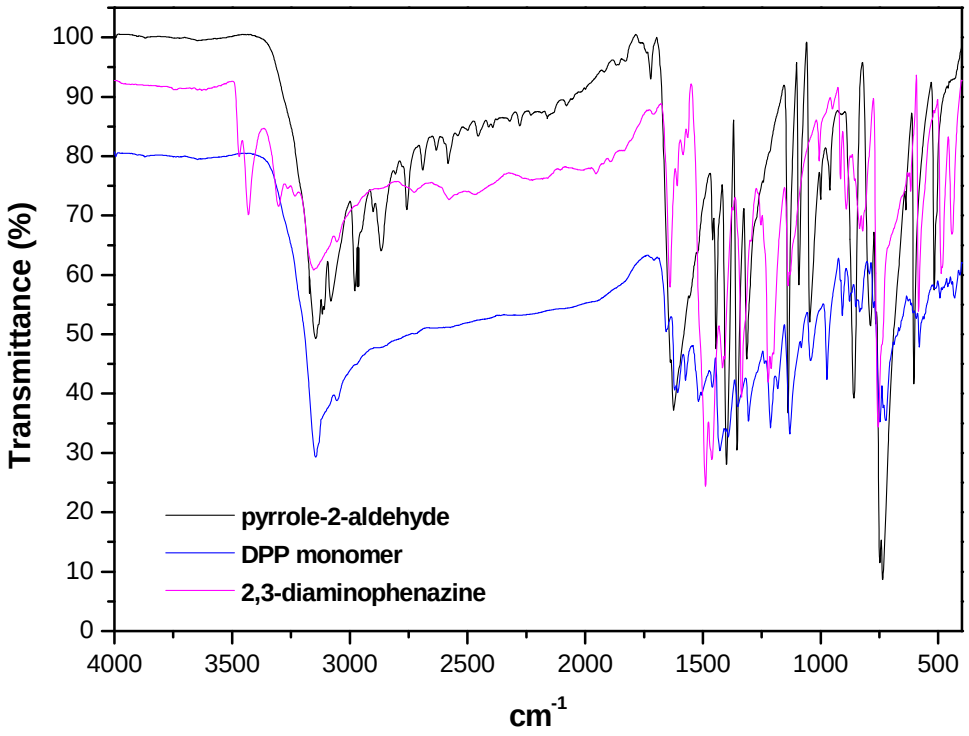

Fig 15: Overlapping FTIR spectra of pyrrole-2-carboxaldehyde; DAP and PDP

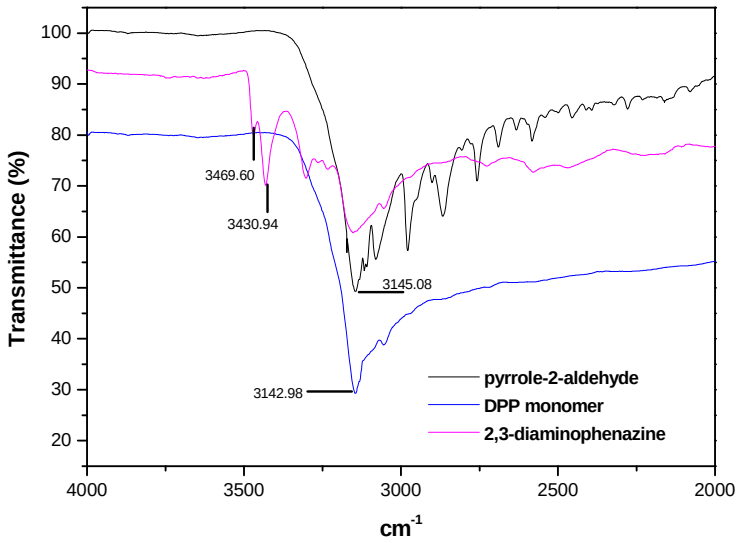

Fig 16: Overlapping FTIR spectra of pyrrole-2-carboxaldehyde; DAP and PDP between 4000 and 2000cm^{-1}.

From Figure 16, the FTIR spectra of DAP, shows 2 peaks at 3469.6cm^{-1} and 3430.94 cm^{-1} respectively, indicative of $\nu(NH_2)$ stretching vibration. This peak is not seen in the FTIR spectra of PDP and thus the NH_2 bond is not present in the chemical structure of PDP. The FTIR spectra of pyrrole-2-carboxaldehyde, shows a peak at 3145 cm^{-1}, which is characteristic of ν(NH) stretching vibration. This peak is still present in the FTIR spectra of PDP (3142 cm^{-1}), indicating the NH bond of PDP. A peak at 738 and 727 cm^{-1} is observed for both pyrrole-2-carboxaldehyde and PDP, which is indicative of an unsubstituted α- position in the pyrrole moeity.

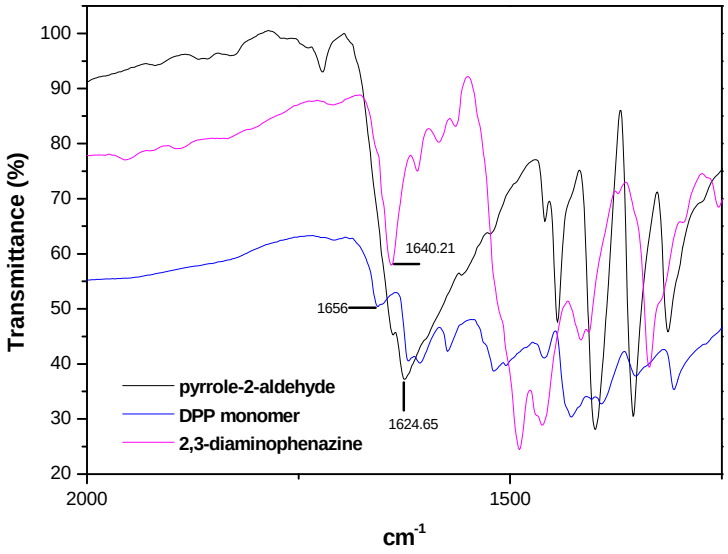

Fig 17: Overlapping FTIR spectra of pyrrole-2-carboxaldehyde; DAP and PDP between 2000 and 1250cm^{-1}.

From Figure 17 the spectra of pyrrole-2-carboxaldehyde show a prominent peak at 1624.65 cm^{-1}. This is due to the *ν*(C=O) stretching band. The spectra of PDP does not show this peak, indicating the absence of the *ν*(C=O) bond in the structure of PDP. A peak at 1640.21cm^{-1} and 1656 cm^{-1} is seen for DAP and PDP respectively. This is as a result of the *ν*(C=N) stretching band present in all three compounds. The results are tabulated in Table 1. All the results from FTIR suggest that the aldehyde and amino moieties of the starting reagents no longer exist and have been converted to the Schiff base linkage (refer to scheme 1) of the newly synthesized PDP.

Table 1: FTIR spectra peak assignment

pyrrole-2-carboxaldehyde		
Assignment	Frequency (cm^{-1})	Literature (cm^{-1})
NH- stretch	3145	3600 [b]
C=O stretch	1624	1735 [a,b]
Unsubstituded α – position	738	700 [b]
2,3- diaminophenazine		
C=N stretch	1640	1635 [a]
NH_2 stretch	3469 and 3430	3420 [a]
phenazine-2,3- diimino (pyrrol-2-yl)		
C=N stretch	1656	1649 [a]
NH- stretch	3142	3600 [b]
Unsubstituded α – position	727	700 [b]

a= Chohen JH and Kauser S, 2000

b= Rice Corey A et al., 2007

4.1.2 NMR analysis

NMR analysis was also done to confirm the structure of PDP. Each peak corresponds to a specific chemical bond in a molecule and thus by observing the appearance or disappearance of peaks for PDP compared to DAP and pyrrole-2-aldehyde, the structure of the desired product can be confirmed. All NMR spectra were done using DMSO as solvent.

The ^{1}H NMR spectra of DAP, pyrrole-2- carboxaldehyde and PDP are shown in Figure 18.

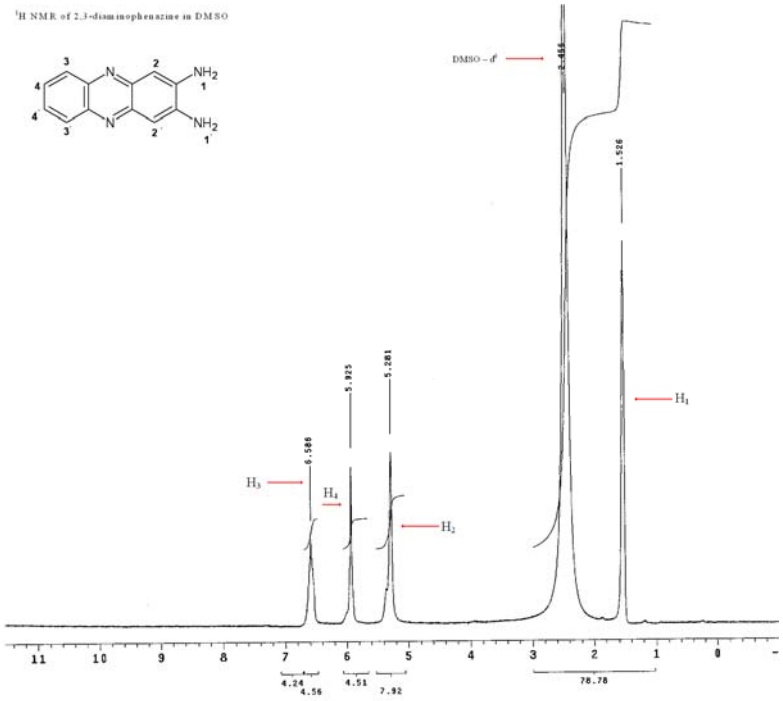

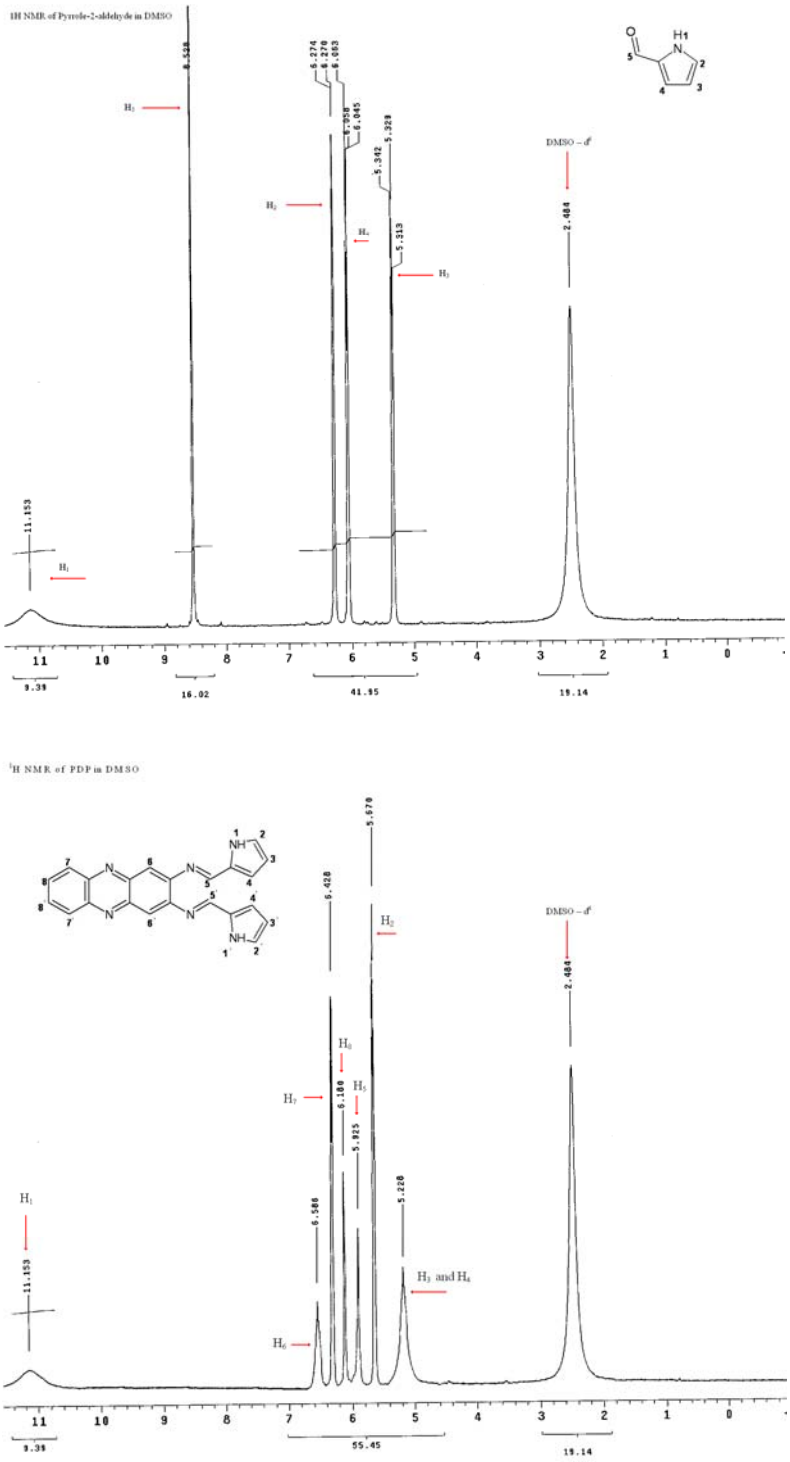

Fig 18: NMR spectra of DAP, pyrrole-2-carboxaldehyde and phenazine-2,3- diimino (pyrrol-2-yl) in DMSO-d^6

DAP: ^{1}H- NMR (DMSO-d^{6}): 1.528 (4H, s, 1-H and 1'-H); 5.281 (2H, s, 2-H and 2'-H); 5.925 (2H, m, 4-H and 4'-H); 6.586 (2H, d, 3-H, 3'-H).

Pyrrole-2-carboxaldehyde: ^{1}H- NMR (DMSO-d^{6}): 5.328 (1H, m, 3-H); 6.063 (1H, d, 4-H); 6.270 (1H, m, 2-H); 8.528 (1H, s, 5-H); 11.152 (1H, d, 1-H).

PDP: ^{1}H- NMR (DMSO-d^{6}): 5.228 (4H, m, 3-H, 3'-H, 4-H and 4'-H); 5.670 (2H, m, 2-H and 2'-H); 5.925 (2H, m, 5-H and 5'-H); 6.180 (2H, m, 8-H and 8'-H); 6.428 (2H, d, 7-H and 7'-H); 6.588 (2H, s, 6-H and 6'-H); 11.153 (2H, m, 1-H and 1'-H).

The ^{1}H NMR spectrum of pyrrole-2- carboxaldehyde showed the aldehydic proton as a singlet at δ 8.528. This singlet disappears in the spectrum of PDP and is seen at in the high field region at δ 5.925, indicating that the C=O bond of DAP is not present, as expected for the desired product. The ^{1}H NMR spectrum of DAP showed the 1-NH_2 and 1'- NH_2 singlet at δ 1.258. This peak disappears in the spectrum of PDP. Thus, the ^{1}H- NMR support the conclusion derived from FTIR.

4.1.3 SEM analysis

SEM analysis was done to assess the morphology of the synthesized product. It was done at a magnification of 1100.

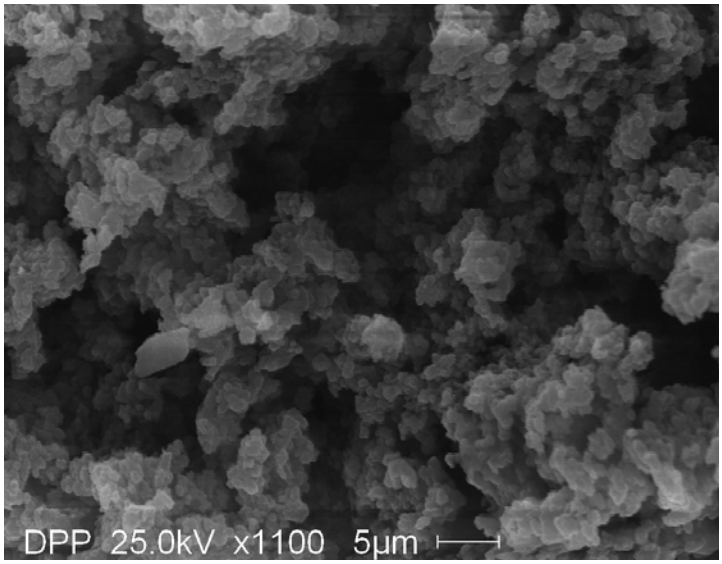

Fig 19: SEM image of PDP

Figure 19 displays the SEM image of PDP. The compound has a micellular morphology, which is attributed to the reaction conditions used.

4.2 Voltammetric measurements

4.2.1 Undoped PPy

The polymerization of undoped polypyrrole, as described in section 3.3.3, is shown in Figure 20. The film had good adhesion on the platinum electrode.

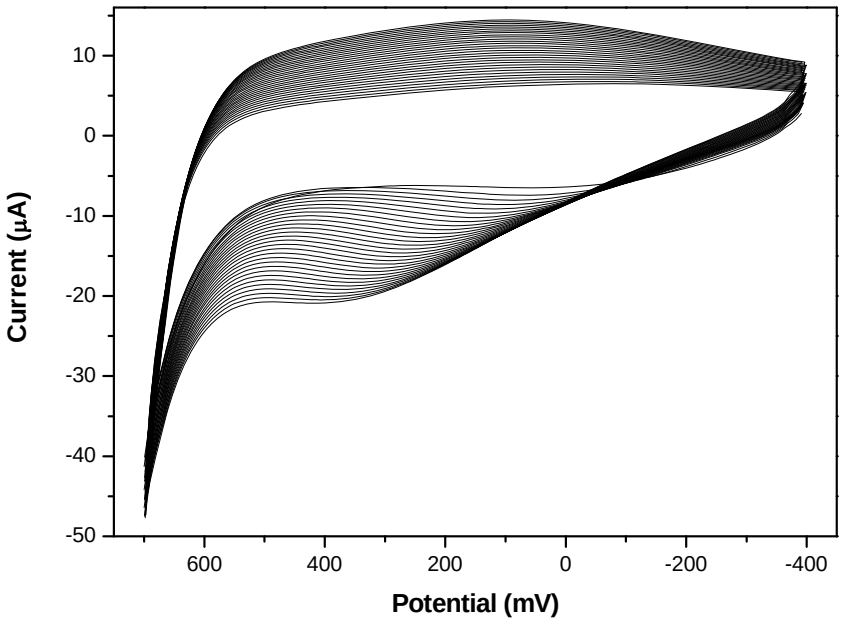

Fig 20: Polymerization voltammogram of 0.1M PPy in 0.1M HCl at 50mV/s on a platinum electrode.

The CV has poor/ ill formed oxidation and reduction peaks. This is due to electropolymerization in the aqueous solvent (0.1M HCl), where the small anionic dopant (Cl^- anion) could not produce the desired modification to produce an electroactive polymer with reversible or quasi- reversible electrochemistry (Mabrouk PA, 2005; Wang L et al., 2001). Thus, the need to use larger dopant ions that could improve conductivity and reversibility is of utmost importance.

4.2.2 Polypyrrole/ NQSA

Figure 21 and Figure 22 shows the polymerization voltammogram and multi-scan rate voltammograms of PPy doped with NQSA respectively, as described in section 3.3.3. As expected, the oxidation and reduction peaks are more distinct than that of undoped PPy, since NQSA is a larger dopant and better charge carrier. The anodic and cathodic peak potentials were 356mV and 306mV vs Ag/AgCl respectively at 5mV/s. The average formal potential ($E^{o'}$), estimated from the peak potentials at 5, 10, 15, 20, 25 and 50mV/s, was calculated as 334.6mV, which is close to the results from OSWV (figure 23) which gave a formal potential (E^{o}) of 329mV. These results are in good collaboration with that of Akinyeye et al., who found the formal potential at 322mV vs Ag/AgCl (Akinyeye R et al., 2007).

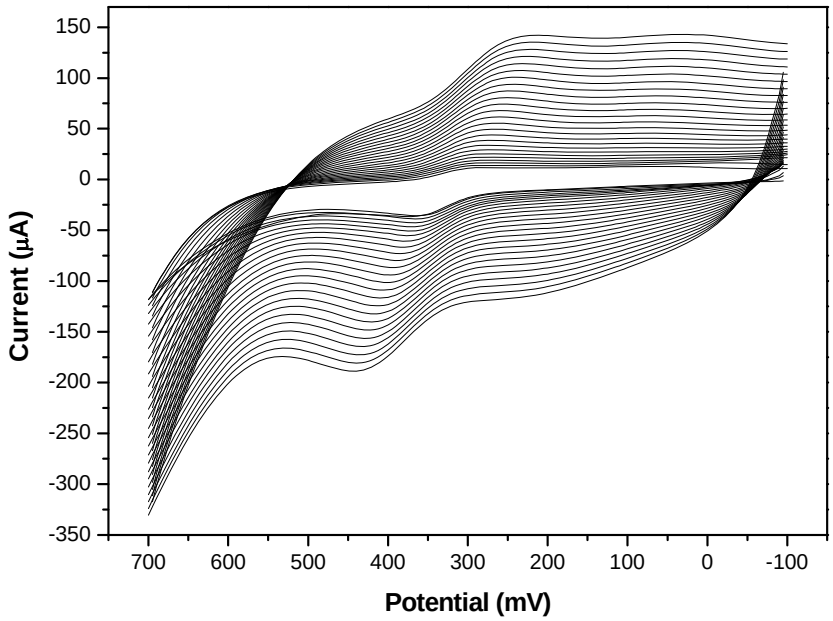

Fig 21: Polymerization voltammogram of PPy doped with NQSA from 0.1mol PPy and 0.05mol NQSA in 0.1M HCl at 50mV/s on a glassy carbon electrode.

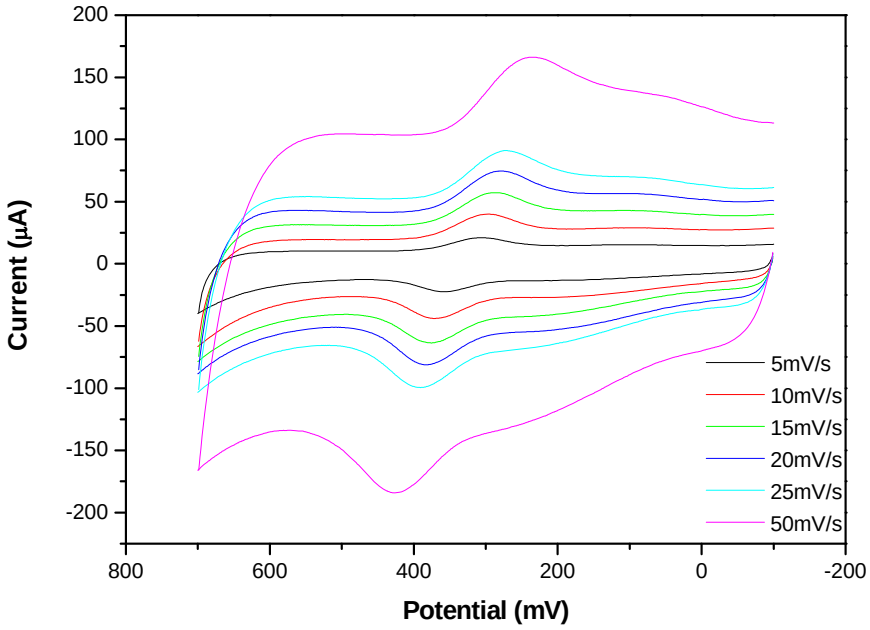

Fig 22: Multi- scan rate voltammogram obtained at a glassy carbon electrode with a thin film of PPy/NQSA in 0.1M HCl at scan rates of 5, 10, 15, 20, 25 and 50mV/s.

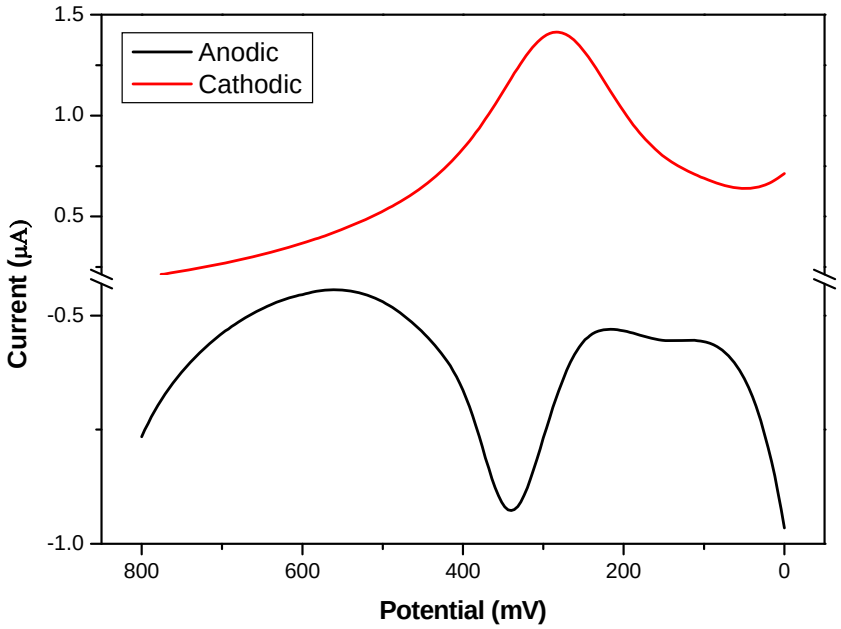

Fig 23: OSWV of GC/PPy/NQSA in 0.1M HCl.

4.2.3 Undoped Poly(2,3- diaminophenazine) (PDAP)

Figure 24 shows the polymerization voltammogram of undoped PDAP.

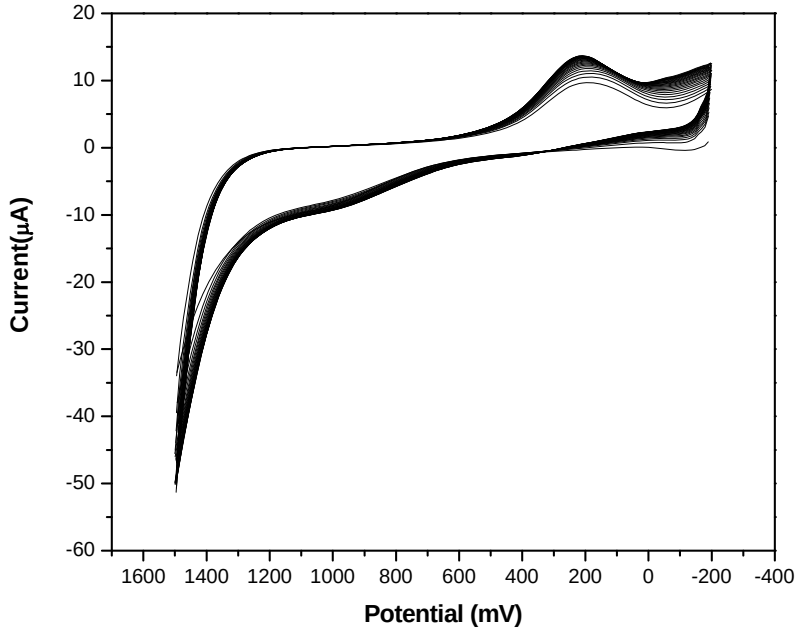

Fig 24: Polymerization voltammogram of undoped PolyDAP from 0.1mol DAP in 0.1M HCl at 50mV/s on a glassy carbon electrode.

The potential at which oxidation of the DAP monomer occurs is at 1500mV and thus the potential window that was used for polymerization was from -200mV to +1500mV. One irreversible redox couple is seen at a potential of +250mV, which corresponds to literature since DAP polymerized in various solvents displayed irreversible redox activity between -800mV to -200mV (Thomas KA and Euler WB, 2001; Niu SY. et al., 2004)). The polymer film showed good adherence to the surface of the glassy carbon electrode.

4.2.5. Undoped and doped Poly (phenazine- 2,3- diimino (pyrrol-2-yl))

Figure 25 shows the repeating unit of poly (phenazine-2,3- diimino (pyrrol-2-yl)). PPDP was synthesized as described in section 3.3.1.

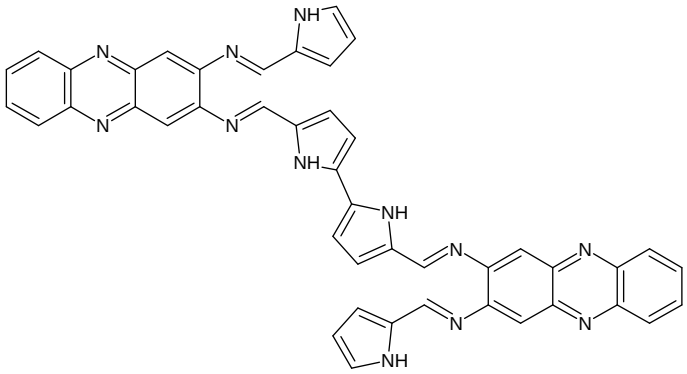

Fig 25: Repeating unit of poly (phenazine 2,3- diimino (pyrrole -2- yl)).

The electrochemically polymerized PPDP and PPDP/NQSA grown at 50mV/s for 25 cycles showed good adherence to the glassy carbon electrode surface. From the polymerization voltammograms (Fig 26a and 26b), one notes that the polymerization current increases as the number of voltammetric cycles increases, indicating that the polymer is indeed forming on the electrode surface and is conductive. As is known, overoxidation and degradation of polypyrrole occurs at high potentials, whilst a too negative potential leads to the evolution of hydrogen (Hiroshi S et al., 2002; Hiroyuki O et al., 2002). Oxidation of the PDP monomer occurs at a higher potential than that of the doped PDP. Thus polymerization was only achievable by cycling the potential from -100mV to +1200mV for the undoped PPDP. Oxidation of the monomer in the presence of NQSA lowers the oxidation potential and thus the potential window of -600mV to +700mV was used.

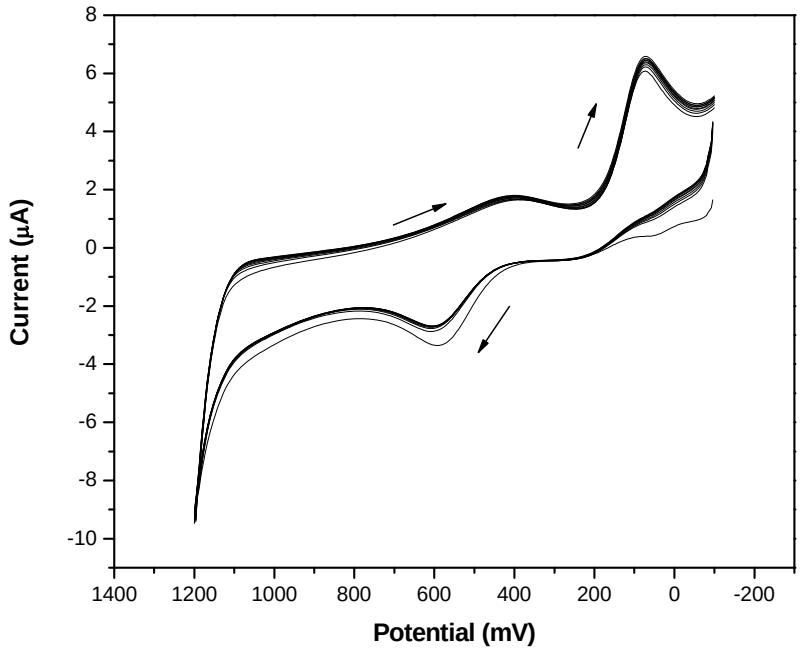

Fig 26a: Polymerization voltammogram of GC/PPDP from 0.5mM PDP in 0.1M HCl/ DMF.

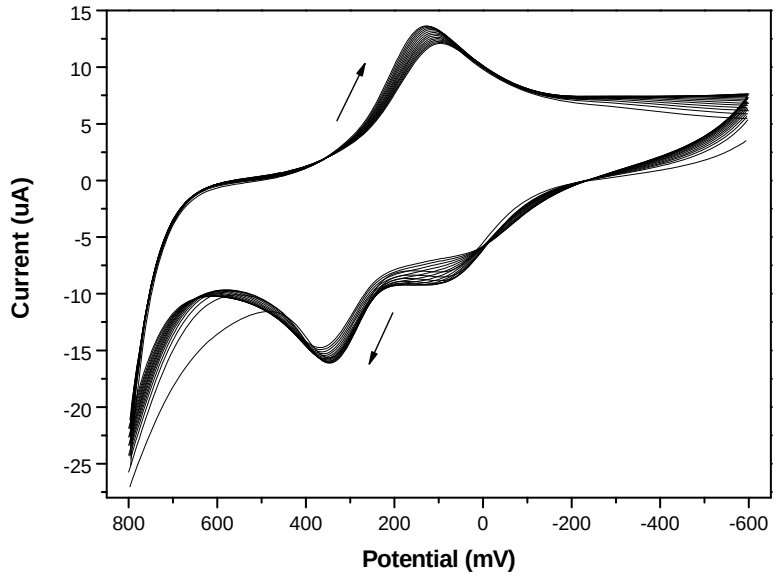

Fig 26b: Polymerization voltammogram of GC/PPDP-NQSA from 0.5mM PDP and 0.05mM NQSA in 0.1M HCl/ DMF (1:1).

The cyclic voltammograms of doped and undoped PPDP (Figure 27a and 27b) shows distinct differences, which is attributed to the presence or absence of NQSA.

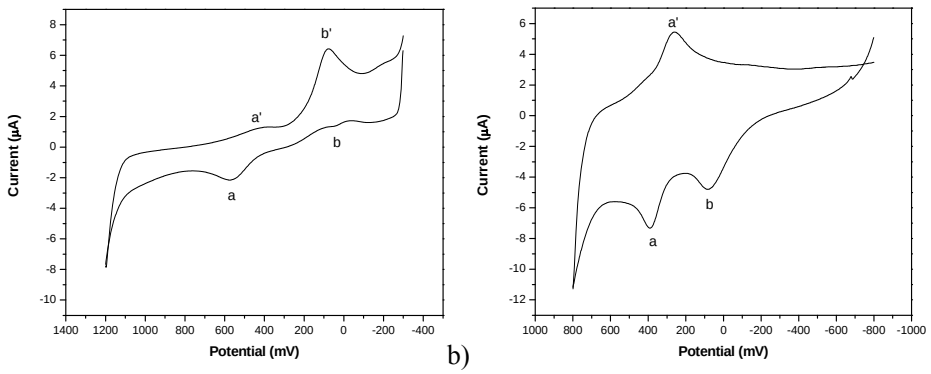

a) b)

Fig 27: CV of a) undoped PPDP and b) PPDP/NQSA at a glassy carbon electrode in 0.1M HCl at a scan rate of 50mV/s.

Undoped PPDP displayed two irreversible redox couples. Couple *a,a'* is similar to undoped PPy (fig 20) and is attributed to the electrochemistry of the pyrrole moiety of PDP, with a oxidation potential of +578mV and reduction potential of +410mV vs Ag/AgCl.. The second couple *b,b'*, is due to the electrochemistry of DAP, as seen from the CV of undoped DAP (fig 24). This couple gave an oxidation potential of +45mV and reduction potential of +76mV.

Doped PPDP shows two redox couples as well. Couple *a,a'* is reversible and at a lower potential compared to that of undoped PPDP and this is attributed to the dopant that enhances the redox behavior of the polymer. From redox couple *b,b'* one notes that peak *b* has intensified at the same potential as for undoped PPDP. This is attributed to the presence of NQSA, which enhanced its electrochemistry. However peak *b'* is no longer present in the CV. This is attributed to the

phenazine moiety of PPDP that has a different electrochemistry in the new copolymer, compared to that of PDAP.

Akinyeye et al. showed that the anodic peak and cathodic peak potential of PPy/NQSA is at +364mV and +301 mV respectively (Akinyeye R et al., 2007). From the multi-scan rate voltammogram of PPDP/NQSA at 50mV/s (Fig 28), it is seen that the anodic peak potential *a,* is at +386mV and the cathodic peak potential *a'* is at +298mV. These potentials are similar to that of PPy/NQSA and thus the redox couple *a: a'* is attributed to the electrochemistry of pyrrole. The second irreversible redox couple displays only one peak, i.e. the anodic potential at +99mV at a scan rate of 50mV/s. DAP polymerized in various solvents displayed irreversible redox activity between -800mV to -200mV (Thomas KA and Euler WB, 2001; Niu SY. et al., 2004)). Thus, peak *b* is attributed to the electrochemistry of the phenazine moiety.

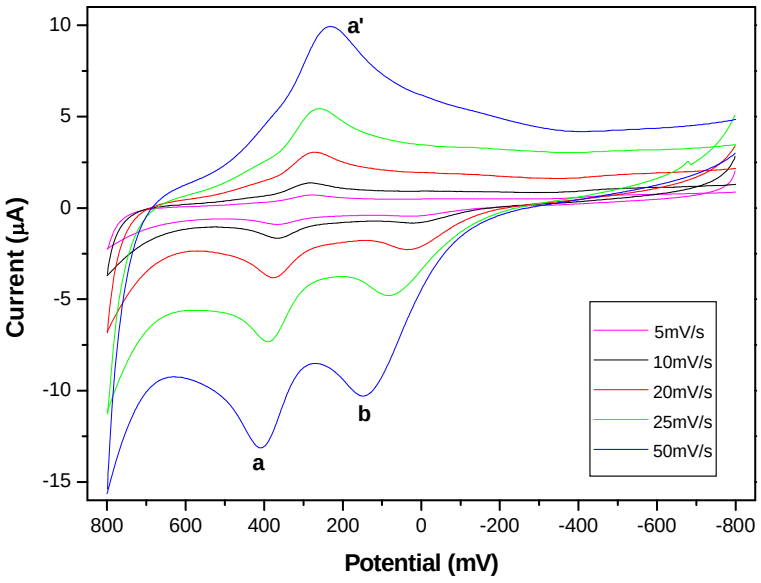

Figure 28: Multi- scan rate voltammogram obtained at a glassy carbon electrode with a thin film of PDPP/NQSA in 0.1M HCl at scan rates of 5, 10, 20, 25 and 50mV/s.

The ratio of Ipc/Ipa ranges from 0.78 for 5mV/s to 0.76 at 100mV/s for *a*:*a*', suggesting a one electron system. The peak separation for the redox couple *a:a'* at 5mV/s is +63mV vs Ag/AgCl, is indicative of a quasi- reversible process. This is also indicates that the polymer is bound to the surface since ΔE_p (E_{pa} - E_{pc}) should be less than 65mV for a surface bound species (Murray RW, 1984; Kelly DM and Vos JG, 1996). The seperation increases progressively from 60mV at 5mV/s to 126mV at 50mV/s coupled with increase in the magnitude of the peak currents with increase scan rates. This shows that the peak currents are diffusion controlled and that diffusion of electrons takes place across the polymer chain, via the conjugated system of pyrrole and phenazine.

The Brown- Anson equation (equation 6) was used to estimate the surface concentration of the polymer ($\Gamma^*_{PPDP/NQSA}$) by plotting the peak currents (I_p) obtained at different scan rates (v), between 5mV/s and 50mV/s, vs. the scan rates.(Brown AP, 1977) (Appendix 2, 5, 8).

$$ip = n^2 F^2 \Gamma^*_{DPPNQSA} (A v/4RT) \ldots\ldots (6)$$

The notations F, A, R, n and T denotes the Faraday constant (96584 $C.mol^{-1}$), working electrode area (0.071cm^2), molar gas constant (8.314 $J.K^{-1}.mol^{-1}$), number of electrons and room temperature (298K) respectively.

The plots gave a trend that confirms the stable film whose density is slightly lower during reduction (1.5 x 10^{-9} mol. cm^{-2}) as compared to oxidation (1.89 x 10^{-9} mol.

cm^{-2}) (redox couple *a:a'*). The plots showed a linear correlation coefficient (r^2) of 0.999, 0.997 and 0.990 respectively for anodic peak *a'*, cathodic peak *a* and anodic peak *b* vs. scan rates. The surface concentration for peak *a'*, *a* and *b* is 1.89 x 10^{-9}mol.cm^{-2}, 1.5 x 10^{-9}mol.cm^{-2} and 1.41 x 10^{-9}mol.cm^{-2} respectively. The speciation of the polymer can be associated with the surface concentration of the electro-active species *a*, *a'* and *b*. From the values of $\Gamma^*_{DPPNQSA}$, it can be seen that the oxidized species *a* is the most abundant and the oxidized form *b* is the least.

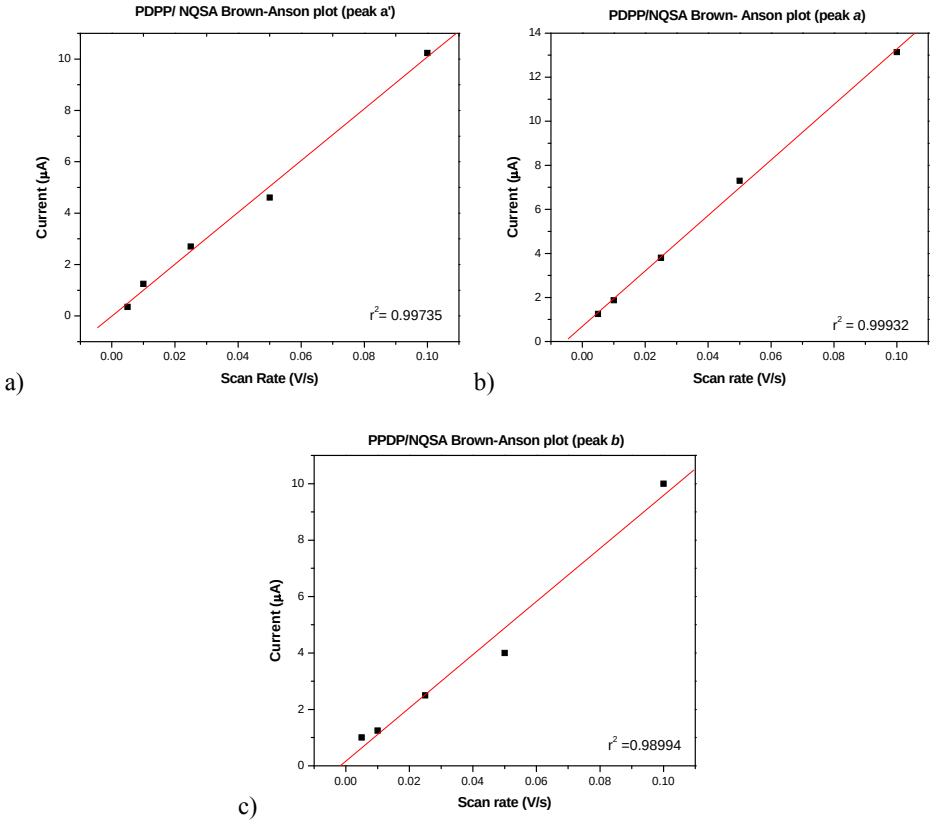

Fig 29: Brown Anson plot of a) peak *a*, b) peak *a'* and c) peak *b*

As mentioned previously the peak currents are diffusion controlled. Thus the Randle- Sevcik equation (equation 7) was applied to determine the diffusion coefficient (D_e) (Bard AJ and Faulkner LR, 2001).

$$Ip,c/v^{1/2} = 0.4463\ (nF)^{3/2}\ A\ D_e{}^{1/2}\ \Gamma^*_{PPDP/NQSA} / L(RT)^{1/2} \quad \ldots\ldots\ldots (7)$$

The notations n, A, D_e, L and C denotes number of electrons, area of the electrode, diffusion coefficient, film thickness and concentration of the electroactive species respectively. Appendix 3, 6 and 9 shows the calculation of D_e by plotting peak current vs. the square root of the scan rate. The correlation coefficients were 0.997, 0.988 and 0.952 for the anodic peak *a*', cathodic peak *a* and anodic peak *b* respectively.

D_e, which is a measure of electron transfer along the polymer chain, was found to be 4.62 x $10^{-7} cm^2.s^{-1}$, 4.61 x $10^{-7} cm^2.s^{-1}$ and 4.39 x $10^{-7} cm^2.s^{-1}$ for the anodic peak *a*', cathodic peak *a* and anodic peak *b* respectively. The values of D_e for both *a* and *a'* are similar, indicating that the deviation from full reversibility does not involve permanent electronic changes in the bulk polypyrrole film upon cycling. (Bard AJ and Faulkner LR, 2001)

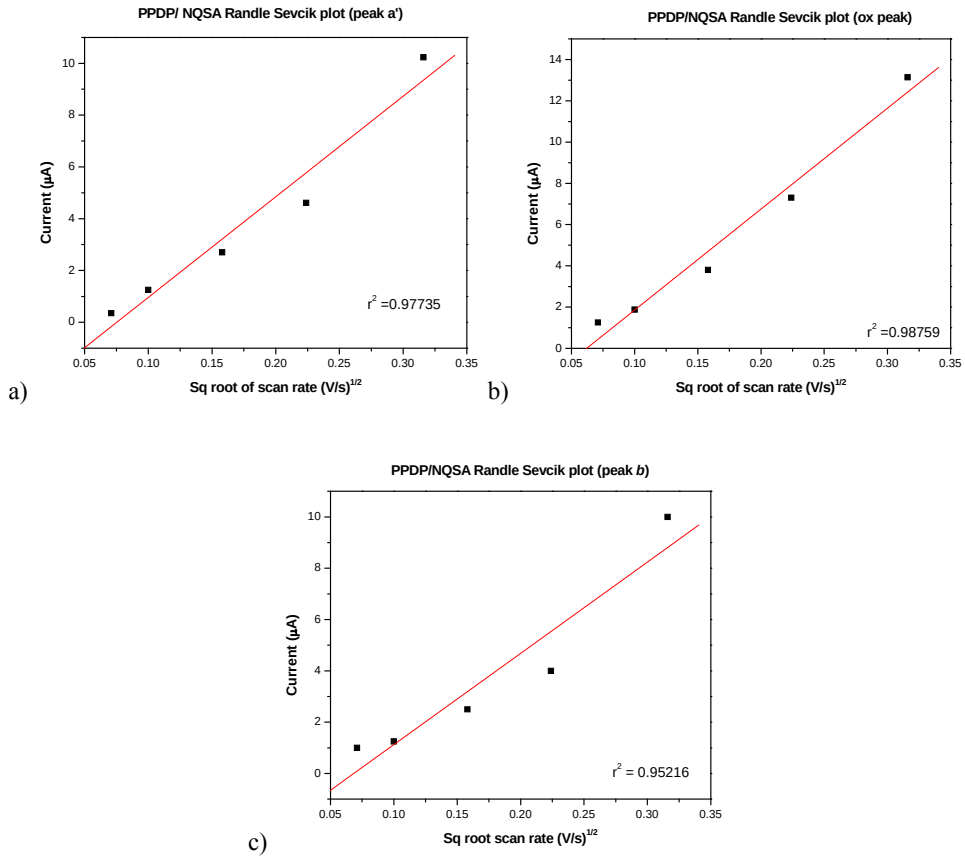

Fig 30: Randle- Sevcik plot of a) peak *a*, b) peak *a'* and c) peak *b*

The cyclic voltammogram at a scan rate of 5mV/s was used to determine the rate constant (k_0) for electron transfer within the polymer chain using the Nicholson treatment for a quasireversible electrochemical system using equation 8 (Bard AJ and Faulkner LR, 2001; Nicholson RS, 1965) (Appendix 4, 7, 10).

$$k' = \psi (\alpha . n . F . \nu . D_e / RT)^{1/2} \ldots\ldots\ldots (8)$$

The transfer coefficient, α, of 0.5 was assumed for the PPDP/NQSA system, as the rate constant does not depend heavily on it, and the kinetic parameter, ψ (dimensionless), was assigned a value of 7 based on the peak seperation (ΔE_p) of 60 mV at a scan rate of 5mV/s. The k_0 value of 1.48 x 10^{-3} $cm.s^{-1}$ was obtained for

the polymer at 5mV/s at all the peak potentials, which confirms the electroactivity of the species. This also indicates that electron hopping along the polymer chain at low scan rate is quite facile. These values are comparable to rate constants of other sulfonated doped polypyrrole conducting polymers, i.e. 2.20 x 10^{-3} cm. s^{-1} for PPyNQSA (Akinyeye R et al., 2007) and 3.75 x 10^{-2} cm. s^{-1} for PPyNSA (Akinyeye R et al., 2006). Other conducting polymers with similar rate constants have been reported, i.e. polyaniline with a k_o value of 5.4 x 10^{-3} $cm.s^{-1}$ (Pauliukaite R et al., 2004) and poly(ethylenedioxythiophene) with a k_o value of 1.5 to 45.3 x 10^{-3} $cm.s^{-1}$ (Sundfords F et al., 2002). Table 2 displays the kinetic parameters as described above.

Table 2: Kinetic parameters for PPDP/NQSA compared to other PPy systems

	PDPP/NQSA (peak a)	**PDPP/NQSA (peak a')**	**PDPP/NQSA (peak b)**	**PPy/NQSA (Akinyeye et al., 2006)**	**PPy/NSA (Akinyeye et al., 2007)**
Γ^* ($mol.cm^{-2}$)	$1.89x10^{-9}$	$1.5x10^{-9}$	$1.41x10^{-9}$	$1.83x10^{-7}$	$2.81x10^{-8}$
D_e ($cm^2.s^{-1}$)	$4.62x10^{-7}$	$4.61x10^{-7}$	$4.39x10^{-7}$	$1.02x10^{-6}$	$1.82x10^{-6}$
k' ($cm.s^{-1}$)	1.48 $x10^{-3}$	1.48 $x10^{-3}$	1.45 $x10^{-3}$	$2.20x10^{-3}$	$3.75x10^{-2}$

The average formal potential estimated from the peak potentials at the different scan rates, is +324mV. OSWV at a frequency of 4Hz and amplitude of 25mV gave a formal potential of +318mV vs. Ag/ AgCl, substantiating the calculated average formal potential (Figure 31).

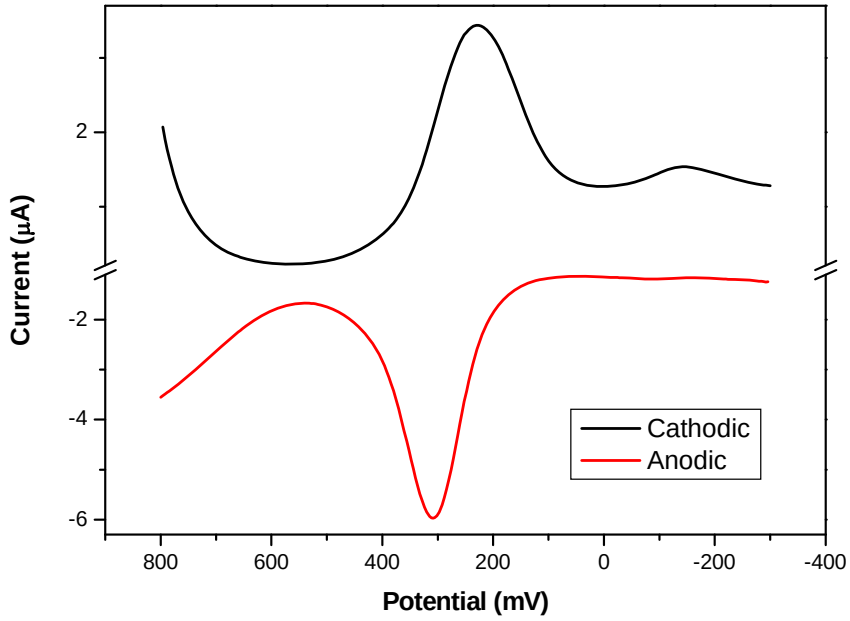

Figure 31: OSWV of GC/PPDP/NQSA in 0.1M HCl.

4.3 EIS measurements

4.3.1 PPDP/NQSA

EIS data was collected in consecutive 100mV steps, in the potential range of 100mV to 500mV. This potential range corresponds to the redox active window of PPDP/NQSA and was done to assess the formal potential and substantiate the value determined from square wave analysis.

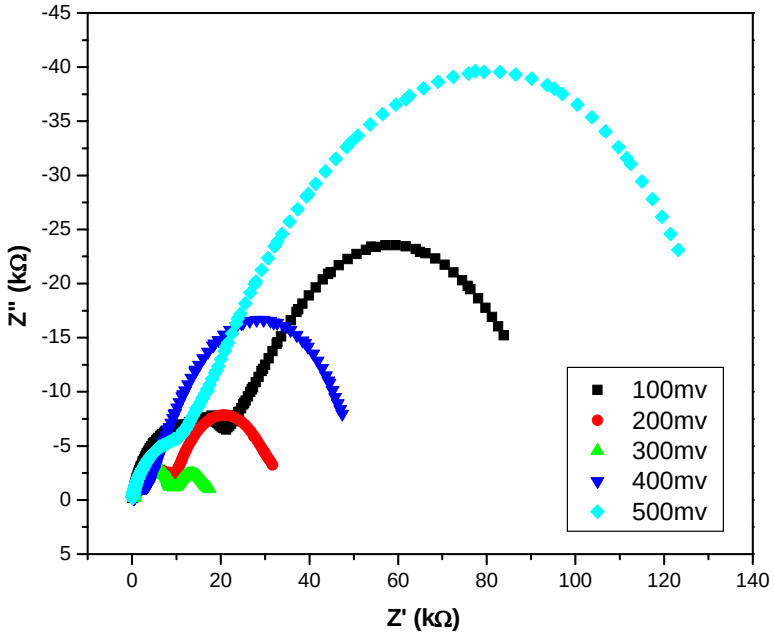

Fig 32: EIS spectra of PPDP/NQSA in 0.1M HCl from 100mV to 500mV vs Ag/AgCl, with 100mV steps.

The potential with the lowest impedance is the formal potential. This is seen at 300mV in Figure 29. The same experiment was repeated from 300mV to 340mV vs Ag/AgCl, with 20mV interval steps. The formal potential, as seen from Figure 30, is found to be at +320mV. This coincides with the value from square wave,

i.e. +318mV. The formal potential of +320mV was then used to determine the film thickness.

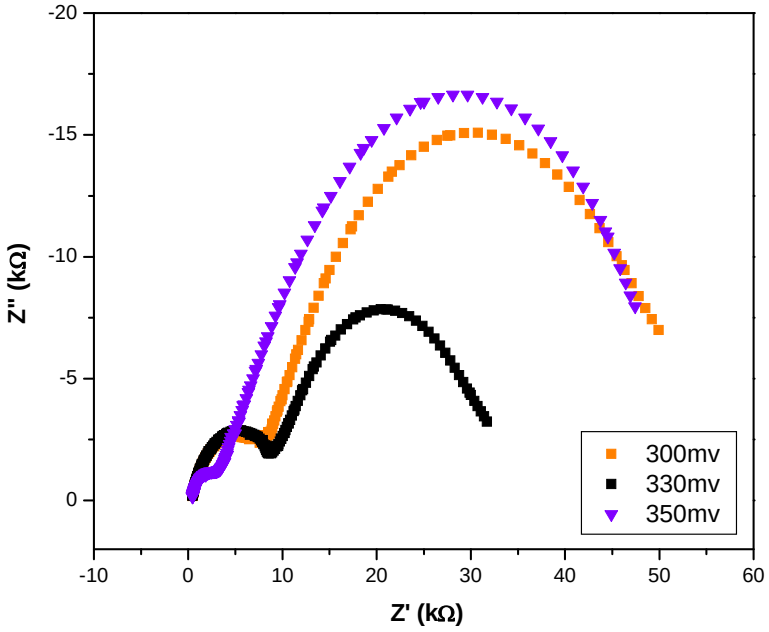

Fig 33: EIS spectra of PPDP/NQSA in 0.1M HCl from 200mV to 350mV vs Ag/AgCl, with 50mV steps.

To quantitatively analyze the behavior of PPDP films, the experimental results were fitted to an equivalent circuit, where the values of the electrical components are associated with the physical/ chemical properties of the electrochemical systems (Barcia OE et al., 2002), using a non- linear least squares fitting method by Zahner (Thales- SIM) fitting program. The equivalent circuit (Figure 30) consists of the solution resistance (R_s) in series with $R_{ct1}C_1$ parallel combination, which is in series with $R_{ct2}CPE_2$ parallel combination. The combination $R_{ct1}C$ models the movement of electron hopping along the polymer backbone. The second component $R_{ct2}CPE_2$ represents the electrode/ solution interface (Grzeszczuk M. and Zabinska-Olszak G., 1997; Mahon PJ. et al., 2000). R_s is the

high- frequency solution resistance, C is the double layer capacitance, R_{ct1} is the high- frequency ionic charge transfer resistance at the polymer/ electrolyte interface or electron transfer resistance at the GC/electrode interface. R_{ct2} is the low- frequency electron transfer resistance of the redox reactions and CPE_2 is the constant phase element for bulk faradaic pseudocapacitance (Hallik A. et al., 2006).

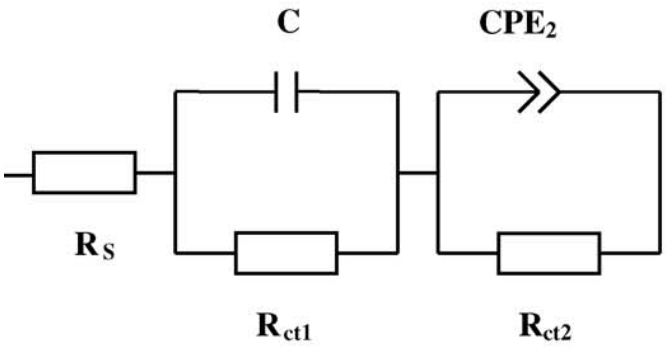

Fig 34: Equivalent circuit used to fit the results from Impedance.

The capacitance is replaced by a CPE (constant phase element), since polymer films have rough or porous surfaces and thus the CPE compensates the geometrical and energetical inhomogeneity of the electrode surface (Lasia A. et al., 1999; MacDonald JR and Johnson WB., 1987). The quality of the fit obtained by using different equivalent circuits was estimated by the relative errors (%) and significance of each parameter values.

The complex plane plot (Figure 32, 33 and 35) shows two distinctive well-defined semi-circles, the smaller one in the high frequency range and the bigger one in the low frequency range. The complex plane plot at 320mV was used to determine the different components of the equivalent circuit and their average values were

found to be: R_S=333.4 Ω, R_{CT1}= 9.318 kΩ, R_{CT2}=21.6 kΩ, C_1=29.29 nF and CPE_2=3.811 μF.

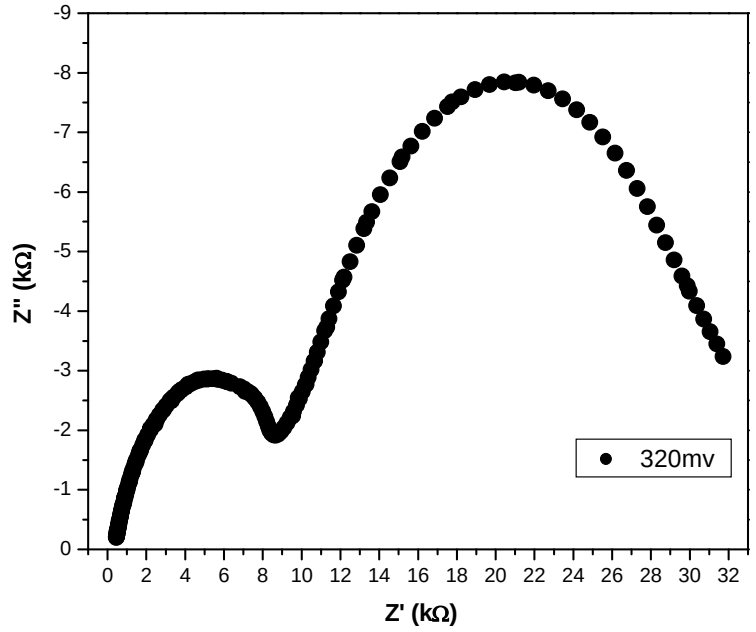

Fig 35: EIS spectra of PPDP/NQSDA at 320mV vs Ag/AgCl

The film thickness of the polymer film can be determined from equation 5:

$$L = \varepsilon_r \varepsilon_o A/C \ldots\ldots (5)$$

where C is the capacitance, ε_r is the dielectric constant (62.7 er) (Hasagawa S et al., 1986), ε_o is the vacuum permittivity (8.85 x 10^{-12} $F.m^{-1}$), A is the geometrical electrode surface area (0.071 cm^2) and L is the film thickness (Giménez-Romero D et al., 2006; Verge MG et al., 2004). At the formal potential the reduced and oxidized species are in equilibrium, thus the film thickness at this potential would be that of the neutral polymer species. The semicircle in the high frequency region is attributed to the charging-discharging of the double layer at the GC/PPDP interface and the low frequency semicircle is due to the charge transport processes in the PPDP/NQSA film (Gime´nez-Romero D. et al., 2006). Thus the film

thickness was determined from low frequency semicircle. The value calculated for L calculated at the formal potential was found to be 1.03 µm. This is comparable with the film thickness of 0.755 µm, as determined from CV (Appendix 1).

EIS measurements were then done at the reduction potential of +320mV in 0.1M HCl. The film underwent cation exchange by subjecting the polymer to the reduction potential of +320mV vs Ag/AgCl for 20 minutes (time- based potentiometry), in different solvents (0.1M NaCl, KCl, $CaCl_2$), followed by EIS at +320mV in these solvents respectively. The complex plane plots for these are seen in Figure 36.

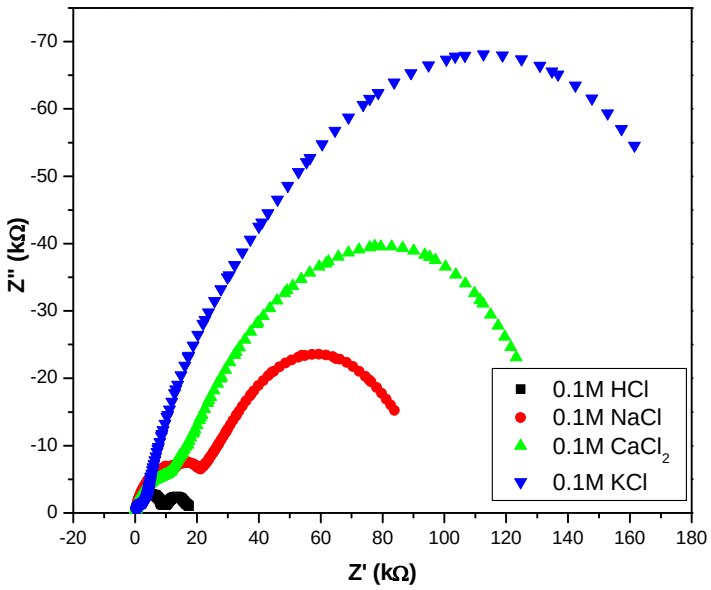

Fig 36: Complex plane plots of PPDP/NQSA in different solvents at +300mV vs Ag/AgCl.

The circuit elements and film thicknesses were calculated as described previously and their values are given in Table 3.

Table 3: Circuit elements and film thicknesses of PPDP/NQSA in different solvents

	HCl	NaCl	$CaCl_2$	KCl
R_s (Ω)	338	352.78	357.5	383
R_{CT1} (kΩ)	8.969	19.63	10.83	2.249
R_{CT2} (kΩ)	27.711	74.56	131.9	232
C (nF)	24.63	21.74	26.54	47.83
CPE_2 (µF)	3.76	3.45	3.26	3.03
L (µm)	1.05	1.14	1.21	1.30

The film thickness at the reduction potential is greater than that at the formal potential in 0.1M HCl. This is due to charged chains that are formed during reduction that repel each other, creating free space for the cations to be inserted.

As can be seen CPE_2 values decrease, accompanied by an increase in film thickness, with an increase in the size of the cation. During reduction electrons are added to the polymer chain, resulting in an overall negative charge across the polymer chain. The cations in solution migrate to the polymer surface to neutralize the charge. The size of cationic radius is $K^+ > Ca^{2+} > Na^+ > H^+$. Thus this trend in increase in film thickness, i.e. KCl > $CaCl_2$>NaCl>HCl, is attributed to the increase in the ionic radii of the cations.

The reluctance of the flux of charge to the electrode surface is the charge transfer resistance. The charge transfer resistance (R_{ct2}) increases upon increase in ionic radius, and is attributed to the increased size of the cation, which has greater difficulty being incorporated into the polymer backbone.

4.3.2 PPy/NQSA

The same procedure was followed for PPy/NQSA as 4.4.1. Figure 37 shows the complex plane plots between 100 mV and 700 mV, using 100mV interval steps in 0.1M HCl and Figure 38 between 280 and 340 mV, with 20 mV interval steps.

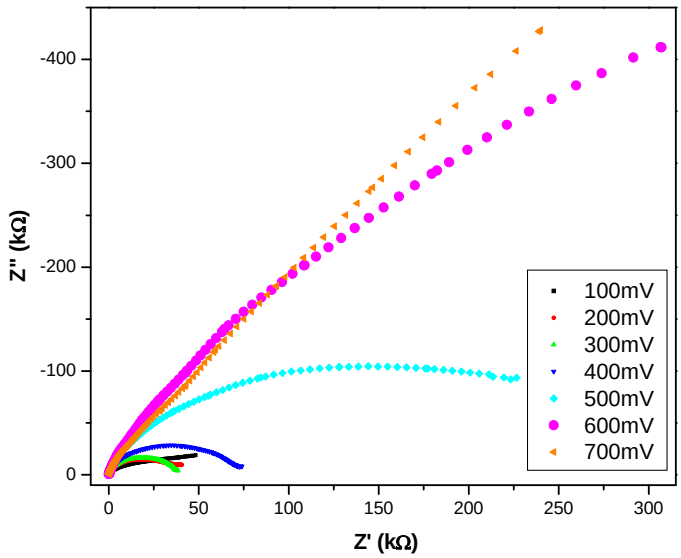

Fig. 37: Complex plane impedance of Ppy/NQSA from 100 to 700mV, with 100mV interval steps, in 0.1M HCl.

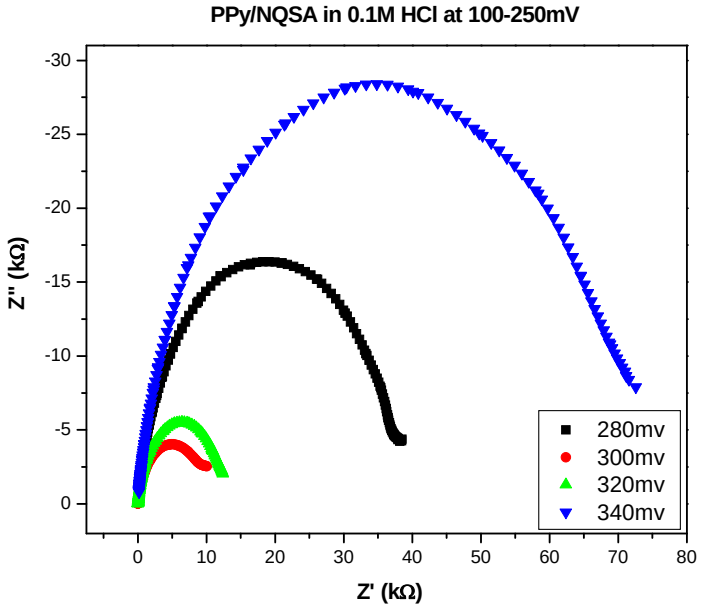

Fig 38: Complex plane impedance of Ppy/NQSA from 200 to 350mV, with 50mV interval steps, in 0.1M HCl.

The formal potential was found to be +320mV vs Ag/AgCl. This is in good agreement of the results found by Akinyeye et al. (Akinyeye R et al., 2007). Figure 39 shows the complex plane plot of PPy/NQSA at +320mV using different solvents.

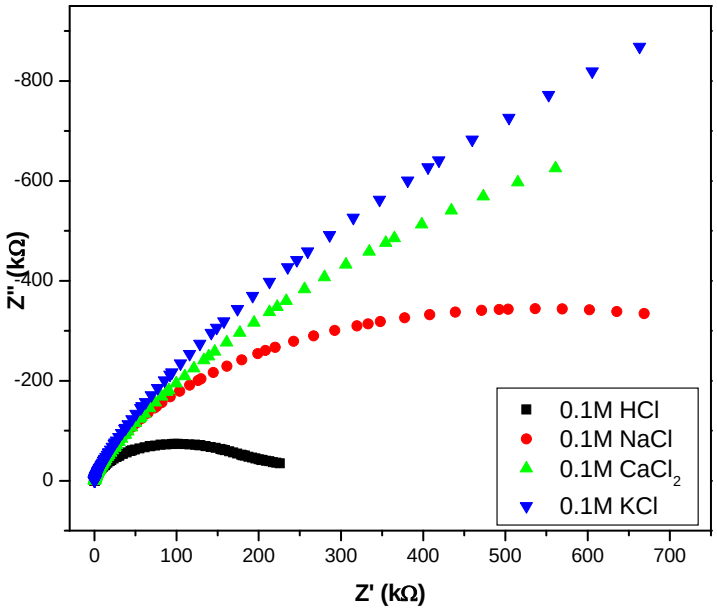

Fig 39: Complex plane plots of PPy/NQSA in different solvents at +320mV vs Ag/AgCl.

The equivalent circuit that was fitted to the results is the same for that of PPDP/NQSA. Table 4 lists the values of the circuit elements calculated as described earlier.

Table 4: Circuit elements and film thicknesses of PPy/NQSA in different solvents

	E^o in 0.1M HCl	HCl	NaCl	$CaCl_2$	KCl
R_s (Ω)	219.7	200.7	224.5	258 x 10^3	307 x 10^3
R_{CT1} (kΩ)	94.7	90	126.5	80.7	102.8
R_{CT2} (kΩ)	68.64	87.6	95.8	157.1	159
C (nF)	736	750	764.8	710	740.2
CPE_2 (nF)	20.5	19.5	15.2	12.9	10.7
L (µm)	0.188	0.20	0.26	0.31	0.37

Table 5 shows a comparison between the film thicknesses of PPy/NQSA and PPDP/NQSA in different solvents.

Table 5: Comparison between the film thicknesses of PPy/NQSA and PPDP/NQSA in different solvents

	E^o in 0.1M HCl	HCl	NaCl	$CaCl_2$	KCl
PPY/NQSA (µm)	0.188	0.20	0.26	0.31	0.37
PPDP/NQSA (µm)	1.03	1.05	1.14	1.21	1.30

From this data, the magnitude of volume change from the neutral to the reduced species in 0.1 M HCl for PPDP/NQSA is 0.023 µm, while that for PPy/NQSA is 0.012 µm. This is attributed to the Π- Π stacking effect of charged pyrrole units of PDPP, compared to PPy where this stacking does not occur. Stacking refers to a stacked arrangement of aromatic molecules that interact with each other through aromatic interactions. An aromatic interaction (or Π- Π stacking) is a non-

covalent interaction between organic compounds containing aromatic moieties, which are caused by intermolecular overlapping of p- orbitals in Π- conjugated systems. Thus upon reduction of PPDP, the charged pyrrole units in the polymer network repel each other to a greater extent than the pyrrole units of polypyrrole due to the overlap of p- obitals of PPDP, as depicted in Fig 40, causing PPDP to undergo a greater change in film thickness that PPy.

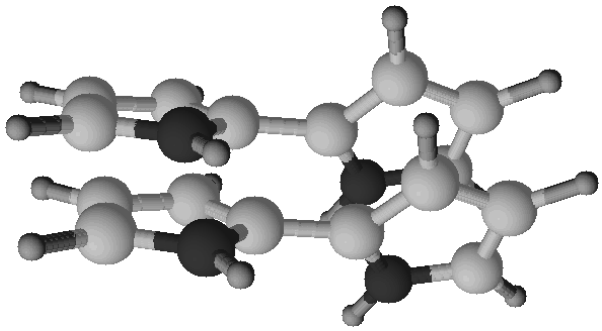

Fig 40: Schematic representation of Π- Π stacking in the pyrrole units of PPDP.

The main drawback that conventional actuators possess is their limited maximum strain. The mechanism of actuation is governed by the movement of ions into and out of the polymer network; thus when the polymer reaches its maximum strain no further ions can be incorporated into its backbone. However, due to the Π- Π stacking of PPDP this strain was increased, evident by the increase in the magnitude of film thickness from the neutral to charged species. This makes PPDP is a better actuator material than PPy.

4.4 SEM analysis of PPDP/NQSA and PPy/NQSA

Scanning Electron Microscope studies were carried out on screen- printed carbon electrodes (SPCE). This technique was used to assess the morphologhy of the modified electrodes. Figure 41a shows the surface of a typical bare SPCE. The graphite particles can clearly be seen.

a)

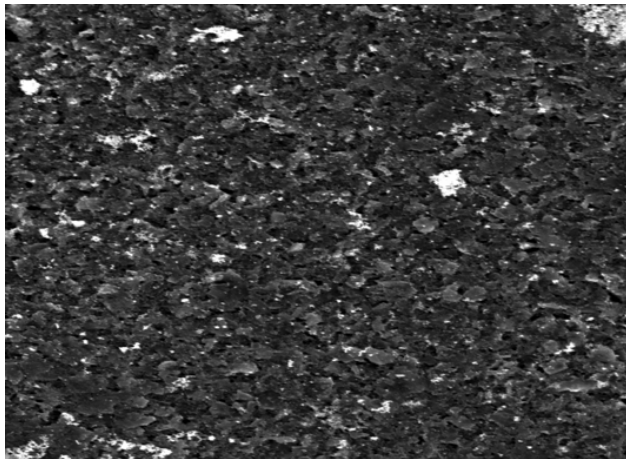

b)

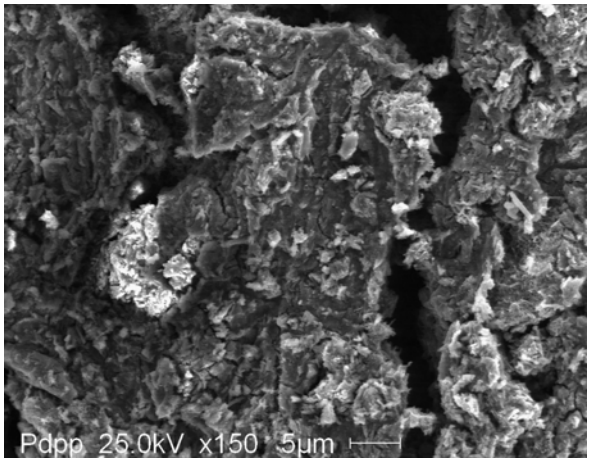

c) 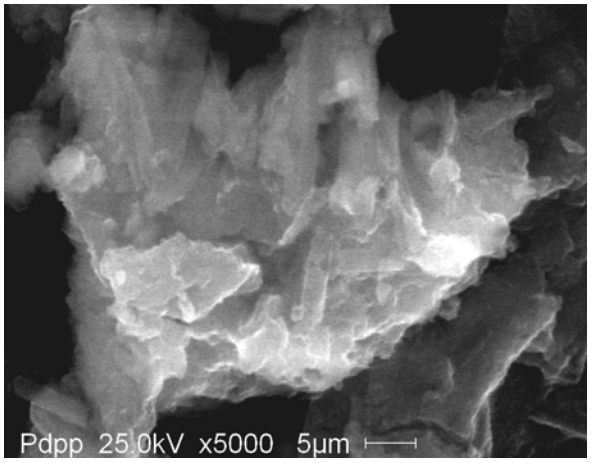

Fig 41: SEM images of screen printed electrodes (area 0.09 cm^2): a) bare SPCE, b) and c) PDPP/NQSA modified SPCE.

The surface of a PPDP/NQSA deposited SPCE is shown in Figures 41 b and c. A very rough, porous, crystalline structure is seen, whose morphology is attributed to the electrochemical synthesis conditions, i.e. concentration of solvent, temperature and pH (Prasad KR and Munichandraiah N, 2001). The polymer covers the greatest part of the surface, indicating that the polymer is surface bound.

Figure 42 shows the SEM images of PPy/NQSA.

a) 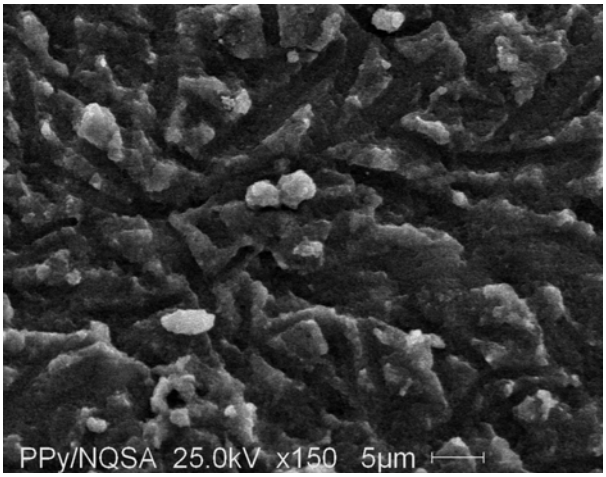

b) 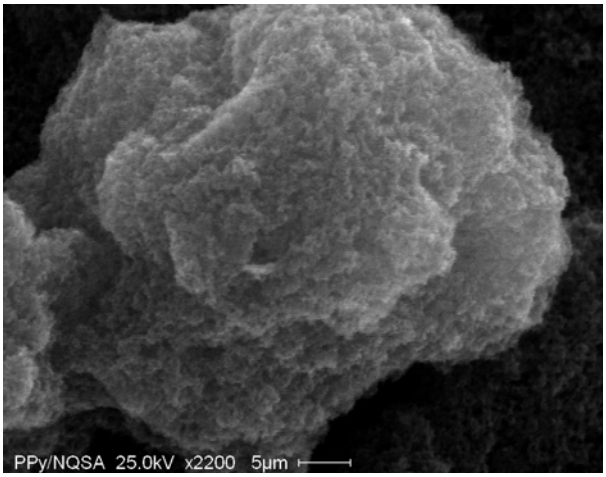

Fig 42: SEM images of Ppy/NQSA modified screen printed electrodes

The SEM image shows that the polymer covered all of the SPCE, having a more granular morphology compared to that of PPDP/NQSA. The topography is smoother and speckled grains can be seen.

References:

Akinyeye, Richard Odunayo; Michira, Immaculate; Sekota, Mantoa; Al Ahmed, Amir; Tito, Duarte; Baker, Priscilla Gloria Lorraine; Brett, Christopher Michael Ashton; Kalaji, Maher; Iwuoha, Emmanuel. **Electrochemical synthesis and characterization of 1,2-naphthaquinone-4-sulfonic acid doped polypyrrole.** Electroanalysis (2007), 19(2-3), 303-309.

Akinyeye, Richard; Michira, Immaculate; Sekota, Mantoa; Al-Ahmed, Amir; Baker, Priscilla; Iwuoha, Emmanuel. **Electrochemical interrogation and sensor applications of nanostructured polypyrroles.** Electroanalysis (2006), 18(24), 2441-2450.

Barcia, O. E.; D'Elia, E.; Frateur, I.; Mattos, O. R.; Pebere, N.; Tribollet, B. **Application of the impedance model of de Levie for the characterization of porous electrodes.** Electrochimica Acta (2002), 47(13-14), 2109-2116.

Bard, A. J.; Faulkner, L. R. **Electrochemical Methods: fundamentals and applications.** Dianhuaxue (2001), 7(2), 255

Bisquert, Juan; Garcia-Belmonte, Germa; Fabregat-Santiago, Francisco; Ferriols, Noemi S.; Bogdanoff, Peter; Pereira, Ernesto C. **Doubling Exponent Models for the Analysis of Porous Film Electrodes by Impedance. Relaxation of TiO2 Nanoporous in Aqueous Solution.** Journal of Physical Chemistry B (2000), 104(10), 2287-2298.

Brown, Alan P.; Anson, Fred C. **Cyclic and differential pulse voltammetric behavior of reactants confined to the electrode surface.** Analytical Chemistry (1977), 49(11), 1589-95.

Chohan, Zahid H., and Kausar Samina. **Synthesis, characterization and biological properties of tridentate NNO, NNS and NNN DONOR thiazole-derived furanyl, thiophenyl and pyrrolyl schiff bases and their Co(ll), Cu(ll), Ni(ll) and Zn(ll) metal chelates**. Metal-Based Drugs (2000), 7 (1).

Gimenez-Romero, D.; Bueno, P. R.; Castano, C.; Gabrielli, C.; Perrot, H.; Garcia-Jareno, J. J.; Vicente, F. **Electrochemical impedance spectroscopy as a tool to estimate thickness in PB films.** Electrochemistry Communications (2006), 8(3), 371-374.

Grzeszczuk, Maria; Zabinska-Olszak, Grazyna. **Effects of the secondary counterions in the electrochemistry of polypyrrole.** Journal of Electroanalytical Chemistry (1997), 427(1-2), 169-177.

Hallik, Allan; Alumaa, Ants; Tamm, Jueri; Sammelselg, Vaeino; Vaeaertnou, Mart; Jaenes, Alar; Lust, Enn. **Analysis of electrochemical impedance of polypyrrole|sulfate and polypyrrole|perchlorate films.** Synthetic Metals (2006), 156(5-6), 488-494.

Kelly, David M.; Vos, Johannes G. **The influence of acetonitrile and methanol on the charge transport properties of [Os(bipy)2(PVP)10Cl]Cl films.** Electrochimica Acta (1996), 41(11/12), 1825-1832.

Krause, Steffi. **Impedance methods.** Encyclopedia of Electrochemistry (2003), 3 196-229.

Lasia, Andrzej. **Electrochemical impedance spectroscopy and its applications.** Modern Aspects of Electrochemistry (1999), 32 143-248.

Li, X.-G.; Huang, M.-R.; Wang, L.-X.; Zhu, M.-F.; Menner, A.; Springer, J. **Synthesis and characterization of pyrrole and m-toluidine copolymers.** Synthetic Metals (2001), 123(3), 435-441.

Mabrouk, Patricia Ann. **Oxidative electropolymerization of pyrrole from neat monomer solution.** Synthetic Metals (2005), 150(1), 101-105.

MacDonald, J. Ross. **Impedance spectroscopy and its use in analyzing the steady-state ac response of solid and liquid electrolytes.** Journal of Electroanalytical Chemistry and Interfacial Electrochemistry (1987), 223(1-2), 25-50.

Mahon, P. J.; Paul, G. L.; Keshishian, S. M.; Vassallo, A. M. **Measurement and modeling of the high-power performance of carbon-based supercapacitors.** Journal of Power Sources (2000), 91(1), 68-76.

Martini, Milena; Matencio, Tullio; Alonso-Vante, Nicolas; De Paoli, Marco-Aurelio. **Electrochemical impedance spectroscopy of dodecyl sulfate doped polypyrrole films in the dark and under illumination.** Journal of the Brazilian Chemical Society (2000), 11(1), 50-58.

Murray, Royce W.. **Polymer modification of electrodes.** Annual Review of Materials Science (1984), 14 145-69.

Nicholson, Richard S.. **Some examples of the numerical solution of nonlinear integral equations.** Anal. Chem. (1965), 37(6), 667-71.

Niu, S. Y.; Zhang, S. S.; Ma, L. B.; Jiao, K. **Electrochemical and spectroscopic studies on the interaction between DNA and the product of enzyme-catalyzed reaction of OPD-H2O2-HRP.** Bulletin of the Korean Chemical Society (2004), 25(6), 829-832.

Okuno Hiroyuki; Kitano Tonomi; Yakabe Hidetaka; Kishimoto Masayoshi; Deore Bhavana A; Siigi Hiroshi; Nagaoka Tsutomu **Characterization of overoxidized polypyrrole colloids imprinted with L-lactate and their application to enantioseparation of amino acids**. Analytical chemistry (2002), 74(16), 4184-90.

Pauliukaite, Rasa; Brett, Christopher M. A.; Monkman, Andrew P. **Polyaniline fibres as electrodes. Electrochemical characterisation in acid solutions.** Electrochimica Acta (2004), 50(1), 159-167.

Rice Corey A; Dauster Ingo; Suhm Martin A **Infrared spectroscopy of pyrrole - 2 - carboxaldehyde and its dimer: a planar beta-sheet peptide model?**. The Journal of chemical physics (2007), 126(13), 134313.

Shiigi, Hiroshi; Okamura, Kentaro; Kijima, Daisuke; Hironaka, Akane; Deore, Bhavana; Sree, Usha; Nagaoka, Tsutomu. **Fabrication Process and Characterization of a Novel Structural Isomer Sensor. Molecularly Imprinted Overoxidized Polypyrrole Film.** Electrochemical and Solid-State Letters (2003), 6(1), H1-H3.

Thomas, K. A.; Euler, W. B. **An electrochemical, spectroscopic, and theoretical study of poly(2,3-diaminophenazine).** Journal of Electroanalytical Chemistry (2001), 501(1-2), 235-240.

Verge, M.-G.; Olsson, C.-O. A.; Landolt, D. **Anodic oxide growth on tungsten studied by EQCM, EIS and AES.** Corrosion Science (2004), 46(10), 2583-2600.

CONCLUSIONS AND FUTURE WORK

6.1 Conclusions

The Schiff-base product phenazine- 2,3- diimino (pyrrol-2-yl) has successfully been synthesized by the condensation reaction of pyrrole-2-carboxaldehyde and 2,3-diaminophenazine. Poly(phenazine- 2,3- diimino (pyrrol-2-yl)) was electrochemically synthesized on a glassy carbon electrode, showing good adherence to the electrode and electrochemistry between +100 and +500mV vs Ag/AgCl.

The actuating mechanism of PPDP/NQSA and PPy/NQSA has successfully been evaluated, using EIS. It is evident that PPDP is a better actuator material than PPy by the magnitude of change in the film thickness from the neutral to the charges species. PPDP underwent a greater change in film thickness than PPy, due to the Π- stacking of pyrrole moieties in the PPDP. This Π- stacking phenomenon allows more ions to be inserted into the polymer backbone, resulting in a greater change in film thickness, thus making this polymer a better actuator than PPy, where Π- stacking does not occur.

It is due to this change in film thickness that PPDP can be used in controlled drug release systems, acting as a hydrogel. The controlled drug release mechanism of hydrogels are based on the release of active ingredient/ drug due to changes in its environment, i.e. pH, temperature, etc. This is comparable with the contraction and expansion mechanism of PPDP. Due to the conformational changes in PPDP, bulkier

ions can be incorporated into its structure. Thus drugs/active ingredients can be stored in the polymer network upon reduction of PPDP, resulting in a 'swelled' polymer. Upon oxidation the drug will then be released in a controlled manner, by application of a appropriate potential into its environment, and the polymer returns to its original form. The same mechanism makes this polymer viable to be used as artificial muscle in robotics.

6.2 Future work

Future work includes assessing the toxicity of PPDP/NQSA to the human body, as one of the requirements for a controlled drug release material is that it should be degradable and not produce harmful by-products upon degradation in the human body. Their mechanical properties, i.e. strain, lifetime, stress, etc. should also be determined to assess its viability as artificial muscle. Designing hinged polymers with quaterpyrrole units between the hinges should also be investigated as quaterpyrrole units will give even larger conformational changes compared to the bipyrrole units of PPDP.

APPENDIX 1: Determination of film thickness

The film thickness of a film can be determined form CV by the following equation (Giminez- Romero et al., 2006):

$$L = Q\, d^3 N_A / 4nFA \text{ ..... (...)}$$

where
L = film thickness
Q = charge
d = length of the unit cell (7.3Å) (Warren MR. and Madden JD, 2006),
N_A = Avogadro's number (6.0223 x 10^{-23} mol^{-1})
n = number of electrons (1)
F = faraday's constant (96584 $C.mol^{-1}$)
A = area of the electrode (0.071cm^2)
The value 4 is given since there is 4 pyrrole units per unit cell

Q is determined by the area under either redox peak.

$$Q = \text{Area} \times 1/V$$

Peak *a*' was chosen and Q was found to be 8.837 x 10^{-3} C.

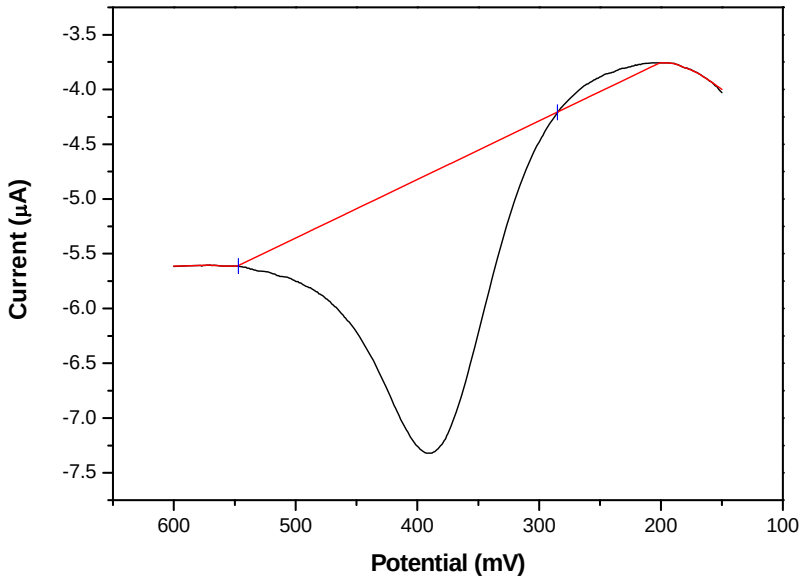

$L = Q\, d^3 N_A / 4nFA$
$= (8.837 \times 10^{-3} C) \times (7.3 \times 10^{-8} cm)^3 \times (6.0223 \times 10^{23} mol^{-1}) / 4 \times 1 \times (96584 C.mol^{-1})(0.071 cm^2)$

$L = 0.755 \times 10^{-4}$ cm = 0.755 µm

APPENDIX 2: Brown Anson Plot of PPDP/NQSA at peak *a*'

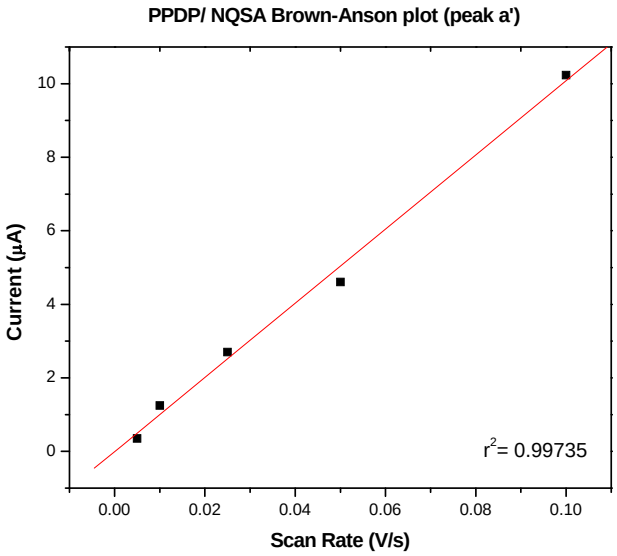

Slope = 1.01 x 10^{-4} A. $(V/s)^{-1}$

Brown- Anson equation

$ip = n^2 F^2 \Gamma^*_{DPPNQSA} (A\ v/4RT)$

where:

*i*p is the peak current
n is the electron stoichiometry
A is the electrode area (cm^2)
C is the concentration (mol/cm^3)
v is the scan rate (V/s)
F is the Faraday's constant (96584 C. mol^{-1})
R is the Molar gas constant (8.314 J / mol K)
T is the room temperature (298K)
Γ^* is the surface concentration

* Diameter of glassy carbon electrode: 0.3cm
Area= ¼. Π. $Diameter^2 = 0.071cm^2$

* Number of electrons: Epa-Epc= 0.059/n volts
n = 0.059/Epa-Epc
= 0.059/(0.367-0.285)
= 0.72
= 1

$ip/v = n^2 F^2 \Gamma^*_{DPPNQSA.} A/(4RT)$
$= n^2 F^2 \Gamma^*_{DPPNQSA} A / (4RT)$
$= (1)^2.(96584\ C^2.\ mol^{-2})^2.\Gamma^*_{DPPNQSA.} (0.071cm^2)./(\ 4x8.314\ J.mol^{-1}K^{-1}x\ 298K)$
1.01 x 10^{-4} A. $(V/s)^{-1}$ = 6.68 x 10^{4} $C^2.mol^{-1}.cm^2.\ J^{-1}$ x $\Gamma^*_{DPPNQSA}$

$\Gamma^*_{DPPNQSA}$ = 1.5 x 10^{-9} mol. cm^{-2}

APPENDIX 3: Randle- Sevcik Plot of PPDP/NQSA at peak *a'*

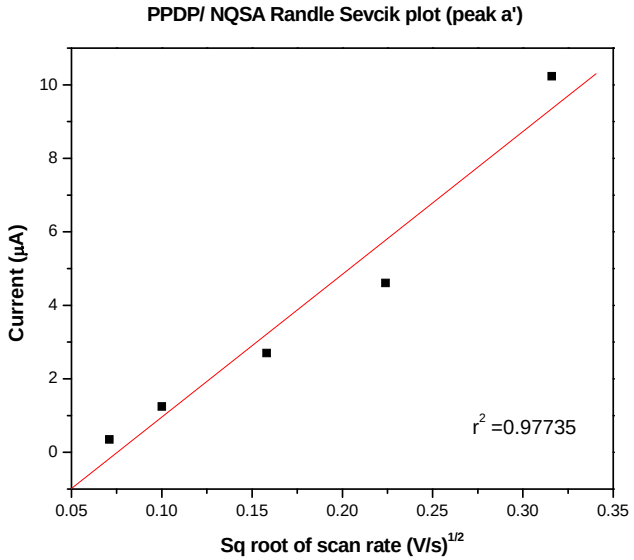

Slope= 3.89 x 10^{-4} A. $(V/s)^{-1/2}$

Randle Sevcik equation*:*

$ip = (2.69 \times 10^5) n^{3/2} A D^{1/2} \Gamma^*_{DPPNQSA} / L \nu^{1/2}$

where:

*i*p is the peak current

n is the electron stoichiometry

A is the electrode area (cm^2)

D is the diffusion current

$\Gamma^*_{DPPNQSA}$ is the surface concentration

L is the film thickness

v is the scan rate (V/s)

$ip / v^{1/2} = (2.69 \times 10^5) n^{3/2} A D^{1/2}$

3.89×10^{-4} A. $(V/s)^{-1/2} = (2.69 \times 10^5)\, n^{3/2} A D^{1/2} \Gamma^*_{DPPNQSA} / L$

$D_e = 4.62 \times 10^{-7}\ cm^2.\ s^{-1}$

APPENDIX 4: Determination of rate constant of PPDP/NQSA at peak *a'*

Determination of rate constant (k') at 5mV/s

This is obtained from the **Nicholson equation**:
$k' = \psi (\alpha . n . F . \nu . D_e / RT)^{1/2}$
where:
Ψ is a dimensionless parameter that is given the value of 7 since Epa-Epc = 60.
k' is independent of α and is assumed to be 0.5

$k' = \psi (\alpha . n . F . \nu . D_e / RT)^{1/2}$
$= 7 ((0.5) \times (1) \times (96584 C.mol^{-1}) \times (0.005 V.s^{-1}) \times (4.62 \times 10^{-7} cm^2.s^{-1}) / (8.314 J\ mol^{-1}K^{-1}) (298K))^{1/2}$

$k' = 1.48 \times 10^{-3}$ cm. s^{-1}

APPENDIX 5: Brown Anson Plot of PPDP/NQSA at peak *a*

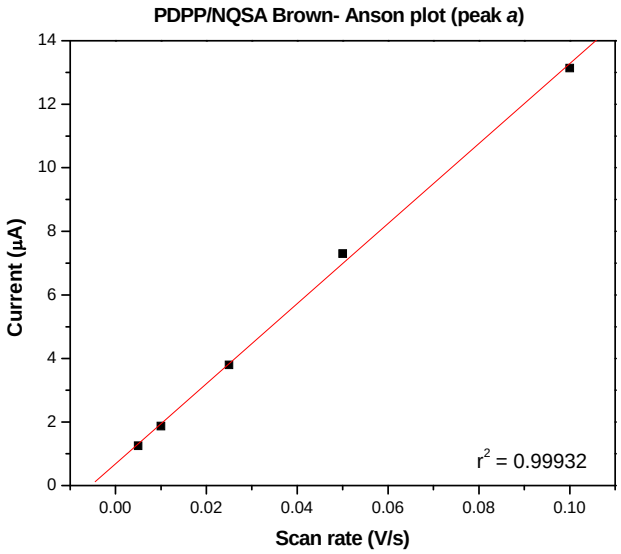

Slope = 1.26 x 10^{-4} A. $(V/s)^{-1}$

Brown- Anson equation

$ip = n^2 F^2 \Gamma^*_{DPPNQSA} (A\ v/4RT)$

where:

*i*p is the peak current

n is the electron stoichiometry

A is the electrode area (cm^2)

C is the concentration (mol/cm^3)

v is the scan rate (V/s)

F is the Faraday's constant (96584 C. mol^{-1})

R is the Molar gas constant (8.314 J / mol K)

T is the room temperature (298K)

Γ^* is the surface concentration

* Diameter of glassy carbon electrode: 0.3cm

Area= ¼. Π. $Diameter^2 = 0.071cm^2$

* Number of electrons: Epa-Epc= 0.059/n volts

n = 0.059/Epa-Epc

= 0.059/(0.367-0.285)

= 0.72

= 1

$ip/v = n^2 F^2 \Gamma^*_{DPPNQSA.} A\ v/(4RT)$

$= n^2 F^2 \Gamma^*_{DPPNQSA} A / (4RT)$

$= (1)^2 . (96584\ C^2. mol^{-2})^2. \Gamma^*_{DPPNQSA.} (0.071cm^2)./(4 \times 8.314\ J . mol^{-1}\ K^{-1} \times 298K)$

1.26 x 10^{-4} A. $(V/s)^{-1}$ = 6.68 x 10^{4} $C^2.mol^{-1}.cm^2. J^{-1}$ x $\Gamma^*_{DPPNQSA}$

$\Gamma^*_{DPPNQSA}$ = 1.89 x 10^{-9} mol. cm^{-2}

APPENDIX 6: Randle Sevcik Plot of PPDP/NQSA at peak *a*

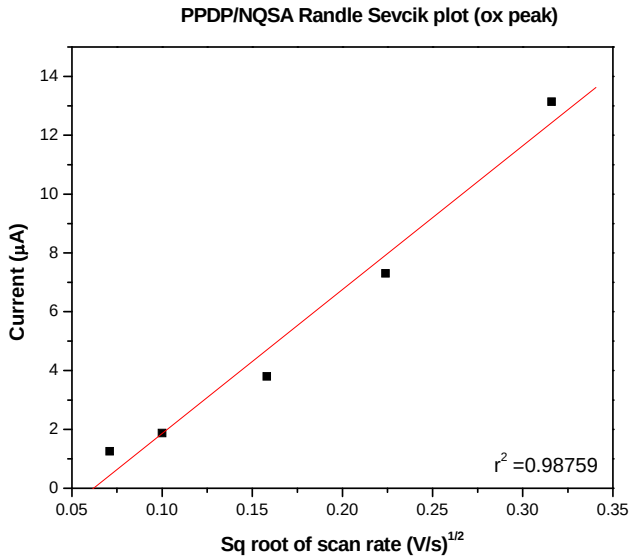

Slope= 4.89 x 10^{-4} A. $(V/s)^{-1/2}$

Randle Sevcik equation:
$ip = (2.69 \times 10^5) n^{3/2} A D^{1/2} C v^{1/2}$
where:
*i*p is the peak current
n is the electron stoichiometry
A is the electrode area (cm^2)
D is the diffusion current
C is the bulk concentration (mol/cm^3)
v is the scan rate (V/s)

$ip / v^{1/2} = (2.69 \times 10^5) n^{3/2} A D^{1/2} \Gamma^*_{DPPNQSA} / L$

4.89×10^{-4} A. $(V/s)^{-1/2} = (2.69 \times 10^5)\ n^{3/2} A D^{1/2} C$

$D_e = 4.61 \times 10^{-7} cm^2 . s^{-1}$

APPENDIX 7: Determination of rate constant of PPDP/NQSA at peak *a*

Determination of rate constant (k') at 5mV/s

This is obtained from the **Nicholson equation**:
$k' = \psi (\alpha . n . F . v . D_e / RT)^{1/2}$
where:
Ψ is a dimensionless parameter that is given the value of 7 since Epa-Epc = 60.
k' is independent of α and is assumed to be 0.5

$k' = \psi (\alpha . n . F . v . D_e / RT)^{1/2}$
$= 7 ((0.5)x(1)x(96584C.mol^{-1})x (0.005V.s^{-1})x (4.61 \times 10^{-7} cm^2.s^{-1})/ (8.314 J mol^{-1}K^{-1}) (298K))^{1/2}$

$k' = 1.48 \times 10^{-3}$ cm. s^{-1}

APPENDIX 8: Brown Anson Plot of PPDP/NQSA at peak *b*

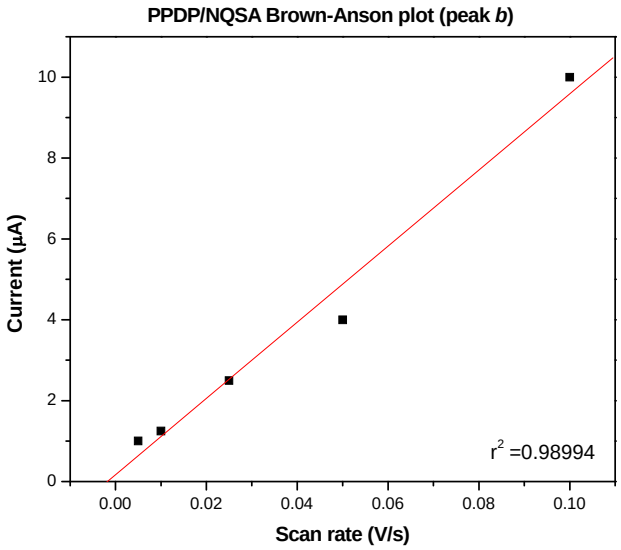

Slope = 9.41 x 10^{-5} A. $(V/s)^{-1}$

Brown- Anson equation

$ip = n^2 F^2 \Gamma^*_{DPPNQSA} (A\ v/4RT)$

where:

*i*p is the peak current
n is the electron stoichiometry
A is the electrode area (0.071cm^2)
C is the concentration (mol/cm^3)
v is the scan rate (V/s)
F is the Faraday's constant (96584 C. mol^{-1})
R is the Molar gas constant (8.314 J / mol K)
T is the room temperature (298K)
Γ^* is the surface concentration

* Diameter of glassy carbon electrode: 0.3cm
Area= ¼. Π. $Diameter^2$ = 0.071cm^2

* Number of electrons: Epa-Epc= 0.059/n volts
n = 0.059/Epa-Epc
= 0.059/(0.367-0.285)
= 0.72
= 1

$ip/v = n^2 F^2 \Gamma^*_{DPPNQSA.} A/(4RT)$
$= n^2 F^2 \Gamma^*_{DPPNQSA} A / (4RT)$
$= (1)^2 . (96584\ C^2. mol^{-2})^2. \Gamma^*_{DPPNQSA.} (0.071cm^2)./(4 \times 8.314\ J . mol^{-1} K^{-1} \times 298K)$
9.41 x 10^{-5} A. $(V/s)^{-1}$ = 6.68 x 10^4 C^2.mol^{-1}.cm^2. J^{-1} x $\Gamma^*_{DPPNQSA}$

$\Gamma^*_{DPPNQSA}$ = 1.41 x 10^{-9} mol. cm^{-2}

APPENDIX 9: Randle Sevcik Plot of PPDP/NQSA at peak *b*

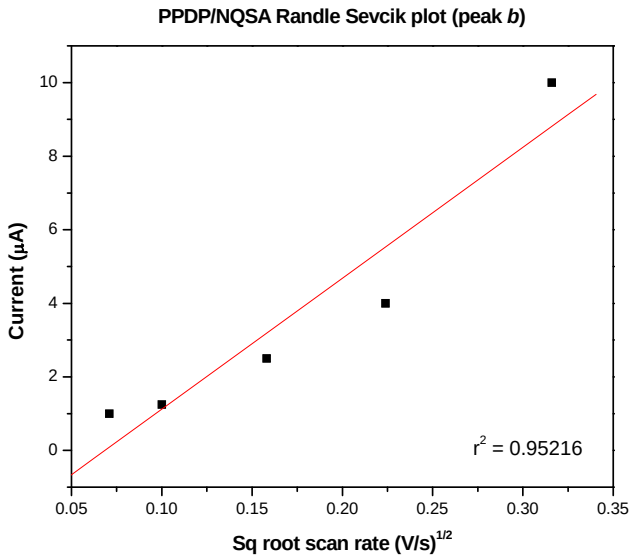

Slope= 3.56 x 10^{-4} A. $(V/s)^{-1/2}$

Randle Sevcik equation:
$ip = (2.69 \times 10^5) n^{3/2} A D^{1/2} \Gamma^*_{DPPNQSA} / L \, v^{1/2}$
where:
*i*p is the peak current
n is the electron stoichiometry
A is the electrode area (cm^2)
D is the diffusion current
C is the bulk concentration (mol/cm^3)
v is the scan rate (V/s)

$ip / v^{1/2} = (2.69 \times 10^5) n^{3/2} A D^{1/2} \Gamma^*_{DPPNQSA} / L$

3.56×10^{-4} A. $(V/s)^{-1/2} = (2.69 \times 10^5)\ n^{3/2}\ A\ D^{1/2}\ \Gamma^*_{DPPNQSA} / L$

$D_e = 4.39 \times 10^{-7} cm^2 . s^{-1}$

APPENDIX 10: Determination of rate constant of PPDP/NQSA at peak *b*

Determination of rate constant (k') at 5mV/s

This is obtained from the **Nicholson equation**:
$k' = \psi (\alpha . n . F . v . D_e / RT)^{1/2}$
where:
Ψ is a dimensionless parameter that is given the value of 7 since Epa-Epc = 60.
k' is independent of α and is assumed to be 0.5

$k' = \psi (\alpha . n . F . v . D_e / RT)^{1/2}$
$= 7 ((0.5) \times (1) \times (96584 C.mol^{-1}) \times (0.005 V.s^{-1}) \times (4.39 \times 10^{-7} cm^2.s^{-1}) / (8.314 J\ mol^{-1}K^{-1}) (298K))^{1/2}$

$k' = 1.45 \times 10^{-3}$ cm. s^{-1}